IAEA-TECDOC-1160

Steady state operation of tokamaks

Proceedings of a Technical Committee meeting held in Hefei, China, 13–15 October 1998

INTERNATIONAL ATOMIC ENERGY AGENCY IAEA

October 2000

The originating Section of this publication in the IAEA was:

Physics Section
International Atomic Energy Agency
Wagramer Strasse 5
P.O. Box 100
A-1400 Vienna, Austria

STEADY STATE OPERATION OF TOKAMAKS
IAEA, VIENNA, 2000
IAEA-TECDOC-1160
ISSN 1011–4289

Printed by the IAEA in Austria
October 2000

FOREWORD

As part of the IAEA mandate to promote peaceful uses of nuclear energy, the IAEA has several activities in the area of nuclear fusion research with the following objectives:

- to enhance international collaboration in plasma physics and fusion research,
- to facilitate technical information exchange,
- to promote spinoff applications, and
- to help developing Member States strengthen their research programmes.

In the area of technical information exchange, the IAEA sponsors a biennial Fusion Energy Conference and technical committee meetings in several areas of plasma physics and fusion technology.

The first IAEA Technical Committee Meeting (TCM) on Steady State Operation of Tokamaks was organized to discuss the operations of present long-pulse tokamaks (TRIAM-1M, TORE SUPRA, MT-7, HT-7M, HL-1M) and the plans for future steady-state tokamaks such as SST-1, CIEL, and HT-7U. This meeting, held from 13–15 October 1998, was hosted by the Academica Sinica Institute of Plasma Physics (ASIPP), Hefei, China. Participants from China, France, India, Japan, the Russian Federation, and the IAEA participated in the meeting. There were 18 individual presentations plus general discussions on many topics, including superconducting magnet systems, cryogenics, plasma position control, non-inductive current drive, auxiliary heating, plasma-wall interactions, high heat flux components, particle control, and data acquisition. There will be future TCMs on this same topic. The IAEA staff member responsible for this publication was T.J. Dolan of the Division of Physical and Chemical Sciences. The IAEA gratefully acknowledges the contributions of P.K. Kaw (Institute of Plasma Research, Bhat, India) who wrote the summary of the meeting, and D. Bora (Institute of Plasma Research, Bhat, India).

EDITORIAL NOTE

This publication has been prepared from the original material as submitted by the authors. The views expressed do not necessarily reflect those of the IAEA, the governments of the nominating Member States or the nominating organizations.

The use of particular designations of countries or territories does not imply any judgement by the publisher, the IAEA, as to the legal status of such countries or territories, of their authorities and institutions or of the delimitation of their boundaries.

The mention of names of specific companies or products (whether or not indicated as registered) does not imply any intention to infringe proprietary rights, nor should it be construed as an endorsement or recommendation on the part of the IAEA.

The authors are responsible for having obtained the necessary permission for the IAEA to reproduce, translate or use material from sources already protected by copyrights.

CONTENTS

SUMMARY

The first IAEA Technical Committee Meeting on Steady-State Operation of Tokamaks was held from October 13 to October 15 1998 in Hefei, China. The meeting was hosted by ASIPP (Academy Sinica Institute of Plasma Physics) and included a tour of the impressive HT-7 facilities. This meeting marks the timely start of TCMs in an important area of tokamak research since several experiments are already yielding impressive results (TORE-SUPRA, TRIAM-1M, HT-7) and several new experiments are under construction (SST1, HT-7U, KSTAR). Most of these devices were discussed at the meeting in a series of 15 technical presentations. In a way, this meeting also marks the beginning of a new research and development co-operation programme being fostered by the IAEA on the recommendation of the International Fusion Research Council.

The basic objectives of the programme on Steady State Operation of Tokamaks are:
- To run long pulse tokamak discharges and to investigate the physics of heat removal and particle control at the boundaries;
- To run steady state tokamaks in advanced configurations ;
- To master the technologies required for the above two objectives.

Definite progress was reported in each of the above areas. Among the ongoing experiments, interesting results were presented from superconducting tokamaks TRIAM-1M, TORE SUPRA and HT-7 and from a conventional tokamak HL-1M (from SWIP — the Southwestern Institute of Physics, Chengdu, China). In low density, low power operations, TRIAM-1M continues to be the pioneer. They have demonstrated a *2 Hour long* discharge with the following parameters:

electron density $n_e \sim 1.5 \times 10^{18}$ m^{-3},
electron temperature $T_e \sim 0.6$ keV,
ion temperature $T_i \sim 0.5$ keV,
magnetic induction $B_T \sim 6$T,
plasma current $I_P \sim 20$ kA and
radiofrequency heating power P_{RF} (2.45 GHz) ≤ 50 kW.

This discharge has produced a heat load of 10^3 MJ/m^2 for a duration $\sim 10^4$ s which may be compared with 10^4–10^5 MJ/m^2 for similar discharges in ITER. The experiment demonstrated the importance of position and fuel control for getting the plasma pulse to last a long time. The authors also emphasized the importance of developing new techniques for diagnostic of plasma position in long pulse discharges; the usual pick-up coil methods cannot be used for times longer than ~3 minutes because of accumulating drifts and the Hall detectors are not suitable in the initial state because of time response limitations. Other multisecond 100 kA low density discharges were reported from HT-7 (using 250 kW LHCD) and HL-1M (using Ohmic drive) and also emphasized the importance of position and fuel control.

High power high density operations for t ~60 seconds were reported from TORE SUPRA and TRIAM-1M. Both experiments reported loss of particle control because of wall saturation and degassing for t >60 seconds. In both cases, this may be a result of acute degassing from non-actively cooled inner components (which reach temperatures up to 2000°C in Tore-Supra), open plasma and inadequate pumping. It appears that a closed divertor configuration with actively cooled inner components and/or adequate pumping may be critical for achieving steady state long pulse discharges. In the latest TORE SUPRA experiments, a current of 1 MA was maintained for 25 seconds with a LHCD power of 2 MW and an auxiliary ICRF heating of 4 MW (giving $E_{tot} \approx 156$ MJ). It was reported that for high density operation, generally auxiliary heating and bootstrap currents are quite important ; a recent simulation showed that at 5×10^{19} m^{-3} typically more than 50 per cent current would be driven by bootstrap effects. Important results on how to avoid hot spots on ICRF antennas and LH grill during high power operations were presented. It was shown that small changes in B_T which remove harmonic resonances from the antenna neighborhood prevent hot spots on the antenna. The hot spots on the LHCD grill are typically due to fast electrons generated by the high $n_{||}$

component of the launched spectrum. They may be avoided by proper septa shaping, using power densities less than ~2.5 KW/cm^2 and the use of guard limiters. Results on the use of new actively cooled bumper limiters (steady state capability ~15 MW/m^2) on ICRF antenna were also presented; it was shown that steady temperatures of the limiters were obtained even with a total input power in excess of 10 MW.

It is most important to set up advanced confinement configurations in steady-state long pulse discharges with current primarily driven by non-inductive methods. Several attempts in this direction were reported from HT-7, TORE SUPRA, TRIAM-1M and HL-1M. In the HT-7 experiment, an attempt was made to set up a reversed shear configurations with an off-axis LHCD using 300 kW of 2.45 GHz waves. The stored energy went up by a factor 3, energy confinement time τ_E by a factor 2 and the discharge terminated by plasma disruption as the density approached the Greenwald limit. In the TORE SUPRA experiment, the magnetic shear control was attempted by changing the spectral peak of $n_{||}$ from 1.8 to 1.5 during a shot. Hard X ray tomography indicated a change in q(r); improvement of electron confinement was also seen. Several current ramp experiments for the production of hollow j(r) have also been done and also show improved electron confinement. Preliminary experiments on improved confinement by rotation induced internal transport barriers produced by off-axis electron and ion heating were also reported from TORE SUPRA. A most unusual sharp ∇T_i sustenance was reported from low density ($n_{e\ i} \leq 2 \times 10^{18} m^{-3}$) TRIAM-1M LHCD experiments. The ion temperature dropped from 2.5 keV at the core to about 0.5 keV at 3.6 cm and the barrier τ like structure was sustained for about a minute or more. It is still unclear how the ion heating is taking place in these low density experiments. An improved confinement plasma ($\tau_E \sim 2\tau_E^{OH}$) with steep n_e, T_e gradients at the edge region was achieved in LHCD phase on HL — 1M tokamak. ELM like perturbations were also observed.

An interesting new direction reported at the meeting (HT-7 experiment) was that of wall conditioning using ICRF. It is well known that wall conditioning techniques for superconducting tokamaks have to be novel because B_T cannot be reduced between shots and so glow discharge cleaning cannot be carried out. HT-7 experiment reported the use of 5-35 kW of ICRF for wall conditioning and boronization experiments. A plasma with $T_e \sim$ 2-6 eV and $T_i \sim 0.4 \sim 2$ keV (with a tail ~30 keV was found to give significant improvement of wall conditions and a high efficiency boronization for fields as high as 2.5 T.

Two proposed new devices were discussed in detail at the meeting. The SST1 experiment (at Institute for Plasma Research, Gandhinagar, India) is designed to be a double null, elongated plasma experiment with pumped divertors, superconducting toroidal and poloidal field magnets, lower hybrid current drive and auxiliary heating by ICRF, neutral beams and ECRH. Plasma is produced by an Ohmic transformer using copper coils giving a V-s. capability of about 1.2 Vs. The design parameters of SST1 are $B_T \sim 3$T, $I_P \sim 0.25$ MA, major and minor radii R/a/b ~ 1.1/0.2/0.4 m, elongation κ ~1.6–2, triangularity $\delta \sim 0.4$–07 , lower hybrid current drive power P_{LHCD} at 3.7 GHz ~ 1 MW, ion cyclotron range of frequencies heating power $P_{ICRF} \sim 1.5$ MW, neutral beam power P_{NB} at 50 keV ~ 1.7 MW, electron cyclotron resonance heating power P_{ECRH} at 84 GHz ~ 0.25 MW and pulse length $t_{pulse} \leq$ 1000 s. The superconducting coils are to be wound from specially designed NbTi/Cu CICC being manufactured at Hitachi Ltd, Japan (test pieces are ready and have undergone successful preliminary short sample and strand tests at Kurchatov Institute, Moscow). The winding of the coils and the manufacture of the basic shell of the machine viz. the vacuum vessel, the cryostat, the coil casings, the Ohmic transformer and the mechanical structure will be carried out by Indian industries. Steady state RF systems are being assembled and prototype development for components of the neutral beam system has been initiated. The first wall of SST1 (comprising of the passive stabilizers, the divertor plates and the baffles) are designed for a steady-state heat removal capability $\leq$ 1 MW/m^2 and are based on mechanically bolted graphite tiles on copper alloy substrates. The machine is expected to have the first plasma in 2002. The formal approval for construction of HT-7U was announced at this meeting. It is a machine with similar design objectives as SST1 ; its parameters are $B_T \sim 3.5$ T, $I_P \sim 1.0$ MA, R/a/b ~ 1.7/.4/.8 m, $\kappa \sim$ 1.6-2,$\delta \sim 0.4$ - 0.8, P_{LHCD} (at 2.4 and 3.7 GHz) ~ 3.5 MW, P_{ICRF} ~3.5 MW, $P_{ECRH} \sim 0.5$ MW, and $t_{pulse} \sim 60$ - 1000 s. The Ohmic transformer is superconducting and has a

capability of 10 Vs. The poloidal field magnets will be wound from special 14 kA. NbTi/Cu CICC conductors which are already designed and are ready for testing. The TF magnet will be based either on the bath cooled system or on forced supercritical Helium system (the relative merits were discussed in a talk by D. Ivanov of Kurchatov Institute) and is likely to use the readily available SSC strands. The first wall system is still in a preliminary stage of design and is likely to be similar to that of SST 1 in the first phase. A neutral beam capability may be introduced in the second phase of HT-7U. First plasma in HT-7U is also slated for 2002–2003. The basic physics objective of both machines is to study the effect of steady state heat removal and particle control at the boundaries on the confinement properties of elongated plasmas with significant triangularity. A particular objective is to maintain advanced confinement configuration with significant bootstrap and noninductive current drive in a steady state discharge.

A third new project presented at the meeting was the project CIEL being proposed on TORE SUPRA. It involves an upgrade of the heat and particle exhaust capability of TORE SUPRA viz. a toroidal pumped limiter able to remove 15 MW of convected power up to 1000 s and a covering of first wall able to remove 25 MW of radiated power (by actively cooled panels) up to 1000 s. It is to be noted that the limiter will be made with third generation fingers (CFC bonded on Cu Cr Zn by active metal casting) of the type that were successfully tested in the antenna limiter in 1998. The CIEL project also involves an upgrade of the RF systems to a total capability of ~20 MW (10 MW ICRF, 8 MW LHCD, 2 MW ECRH). Simulations show that densities up to 10^{20} m^{-3} can be achieved with a bootstrap current fraction of up to 80 per cent. Project CIEL is likely to be operational in the year 2001.

An interesting futuristic talk on the near term application of steady state superconducting tokamaks was presented by Y.X. Wan (China). He pointed out that in considering energy alternatives for China, it is proposed that in a few decades 15–20% of electricity production will be based on nuclear fission power. Fusion scientists are considering how they can contribute to fissile fuel production and treatment of waste products for the near 300 power plants which will have to be in operation. They estimate that a machine of the size of JET (R/a ~ 2.8/1.0m) with a D-T mixture at a temperature ~10 keV and a duty factor of 15–50% will produce a wall loading of order 0.2 MW/m^2 which can treat an actinide waste of 250 kg per year. If the size of machine is increased to (R/a ~ 4.0/1.0 m) and duty factor is kept at 50%, one would get a wall loading of 0.42 MW/m^2 which can generate about 100 kg. of fissile fuel per year. These numbers are very attractive. However, to make the time frame (2015–2020) proposed for such devices realistic, one needs a thorough discussion on areas such as materials on which very little work is going on at the moment.

Overall, this meeting has made an exciting beginning to intense discussions in an important area of fusion research — in fact, the only area of tokamak research in which new experiments are under construction today. There is need for collaboration amongst the various groups especially in key areas of technology such as development of first wall components with high power steady state capability, development of CW RF and neutral beam systems, etc. It was decided to enlarge the scope of this meeting in future and to include all toroidal devices with steady state operation (such as the recently commissioned LHD machine where many of the technologies are similar). The next meeting is likely to be held in 1999 in Kyushu, Japan where the TRIAM-1M experiment is being conducted.

TOWARDS HIGH-POWER LONG-PULSE OPERATION ON TORE SUPRA

TORE SUPRA Team[1]
(Presented by A. Becoulet)

Association EURATOM-CEA sur la fusion,
Centre d'études de Cadarache,
Saint-Paul-lez-Durances, France

Abstract

The Tore Supra tokamak was given the main mission to investigate the route towards long pulse plasma discharges. This includes the problem of heat exhaust and particle control (via the development of high-performance plasma facing components), and in parallel the physics of fully non inductive discharges and its optimization with respect to the confinement. Tore Supra is thus equipped with a superconducting toroidal magnet (maximum magnetic field on axis 4.5T), a full set of actively cooled plasma facing components (PFC), and a heating & current drive capability based on high power RF systems connected to actively cooled antennas. The encouraging results already obtained, as well as recent progress in PFC, allowed us to envisage a significant improvement in the heat exhaust capability of Tore Supra. The so-called CIEL-project [1] consists in a complete upgrade of the inner chamber of Tore Supra, planned to be installed during the year 2000. The present paper deals with the experimental and modeling activity linked to the preparation of the long-pulse high-power discharges using the present Tore Supra equipment: heating and current drive scenarios, power coupling, confinement and transport studies, discharge control... An overview of the results obtained in that field is presented, as well as the progress required in the coming years, and the expected performance, for the CIEL phase, in terms of current drive and confinement.

1. Additional Heating and Non Inductive Current Drive on Tore Supra

The present auxiliary heating system of Tore Supra [2-3] consists of a lower hybrid current drive (LHCD) unit (16 × 500kW-klystrons, 3.7GHz, 2 multijunction launchers) combined with an ion cyclotron range of frequency (ICRF) system (6 × 2.2MW-tetrodes, 40-80MHz, 3 double-loop resonant antennas). The maximum power expected to be coupled to the plasma with the present system is in the range of 10-11 MW for ICRF and 5-6 MW for LHCD. Both systems have current drive capabilities (i.e. tunable phasing), actively cooled antenna structures (lateral bumpers (ICRF+LHCD); Faraday screen, current straps, matching capacitors (ICRF)), and are designed at present for 30s (ICRF) or 210s (LHCD) pulses. Various recent improvements are to be noted as key elements towards a more reliable operation of the system:

- *ICRF operation*: automatic matching based on the tuning of the antenna variable capacitors during pulses, with a minimum time response of the order of 100ms [4]; use of Thomson Tubes Electroniques TH525 tetrodes allowing a higher output power (~2.2MW), as well as a higher dissipated power (up to 2MW) [2].
- *LHCD operation*: VME operation system favoring various real time feedback loops, including one limiting the output power in case of high-Z impurity production.
- *Infrared camera monitoring*: numerical data acquisition and processing of the infrared camera system, allowing a more exhaustive analysis and control of both PFC and antennas.

The progress towards high power long pulse discharges presently follows two main routes. The first one consists in achieving discharges which combine the two RF systems at their maximum power capability. As mentioned above, this aspect of course requires a reliable operation of the generator and antenna systems, involving continuous maintenance and development effort. It also involves the understanding and optimization of the power coupling. As a matter of examples, one can mention several key points, recently documented:

[1] See the Appendix.

– *acceleration of electrons in front of LHCD multijunction grills*: experiments and modeling on several machines have shown the possible dissipation of LHCD power by the edge electrons, generating damages [5-7]. Minimization of such effects requires a limitation of the power density at the grill mouth, as well as a careful design of the grill itself (septa shaping, location of guard limiters). Such improvements are being implemented on the present and future Tore Supra [3] launchers to allow a safer long pulse operation.
– *careful ICRF layers optimization*: due to the Tore Supra aspect ratio, high harmonic cyclotron layers often locate at the very edge of the plasma (low field side) during ICRF operation. This mainly concerns the third harmonic of Deuterium in D(H) minority heating, and the fourth harmonic of Deuterium (second harmonic of hydrogen) in fast wave electron heating (FWEH) scenarios. Though they do not significantly alter the expected power deposition balance, those layers can be responsible for a strong heat deposition on the antenna Faraday screens when located a few centimeters in front of it (fig1). A careful positioning of such layers, accounting for the important local magnetic field ripple, is thus fundamental for long pulse operation.

The Tore Supra ICRF antennas have demonstrated several time their individual capability of operating at the nominal power of the generator system, namely from 4 to 4.2 MW. The actual antenna limitation is in fact more relevant to a maximum voltage of 40-45kV, located at the extremities of the current strap. Combined operation with several ICRF antennas is of course more constrained. The first effect concerns the increase of the overall power, and thus of the heat load on the antenna structures. This point becomes crucial for long pulse operation and will be discussed mainly in the last section. The second aspect involves the possible "cross-talk" effects between antennas. Power flowing from one antenna can be seen by the other antennas as reflected power, possibly confusing the safety systems based on the reflected to incident voltage ratio. This effect is exacerbated when operating in low single pass damping scenarios, as FWEH or mode conversion heating, which develop strong cavity mode structures. Several solutions are presently envisaged: i) polychrome operation, consisting in associating a different frequency to each antenna. The drawback of this method is that the required frequency split (±200kHz at least) is not always compatible with the careful control of the edge high harmonic cyclotron layers. ii) the simultaneous management of the three antenna safety systems, which insures that they are switched on and off at exactly the same times. This solution is being implemented. iii) new arc detection systems (optic fibers, detection of sub-harmonic frequencies generated by arcs, ...) replacing the existing safety system. Such a solution still requires R&D. Though no definitive solution has been fully implemented yet, up to 10 MW of ICRF were coupled into the Tore Supra plasmas by the combined operation of the three antennas, both in minority heating scenarios (damping per pass close to 100%) and in FWEH schemes [8] (at 2T, damping per pass of the order of 10%). This performance is close to the present generator capability of the ICRF system. Solving the problem generated by cross-talk effects would however mean more reliability and stability for these high power discharges. This reliability can even become a pre-requisite for certain types of discharges, as the ones operated at high fraction of radiated power (with or without the ergodic divertor) for which a power switch-off leads to disruption, or the ones operated at high-bp for which a power switch-off leads to a fast backward motion of the plasma and thus to major difficulties for recovering.

The combined operation of the two LHCD grills is not altered by such "cross-talk" effects. Maximization of LHCD coupled power is mainly governed by a careful control of the reflected power of each antenna, i.e. by the optimization of the edge conditions at the grill mouth (once the antenna conditioning is satisfactory). Up to 5.3MW were obtained energizing the two grills simultaneously for 6s. The plasma-grill distance can also be adjusted during the pulse, and controlled by a feedback loop, for instance on the reflection coefficient. Using the same system in a pre-programmed way, the power coupling has been maintained as the plasma-grills distance was slowly increased up to 16cm, in regions where the plasma heat load is negligible.

The ultimate goal is of course to combine both RF systems on the same target plasma. One must here again distinguish between the overall heat load problem (more relevant to long pulses and discussed below), and the problem of compatibility between the constraints. The limitation of the voltage in the ICRF antennas forces to maximize the loading resistance if one wants to maximize the coupled power.

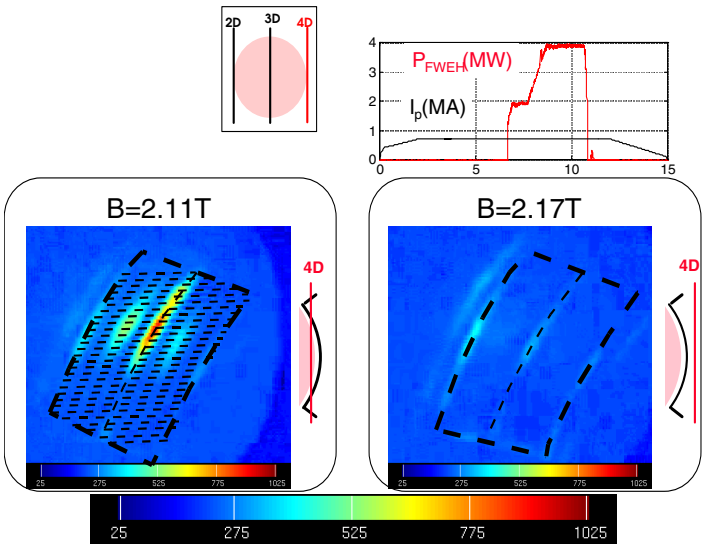

FIG. 1: FWEH experiment (2 × 2MW with two ICRH antennas, dipole phasing). Influence of the 4D(2H) cyclotron layer exact location on the Faraday screen temperature measured by infrared cameras.

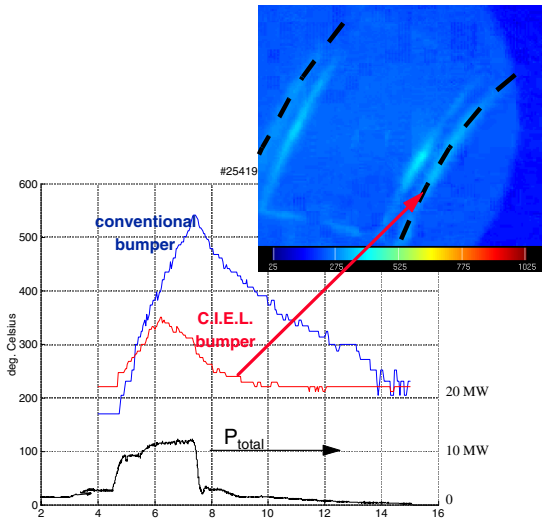

FIG. 2: (#25419) 9.5MW of ICRH (3 antennas)+1.8MW of LHCD(1 grill)+0.3MW of Ohmic. Time traces of the ICRF antenna lateral bumpers temperatures, comparing the conventional ones (carbon tiles) and the new CIEL concept (CFC tiles). An infrared picture also illustrates the new bumper behavior (on a 25-1025¡C scale).

This is achieved either by increasing the plasma density (in fact the plasma edge density) and/or by decreasing the antenna-plasma distance. For the Tore Supra ICRF antennas, coupling the full power requires a loading resistance larger than 5 W/m, which corresponds to line densities larger than 4-5.10^{19}m^{-2} and antenna-plasma distances of the order of 2-3cm. The edge conditions are of course of importance: recycling conditions, gas, limiter or ergodic divertor configuration,... have an influence on the antenna loading resistance. One finally must keep in mind that a reliable operation requires some antenna voltage margins, in order to cope with transient effects, like giant or monster sawtooth crashes, plasma motions, ... Following this idea, a feedback loop system limiting the antenna voltage to a preset value is under study. On the LHCD side, the optimum coupling conditions are unfortunately opposite: the density at the grill mouth should be maintained close to its (low) ideal

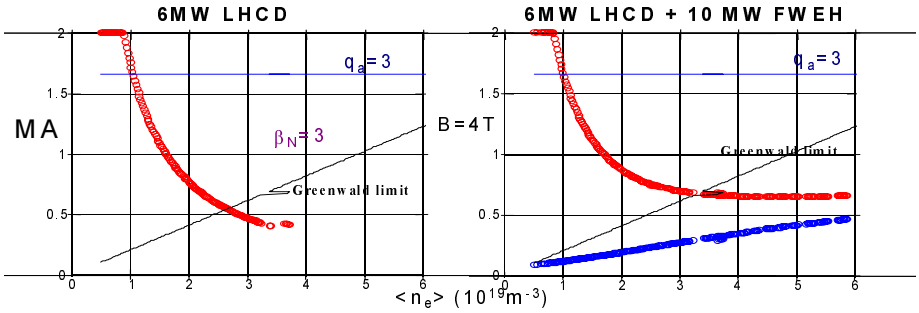

FIG. 3: Fully non inductive plasma current (red) driven by 6MW of LHCD (left), and 6MW of LHCD + 10MW of FWEH (right) (driving bootstrap current (blue)) on Tore Supra versus the volume averaged density. The Greenwald, q_a=3 and β_N=3 limits are also displayed.

cutoff value. Moreover, for a given power density at the grill mouth, the higher the local density the larger amount of fast electrons in the plasma edge, possibly causing damages to the magnetically connected objects. The success is finally sensitive to the chosen scenario and plasma behavior. The latest performance achieved in this domain (fig2) is a 11.6MW/1.6s discharge (#25419, 32MJ for the overall discharge), consisting of 9.5 MW of ICRF (3 antennas) + 1.8MW of LHCD (1 grill) + 0.3MW of ohmic power. It has been achieved in a He(H) minority heating scenario (B=3.5T, Ip=1.4MA, nl=6.10^{19}m^{-2}) where the fundamental hydrogen cyclotron layer is located slightly off-axis on the high field side, in order to limit the sawtooth activity (Te(0)~5keV). The voltages on the ICRF antenna was in the range of 35kV and the coupling resistance of 6W/m. The time duration was limited on that discharge by the temperature reached on the main pumped limiter on which the plasma was lying. Note that the diamagnetic stored energy reached the record value for Tore Supra of 1.24MJ (thermal energy confinement time ~85ms).

The second route consists in achieving long pulse discharges in order to progressively qualify new PFC components, in the various integration aspects: power and particle injection and exhaust capabilities, machine operation, diagnostics, data acquisition, feedback loops..., and address the feasibility of steady-state discharges. The pre-requisite of such studies is of course to drive non-inductively a significant fraction of the plasma current, mainly through the intensive use of LHCD (see below). The plasma current has already been sustained on Tore Supra for 2 minutes at the level of 0.8 MA, using 2.4MW of LHCD. The total injected energy (LHCD+ohmic) reached the record value of 280MJ [9]. The slow density increase usually observed after one minute of operation on such discharges confirmed the absolute necessity of a complete particle control system for further progress (i.e. active cooling of each element plus efficient pumping). Fully non inductive discharges were performed for durations up to 75s, using a double feedback control: the loop voltage was imposed to be zero by retroaction on the ohmic system, and the plasma current value was controlled by a feedback loop on the injected LHCD power (Ip=0.6MA, P_{LHCD}=2MW). In order to progressively increase the power level on such discharges, ICRF power has also been superimposed. This allowed us to couple up to 4MW of ICRF (hydrogen minority heating) plus 2.2MW of LHCD during 26s, representing a total input energy of 170MJ. Note that this performance was also favored by the fact that 1/6 of the Tore Supra carbon inner wall was replaced by more high-performance PFC components, made of Carbon Fiber Composites (CFC) and intentionally slightly misaligned beyond the remaining 5/6 [10].

The success of the overall programme is of course not independent of the chosen scenarios and of the resulting confinement properties and plasma stability. The required non inductive current is based on Tore Supra on two components. The first one is LHCD, the second bootstrap current. Fully non inductive discharges, driven by LHCD on time durations long enough to reach steady-state under various plasma conditions, allowed us to determine the experimental behavior of the LH current drive efficiency for the Tore Supra conditions. Besides the predicted dependence in Zeff, it is found to depend linearly on the magnetic field, and to very slowly decrease with density. No clear evidence of a dependence with the volume averaged electron temperature is found. More details on the non

inductive current profile behavior are discussed in the next section, as well as in Ref [5]. Extrapolations of such a current drive efficiency clearly show (fig3) that some extra LHCD power and/or alternative non inductive current are required to reach steady-state discharges in the relevant range of 0.5²Ip(MA)²1.5 and 1 ² <n>($10^{19}$$m^{-3}$) ² 5.

Significant effort is thus being made in the bootstrap current generation using the direct coupling of the fast magnetosonic wave to electrons, in the ICRF [8]. This so-called fast wave electron heating (FWEH) scheme involves Landau damping and transit time magnetic pumping of the fast wave on the parallel motion of the bulk electrons. The Tore Supra database now covers a magnetic field range between 1.3T and 3.5T, and an input power range up to 9.5MW. Bootstrap current fractions up to 50% have already been reached for several seconds. The corresponding ICRF frequency is chosen so that the plasma is bounded by the second and fourth cyclotron harmonic layers of the bulk ions (Deuterium or Helium 4). The third cyclotron harmonic layer thus crosses the plasma centre, but the possible competition with the FWEH is insignificant on present discharges as the bulk ion temperature remains low enough. For the first time in a tokamak, the fast wave has also been damped by electrons in a scenario where no competing ion cyclotron damping is present in the plasma (42MHz, 3.9T), confirming without any ambiguity the FWEH process. The power deposition profile is strongly peaked in the plasma centre and the bootstrap current is then driven by the resulting strong electron pressure gradient. The corresponding amount of bootstrap current is found not to depend on the operating magnetic field, and the following ad-hoc expression of the bootstrap current fraction was fitted, adding the TEXTOR and TFTR bootstrap databases to the Tore Supra one [11]:

$$Ibs/Ip \approx Å\ 0.5\ e^{0.5}\ bp\ (a_p/a_j)^{0.5}$$

where e is the inverse aspect ratio, bp the poloidal beta, a_j the peaking factor of the current density (defined as the ratio between the central current density and the average current density Ip/pa^2) and a_p the central pressure value normalized to the volume averaged pressure.

Alternative scenarios, combining ICRF and LHCD, are also under consideration. We first investigated some possible "synergistic" current drive effects expected between both waves. The experiment was based on the possibility for the wave mode-converted from the fast wave at a two-ion hybrid layer location (monopole operation) to couple to the fast electrons generated by LHCD. LHCD and ICRF powers have thus been coupled in H-He3 plasmas optimized for ICRF mode conversion heating [12], and various scans in plasma current, density and ion mixture were performed. Operation at zero loop voltage was also studied. More than 60 discharges allowed us to conclude that, in such conditions, no effect on current drive efficiency was noticed, as well as no modification of the fast electron population was seen on the hard-X ray tomography system [13].

The "FWEH-driven" bootstrap current is thus now considered on Tore Supra as the major candidate for supplementing the LHCD non inductive current on high-density long-pulse operation. The characteristic of such a scenario is that the power transfer between the heating waves and the plasma mainly results in a strong bulk electron heating, combined with a significant fraction of non inductive current. The resulting transport is then dominated by the electron L-mode transport, improved by possibly significant magnetic shear modification effects[14], the ion energy content being governed by the collisional equipartition rules. In the present Tore Supra discharges, two kinds of improved regimes have been observed: one mainly observed an enhancement of the confinement linked to the increase of the mid-radius magnetic shear, under the influence of bootstrap current for instance, and/or an enhancement of the central performances due to a flat or slightly reversed central magnetic shear when operating close to 100% LHCD-driven discharges (so-called hot core LHEP discharges). The obtained performance [8] show H-factors up to 1.6 (with respect to the ITERL-97-P thermal scaling law [15]).

2. Current profile modifications and control

In addition to a fully non inductive plasma current, the long-pulse discharges require an active control of the current density profile, both for transport optimization and MHD stability. It is thus essential to

rely on several non inductive current sources, which allow to shape the current profile, as well as on real-time determination of the major (local and global) characteristics of the current profile (central safety factor, minimum safety factor location and value, internal inductance, ...). One can then set appropriate feedback loops on the current sources. This long term work, both technical and physical, is underway on Tore Supra.

Weak (positive or negative) magnetic shear discharges may for instance develop MHD activity of various types, requiring a careful adjustment of the current profile (including bootstrap), pressure profile, etc. For instance, tearing modes have been observed [16] tp limit performance of some Tore Supra long-pulse discharges with a dominant fraction of LHCD non inductive current (so-called LHEP phase)(fig4). In such discharges, the central safety factor is slightly below a low-order rational value (3/2 or 2) associated with a local flatness of the current profile (weak shear region up to r/a~0.3). On the case shown on Fig. 4, the onset of a m/n=2/1 tearing mode is reached after 13s of operation, as the current and pressure profile still slowly evolve. The LHEP phase is abruptly terminated, and the postlude plasma exhibits a strong "sawtooth-like" MHD activity driven by coupled m/n=2/1 and m/n=3/1 modes and preventing recovery of the confinement enhancement associated with the LHEP phase.

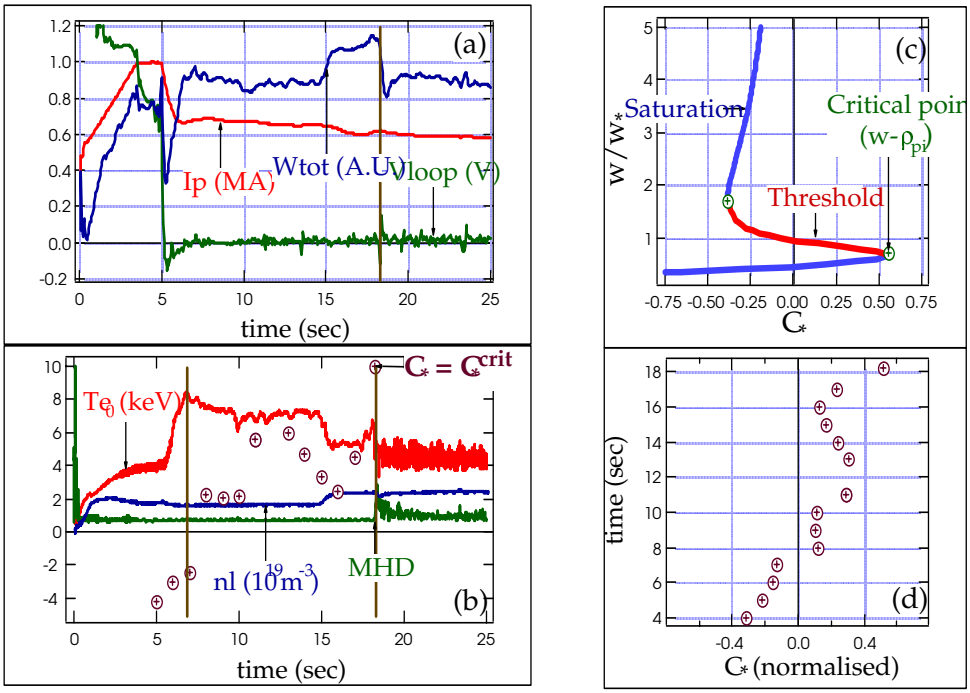

FIG. 4: (a-b) A ToreSupra LHEP-discharge exhibits a transition from improved LHEP-regime towards degraded-regime, with MHD-onset at t=18.2 sec. (c-d) Stability diagram and evolution of the control parameter (see Ref [16]) for the discharge.

An efficient feedback system is thus required in order to extend the duration of such regimes significantly. Improvements in current density profile measurements (through polarimetry diagnostic (from 5 towards 9 channels), development of a MSE diagnostic, VME data acquisition...) are underway. However, one of the key points remains the capability for the heating & current drive systems to efficiently act on the pressure and current density profiles. An example is given on Fig. 5, where a feedback loop was set between the plasma internal inductance (l_i) and the $n_{//}$-spectrum of the LHCD launchers. The injected $n_{//}$ index can freely vary between 1.4 and 2.8. In this experiment, the preset-l_i was required to vary from 1.7 to 1.55 during the discharge. Figure 5 shows the corresponding response in terms of LHCD launcher phase and power, as well as the actual l_i-evolution, confirming

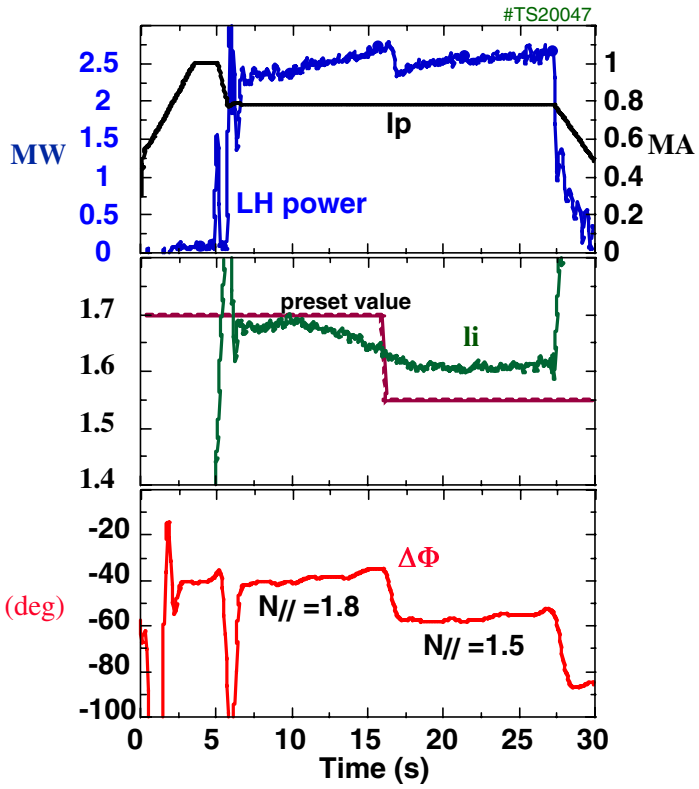

FIG. 5: (#20047) time evolution of a Tore Supra discharge where the internal inductance (li) value is required to follow a preset value feedback controlled on the LHCD parallel index $N_{//}$.

the possibility of control. But, of course, the relation between the LHCD power deposition profile and the phase of the launchers, as well as between l_i and the current profile, are more sophisticated, and this experiment represents to that respect a proof of principle. The new hard X ray (HXR) tomography system[5,13] installed on Tore Supra is now extensively used for a more exhaustive fast electron behavior analysis, both in time (4ms resolution), velocity (8 energy channels) and poloidal (59 lines of sight, 5cm resolution) spaces. One of the first strong conclusions of this analysis (discussed in [5]) is that, in reversed shear ramp-up experiments, the LHCD power deposition profile remains peaked, until the q=1 surface appears in the discharge. Moreover, a correlation between the radial position of the HXR maximum of emission and the q=1 surface location is then observed, revealing a strong connection between the deposition and the current profiles. The present LHCD system can thus hardly sustain high-q_a shear reversal situations, unless the wave accessibility conditions are not fulfilled, as already demonstrated at very low magnetic field [17]. Such conclusions encourage several prospective studies engaged on Tore Supra. These studies both include the present equipment, through the combination with FWEH-driven bootstrap current for instance, as well as on-going developments (installation of an ECRH/ECCD system (see below)) and new possible developments (combination with a vertical LHCD launcher insuring an edge absorption barrier for the LHCD power launched by the main grills located in the equatorial plane).

From the transport point of view, a major interest for Tore Supra remains the possibility of triggering, and sustaining, wide internal transport barriers (ITB) with RF heating and current drive alone. One of the most successful techniques, applied on many tokamaks, consists in coupling the power very early in the discharge, during the plasma current ramp-up, in order to take advantage of the ohmic hollow current profile and slow down its diffusion towards the centre. This technique however suffers from two major drawbacks on Tore Supra: i) when using ICRF additional power, a relatively high density is required (see above) to couple a sufficient amount of power. The time required for reaching such densities is too long compared to the very short current diffusion time scale (a few hundreds of ms in the start-up phase), ii) when using LHCD power, the current deposition profile, as

(a)

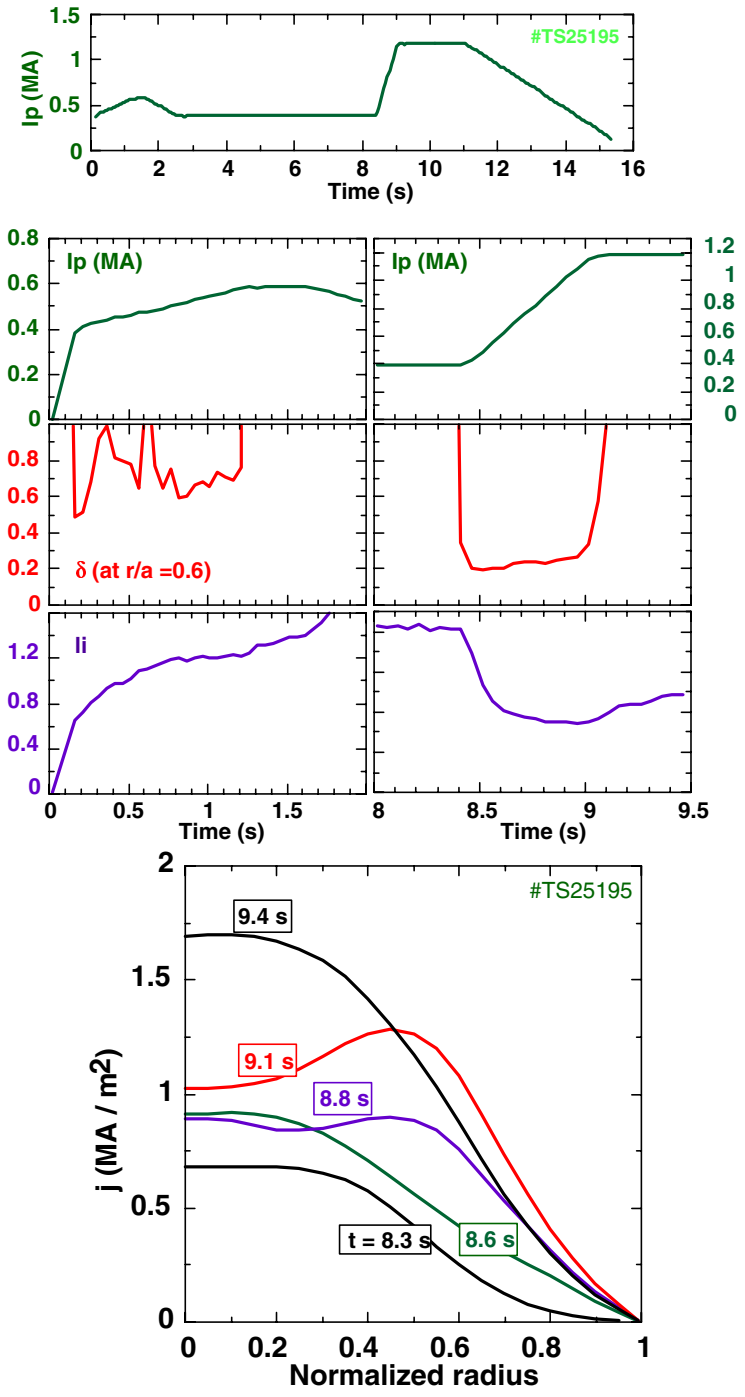

(b)

FIG. 6: (a) (#25195) Comparison of two plasma current ramp-up phases. The first one, during plasma start-up (left) leads to a skin depth (computed at r/a=0.6) of 0.6 and a weak effect on li, the second one, after an 8s low current plateau (with 1.6MW LHCD), leads to a skin depth of 0.2 and a significant shear reversal, as confirmed on FIG. 6b. (B) current density profiles during #25195.

discussed previously and in [5], is peaked at low plasma current. This partially spoils the efforts for sustaining a wide hollow current profile on time scales much longer than the resistive time. An alternative way is thus being investigated at present. It first consists in setting a low (~500kA) plasma current discharge on which ICRF minority heating (and/or LHCD) is established, on a time duration long enough (8-10s) to reach a steady-state. The plasma current and the power are then rapidly ramped-up and a hollow current phase is reached. In that case, one can optimize the resistive skin depth by properly shaping the ramp-up frequency w=(1/Ip)(dIp/dt). Figure 6 shows an example of a fast current ramp-up phase (from 0.5 to 1.2MA) leading to a normalized skin depth 1/a.sqrt(2h/w) = 0.2 (instead of 0.6 during the start-up phase) (h is the plasma resistivity). The internal inductance drops to ~ 0.6, and the central shear is negative. The next step will consist in increasing the additional power and controlling the reversed shear region by adjusting the power deposition location (off-axis ICRH and/or ECRH heating).

Such a scenario should insure a significant current profile control, in which the electron heating is dominant. The final step consists then in increasing the ion pressure gradient, in order to enhance the rotation shear and improve the transport. This challenge for RF heating systems requires further scenario studies. Those scenarios are presently being investigated. Promising results in this field were obtained in high hydrogen minority discharges, at relatively high density (80% of the Greenwald limit). In such discharges, ion and electron energy contents are more balanced, and a significant toroidal rotation is induced by ICRF. An improved confinement was observed, during more than 2s, in both ion and electron channels, corresponding to an H factor of 1.6 (with respect to ITERL-97-P)[18]. Other possibilities, involving Helium3 or Impurity minority heating for instance are also under investigations.

3. Towards the CIEL discharges

The power exhaust capability of the so-called "CIEL" plasma facing components will be of the order of 20-25 MW (conducted + radiated), in steady-state (i.e. several hundred of seconds)[1,19-20]. In order to fully benefit of such a capability, the heating and current drive systems follow a long-term improvement programme, including several levels from the generators to the antennas. Among the numerous elements presently under development, one can underline:

– *ICRF operation*: one of the ICRF antennas has been equipped with a new set of lateral protection elements [21] (fig7), using for the first time in this environment the active metal casting technology (CFC tiles bonded on copper alloy water cooled fingers) [22], which is the basis for all the PFC in CIEL. Extensive validation tests were performed under various conditions: ICRF minority heating, FWEH, combination with LHCD, ergodic divertor configuration, antenna-plasma positions, etc. Up to now, those elements showed a quite satisfactory behavior, as illustrated on Fig. 2, where the antenna temperature is shown during the 11.6MW/1.6s shot (#25419) described above, and compared to another antenna using the conventional carbon tiles lateral protections at the same level of power and radial position. The two other ICRF antennas will be progressively equipped with such protections. VME data acquisition is also underway for the ICRF system, allowing feedback loops on the antenna position, coupling resistance or limitations of the voltages for instance. An active feedback on the antenna phasing is also being developed [23].

Concerning the future developments, the generators and several antenna elements must be adapted to longer pulses. One of the challenges is certainly the improvement of reliability of the antenna matching elements, presently built with actively cooled variable vacuum capacitors [24].

– *LHCD operation*: a renewal of the LHCD multijunction launchers is underway. The new design [3][25] involves a larger radiation surface (i.e. a lowering of the power density at the grill mouth), as well as the new lateral protections mentioned above for ICRH antennas. The first new grill is planned to be installed and tested in summer 99. New concepts, like Passive-Active

Multijunction, insuring a better cooling capability are also being considered, in collaboration with ENEA-Frascati, where the concept will be tested first [26].

– *ECRF*: in collaboration with the Ecole Polytechnique Federale de Lausanne, Forschungszentrum Karlsruhe, and Thomson Tubes Electroniques, Tore Supra is implementing a 118GHz/3MW/210s ECRF system. The prototype gyrotron (500kW) is already being tested in Cadarache [27], and the full power is planned to be available for the operation on CIEL. Beyond the extra input power brought by this system, its flexibility in terms of injected angles allows to envisage local heating and current drive effects, strong enough to stabilize performance limiting tearing modes [28], and/or to modify the local current profile significantly, with a capability of setting (slow) feedback loops on the injected angles.

– *Infrared camera monitoring*: both the 360¡ of toroidal pumped limiter (TPL) and each antenna will be monitored with numerical data acquisition, allowing an active safety control.

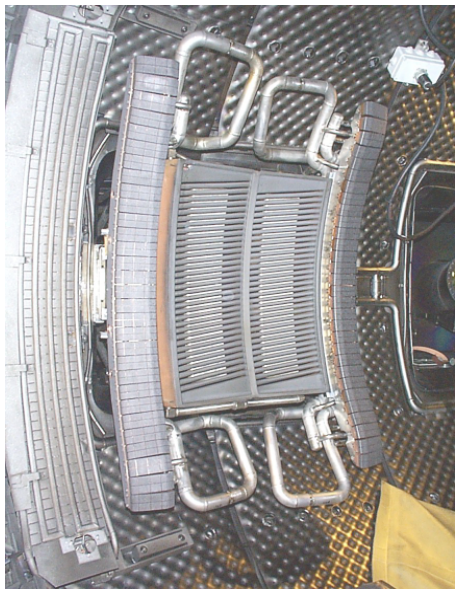

FIG. 7: New lateral bumpers on one of the ICRH antennas.

The heating and current drive systems, after the necessary upgrades, should typically deliver in steady-state 10-12MW of ICRF, 6-8MW of LHCD and 2-3 MW of ECRF. Zero-D extrapolations of the present database combining LHCD, bootstrap current, the Zeff behavior in limiter configuration, the confinement and its enhancement with respect to the bootstrap current fraction, gives us the basic steady-state performance of CIEL discharges [8], in terms of (fully non inductive) plasma current versus volume averaged density (see Fig. 8a). They mainly lead to two types of scenarios. The first one takes place at low density: the plasma current is of the order of 1.5-1.7MA (q_a close to 3), with a negligible fraction of bootstrap current. The lower density however allows only to control the wall-particle inventory, but not the density profile. Furthermore, the plasma does not radiate a significant fraction of the outcoming power. This regime shows a moderate confinement enhancement. The second mode of operation is more "advanced". It consists in working much closer to the Greenwald limit of density; the plasma current is of the order of 0.8-1 MA (q_a close to 5-6), with a confinement enhancement factor of the order of 2 (with respect to ITERL-97-P). The bootstrap current fraction reaches 50%, and the density level then allows an efficient edge pumping by the Toroidal Pumped Limiter (Fig. 8b), as well as a large fraction of radiated power. Normalized beta values are of the order of 1.5 at 4T, and reach 3 at 2T. Note that this extrapolation is rather conservative, in the sense that it does not rely on further confinement enhancement due to possible hollow current profiles and/or shear flow effects, triggering internal transport barriers.

(a)

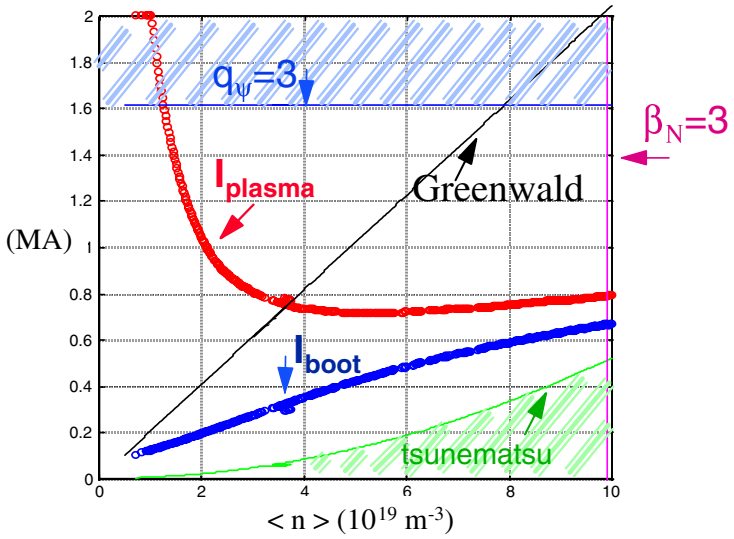

(b)

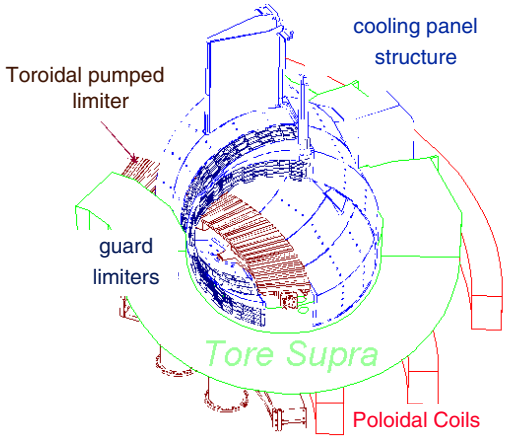

FIG. 8: (a) Fully non inductive plasma current (red) driven by 8MW of LHCD + 10MW of FWEW (driving bootstrap current (blue)+ 2MW of ECRH) on Tore Supra versus the volume averaged density. The Greenwald, Tsunematsu, q_a=3 and β_N=3 limits are also displayed (B=4T). (b) schematic view of the Tore Supra inner vessel during the C.I.E.L. phase.

4. Conclusions

Achievement of high power long pulse discharges is the long term goal of the Tore Supra tokamak programme. It represents a huge integration effort involving all the tokamak technology and physics domains: 100% heat and particle exhaust, fully reliable additional RF power at high level, current profile control, MHD control, possibly in the high performance plasmas. The Tore Supra equipment is progressively evolving in that direction, with first a complete upgrade of the inner vessel components (planned to be installed in year 2000), and second the progressive upgrade of the heating and current drive systems. Scenarios studies (current drive, current profile modifications, long pulse operation, MHD studies, feedback loops, etc.) are also underway. Many encouraging results were already obtained: 2 minute pulses, long fully non inductive discharges, high power shots, high

bootstrap fraction plasmas, magnetic shear reversal discharges, etc. At the same time, the understanding and modeling of the corresponding physics is improved: fast electron diagnostic, edge RF physics, MHD, confinement versus current profile, etc. The integration of all these aspects progressively takes place, allowing a more reliable and safe operation.

REFERENCES

[1] LIPA, M., et al., Proc. Of the 17th IEEE/NPSS Symp. On Fus. Engineering, San Diego, USA, 1997.
[2] Equipe Tore Supra, presented by B. BEAUMONT, Proc. of the 12th Top. Conf. On RF power in plasmas, Savannah, 1997, (AIP, Editors P. Ryan and T. Intrator), p23.
[3] TONON, G. et al., this conference. (IAEA-F1-CN-69/CDP/02)
[4] LADURELLE, L. et al., proc. of the 19th SOFT, LISBOA (PORTUGAL), p593.
[5] PEYSSON Y., GONICHE M. et al, this conference. (IAEA-F1-CN-69/CDP/03)
[6] FUCHS V. et al., Phys. Plasmas 3 (1196) 4023.
[7] RANTAMAKI, K.M., et al., proc. Of the 2nd European Top. Conf. On RF Heating and Current Drive of Fusion Devices, BRUSSELS (BELGIUM) 22A (1998) 173.
[8] BECOULET A., et al, Plas. Phys. Contr. Fusion 40-8A (1998) A157.
[9] Equipe Tore Supra, presented by B. SAOUTIC, Proc. of the 16th IAEA Fusion Energy Conf., Montréal, 1996, volI, 147.
[10] MITTEAU, R. et al, proc. of the 20th SOFT, MARSEILLE (FRANCE), p129.
[11] HOANG, G.T., et al, proc. Of the 24th EPS Conf., 1997, BERSCHTESGADEN (GERMANY), 21A-III, p965.
[12] SAOUTIC, B., et al., Phys. Rev. Lett. 76 (1996) 1647.[13] PEYSSON, Y., et al., proc. Of the 24th EPS Conf., 1997, BERSCHTESGADEN (GERMANY), 21A-I, p229.
[14] HOANG, G.T, et al., Nucl. Fusion, 38 (1998) 117.
[15] KAYE, S.M, ITER CONFINEMENT DATABASE WORKING GROUP, Nuclear Fusion 37 (1997) 1303.
[16] ZABIEGO, M., et al., Proc. of the 7th European Fusion Theory Conference, JULICH, (GERMANY)1997, ed. By A. Rogister.
[17] Equipe Tore Supra (presented by LITAUDON, X.), Plas. Phys. Contr. Fusion, 38-12A (1996) A251.
[18] MONIER-GARBET P., et al., to appear in proc. Of the 25th EPS Conf., 1997, BERSCHTESGADEN (GERMANY).
[19] DOCEUL, L., et al., proc. of the 20th SOFT, MARSEILLE (FRANCE), p117.
[20] Equipe Tore Supra, presented by P. GARIN, proc. of the 20th SOFT, MARSEILLE (FRANCE), p1709.
[21] AGARICI, G., et al., proc. of the 20th SOFT, MARSEILLE (FRANCE), p331.
[22] MONCEL, L., et al., proc. of the 20th SOFT, MARSEILLE (FRANCE), p133.
[23] LADURELLE, L., et al., proc. of the 20th SOFT, MARSEILLE (FRANCE), p287.
[24] BREMOND, S., et al., proc. of the 20th SOFT, MARSEILLE (FRANCE), p343.
[25] BIBET, Ph. et al., proc. of the 20th SOFT, MARSEILLE (FRANCE), p339.
[26] MIRIZZI, F., et al., proc. of the 20th SOFT, MARSEILLE (FRANCE), p465.
[27] PAIN, M., et al., proc. of the 20th SOFT, MARSEILLE (FRANCE), p359.
[28] GIRUZZI, G., et al., EUR-CEA-FC-1619, accepted for publication in Nucl. Fus.

APPENDIX

TORE SUPRA Team

G. Agarici , F. Albajar vinas, J.M. Ane, T. Aniel, G. Antar, J.F. Artaud, A. Azeroual, S. Balme, V. Basiuk, M. Basko, P. Bayetti, B. Beaumont, A. Becoulet, M. Becoulet, V. Bergeaud, G. Berger-By, M. Berroukeche, B. Bertrand, Ph. Bibet, J.M. Bottereau, F. Bottiglioni, C. Bourdelle, R. Bregeon, S. Bremond, R. Brugnetti, J. Bucalossi, Y. Buravand, H. Capes, J.J. Capitain, M. Chantant, Ph. Chappuis, E. Chatelier, M. Chatelier, X. Chen, L. Cherigier, L. Chiarazzo, D. Ciazynski, F. Clairet, L. Colas, J.J. Cordier, L. Courtois, B. Couturier, J.P. Crenn, P. Da silva rosa, C. Darbos, B. de Gentile, C. De Michelis, C. Deck, P. Decool, C. Desgranges, P. Devynck, L. Doceul, H. Dougnac, J.L. Duchateau, T. Dudok de Wit, R. Dumont, A. Durocher, D. Elbeze, F. Escourbiac, J.L. Farjon, Ph. Fazilleau, C. Fenzi, M. Fois, D. Fraboulet, P. Francois, Ph. Froissard, L. Garampon, X. Garbet, L. Gargiulo, P. Garin, E. Gauthier, A. Geraud, F. Gervais, Ph. Ghendrih, T. Gianakon, R. Giannella, C. Gil, G. Giruzzi, P. Gomez, M. Goniche, G. Granata, V. Grandgirard, B. Gravil, M. Gregoire, S. Gregoire, C. Grisolia, A. Grosman, D. Guilhem, B. Guillerminet, R. Guirlet, J. Gunn, Y. He, R. Hemsworth, P. Hennequin, F. Hennion, D. Henry, P. Hertout, W. Hess, M. Hesse, G.T. Hoang, J. Hourtoule, P. Houy, J. How, T. Hutter, F. Imbeaux, C. Jacquot, R. Jimenez, E. Joffrin, J. Johner, J.Y. Journeaux, F. Kazarian, L. Ladurelle, D. Lafon, J. Lasalle, F. Laugier, C. Laviron, G. Leclert, F. Leroux, P. Libeyre, M. Lipa, X. Litaudon, T. Loarer, Ph. Lotte, P. Magaud, P. Maget, R. Magne, J. Mailloux, W. Mandl, G. Martin, A. Martinez, L. Masse, R. Mast, P. Mason, M. Mattel, G. Mangle, F. Minot, J.F. Misguich, R. Mitteau, I. Monakhov, L. Moncel, P. Monier-Garbet, D. Moreau, J.P. Morera, B. Moulin, D. Moulin, M. Moustier, C. Munnier, R. Nakach, F. Nguyen, S. Nicollet, M. Ottaviani, M. Pain, J. Pamela, G. Pastor, M. Paume, A.L. Pecquet, B. Pegourie, Y. Petrov, Y. Peysson, P. Platz, C. Portafaix, M. Prou, R. Pugno, A. Quemeneur, E. Rabaglino, R. Reichle, J.D. Reuss, G. Rey, F. Rochard, A. Romannikov, B. Rothan, R. Sabot, F. Saint-Laurent, F. Samaille, A. Santagiustina, B. Saoutic, T. Schild, J. Schlosser, J.L. Segui, J. Simoncini, A. Simonin, P. Spuig, F. Surle, M. Tena, J.M. Theis, G. Tonon, R. Trainham, J. Travere, A. Truc, E. Tsitrone, B. Turck, J.C. Vallet, D. van Houtte, D. Voslamber, C. Wachter, G. Wang, J. Weisse, M. Zabiego, X.L. Zou, E. Zucchi, K. Zunino

STEADY STATE OPERATION OF THE SUPERCONDUCTING TOKAMAK TRIAM-1M

K. HANADA, S. ITOH, K. SATO, K. NAKAMURA, H. ZUSHI,
M. SAKAMOTO, E. JOTAKI, K. MAKINO
Advanced Fusion Research Center,
Research Institute for Applied Mechanics,
Kyushu University,
Fukuoka, Japan

Abstract

A 2-hour limiter discharge in circular configuration was successfully maintained using both Hall generators to be free from the drift of integrator and position control by TV image to avoid the concentration of heat load. The property of wall saturation is discussed as the serious issue for steady state operation, which strongly depends on electron density. In the high density region, the discharges sometimes terminate due to uncontrollable increase in electron density caused by wall saturation. The plasmas with high k ~1.5 can be demonstrated for longer than 1 min. The duration of discharge is limited by vertical displacement event (VDE). The avoidance of VDE is a crucial point to achieve long discharges with high k. New technique to monitor the accurate magnetic field with high time resolution for a long time is required to achieve the longer discharge with high k. A high ion temperature (HIT) discharge characterized by high ion temperature up to 5keV and by steep temperature gradient up to 85 keV/m is successfully sustained for longer than 30 sec by 2.45 GHz LHCD on single null divertor configuration. This indicates that the transport barrier of ion temperature can be maintained in steady state.

1. Introduction

The steady state operation and the achievement of high performance plasma are most important issues for tokamak fusion reactor. In these years, various improved confinement modes have been found in many devices [1-4]. As for steady state operation of tokamak discharges, although in Tore Supra, the high pressure plasma could be sustained for 2 minutes [5], the steady state discharge over 1 hour have been proceeded only in the superconducting (SC) machine TRIAM-1M [6]. The long sustainment of high pressure plasma of $\overline{n_e}$ ~1.5 × m^{-3} is also demonstrated for 1 min [6]. In this case, the abrupt uncontrollable increase in n_e sometimes occurs, which is caused by wall saturation.

The plasma shape with the high elongation, k, and the high triangularity, d, is important factor for the achievement of high performance, because the limitation of the MHD stability in the pressure gradient becomes better. However, the sustainment of high k discharge had been tried in many machine, vertical displacement event (VDE) prevents from achieving the long discharge with high k. In JET, a 1-min discharge with k~1.4 can be obtained in limiter configuration. In TRIAM-1M, the plasmas with high k ~1.5 can be demonstrated for longer than 1 min in the single null divertor configuration.

Recent progresses of high performance are supported by the transport barrier in the core and edge region [1-4]. The sustainment of the transport barrier is a key issue for the steady state high performance operation of tokamak, however the long sustainment of transport barrier is difficult, because the instability based on the high pressure gradient is excited near the transport barrier. Moreover, as the high temperature leads to long current diffusion time, the duration of plasma is not sufficient for steady state condition. Recently the steady state high performance plasma with transport barrier is also achieved on TRIAM-1M.

In this paper, a brief survey of developments to achieve the 2-hour discharge is described at first and subsequently the issues for steady state operation of tokamak are pointed out. After that, the recent progresses concerning steady state high performance plasma are described.

2. Experiments of Super Ultra Long Discharge (Suld)

2.1. Developments and issues for steady state operation

TRIAM-1M is the high-field superconducting tokamak with 16 toroidal field coils made of Nb_3Sn (R = 0.8m, a × b = 0.12m × 0.18m) [7], which can produce the steady state strong magnetic field continuously. The maximum field reaches 11 T at windings and 8 T at the plasma center. Two heating sources are installed for current drive. One is a 2.45 GHz LHCD system (1 klystron of the maximum power; 50kW, 4×1 grill) and the other is an 8.2 GHz LHCD system (8 klystrons, the total maximum power, 200 kW, 8×2 grill). The vacuum vessel is made of SS304L and the three poloidal limiters are made of Mo. The ECR discharge cleaning is carried out for wall conditioning of the plasma chamber before every experimental campaign.

In 1995, the long pulse tokamak plasma for longer than 2 hour was achieved in limiter configuration [6], based on the essential developments as the following; 1) construction of superconducting (SC) magnets made of Nb_3Sn, 2) stable operation of tokamak with SC magnet, 3) continuous wave (CW) microwave system for non-inductive current drive, 4) the plasma production by flux swing generated by the decrease in the center solenoid coil current, 5) magnetic measurement using Hall generator, 6) position control using TV image, 7) fueling control using Ha signal, and 8) data acquisition system for long operation. The progresses of steady state operation on TRIAM-1M are summarized in Fig. 1.

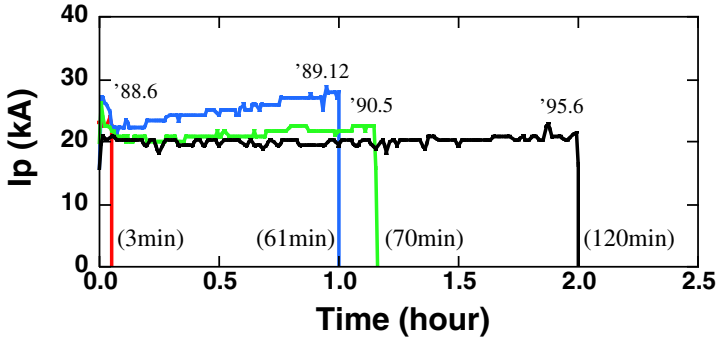

FIG.1. Progresses of steady state operation using 2.45GHz LHCD on TRIAM-1M. The main parameters are similar in all of the discharges in this Figure, I_p~20kA, $\overline{n_e}$ ~1.5x10^{18}m^{-3}, T_e~0.6keV, T_i~0.5keV, B_t=6T, P_{RF}~20kW.

As for the magnetic measurement, the conventional method, that is the combination of magnetic coils with integrators, is not reliable for long discharge, because of the accumulated drift of the integrators. To solve the drift problem, Hall generators are adopted to monitor the plasma position. The Hall generators can measure the local magnetic field directly, therefore they are free from the problem of the drift of integrators. However, the time response of the Hall generators is not so high for the fast change in the magnetic field as observed in the break-down and current ramp up phases. Therefore, the plasma position was controlled with the conventional magnetic coil system at the initial phase of the discharge, and the Hall generator system was used in the subsequent phase.

The heat load sometimes concentrates on a certain point of a poloidal limiter, where it becomes bright (hot spot). The hot spot is the source of impurity, and the performance of the plasma was sometimes deteriorated. The position control using the TV image of the plasma cross section and the poloidal limiter is used to avoid the appearance of the hot spot. When the hot spot appears, the bright point on the limiter is caught by the TV image and the

automatic control system makes the plasma moved in the suitable direction to eliminate the hot spot.

The fueling control using Ha signal is carried out for taking the hydrogen recycling property into consideration. Temperature of wall and hydrogen recycling property changes gradually during the discharge as well as shot by shot. Moreover the amount of the fuel adsorbed on the wall varies, because it depends mainly both on the previous shots and on the present shot. Therefore, the fueling control must be adapted itself to adjust the change in the wall condition. In order to cope with it, the fueling control system has been improved by the feedback control using the Ha signal. The intensity of Ha line corresponds to the influx of the fuel to the core plasma. As the influx of the fuel is proportional to the electron density in steady state operation regime, the fueling control using the Ha intensity is also sensitive to electron density.

As for the data acquisition system, the continuous monitoring and data acquisition system, which is called "cyclic processing", was also developed [8]. On this new system, multiple lines of data processing are running simultaneously and each line of processing is switched in the regular interval. This system has been successfully applied to 2-hour discharge. Moreover event trigger method was also established to acquire the data with a high time resolution around some interesting events during long duration discharges [9]. In the case of long time or steady state operation, it is important to monitor and control the plasma condition continuously during the discharge. However, conventional systems cannot follow these operation as it shows the results after each discharge. Moreover the memory prepared in a CAMAC module is not sufficient, therefore it is impossible to store the data with high time resolution for the whole of a long discharge. These issues become more serious with the increasing of the discharge duration time.

2.2. Wall property during long-time discharge

The heat load of the 2-hour discharge on TRIAM-1M to the limiter (more than 1GJ/m^2) is compared to that to the divertor plate of ITER. This huge heat load generates the hot spot and intense sputtering on the limiter, which sometimes make the plasma performance deteriorated. This circumstances concerning heat load are suitable to investigate the plasma wall interaction.

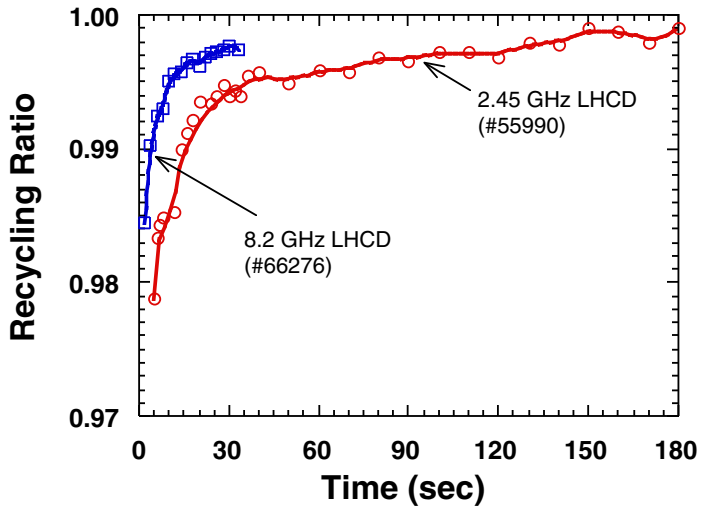

FIG. 2. Time evolutions of the recycling ratio of the low density discharge ($\overline{n_e}$ ~ 0.2 × 10^{19}m^{-3}, I_p ~ 21kA, B_t = 6T) sustained by the 2.45GHz LHCD with ~20kW (open circles) and the high density discharge ($\overline{n_e}$ ~1 × 10^{19}m^{-3}, I_p~23kA, B_t = 7T) sustained by the 8.2GHz LHCD with ~100kW (open squares).

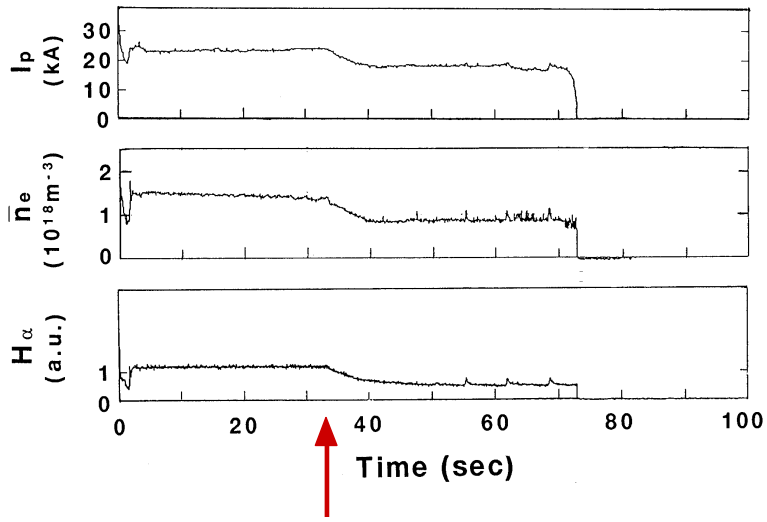

FIG.3 Time evolutions of plasma current, electron density and intensity of Ha. The arrow of the Figure shows the timing of termination of both pumping and fueling. It should be noted that the particles can be balanced well under the condition that the recycling ratio is completely unity for longer than 30 s.

The plasma was maintained in the limiter configuration by the microwave of 2.45 GHz, 20kW and the plasma current (~20kA) was driven by the energetic electrons drifting in the toroidal direction. In the limiter configuration, heat load by the plasma sometimes concentrates on the poloidal limiter. The many plasma parameters, for example density, plasma current, temperature, and so on, are kept constant. The impurities estimated by the vacuum ultra violet (VUV) become constant (O ~2%, Mo ~0.2%) [10] and they do not change significantly during discharge [11]. This is a preferable phenomenon for the steady state operation, because the contamination and concentration of impurity in the core plasma prevent from maintaining the plasma. These plasma parameters become constant in early time of the discharge, because characteristics time scale depends on the energy confinement time, t_E (~ a few ms) and current diffusion time, $t_{L/R}$ (~200ms). The recycling ratio, which significantly affects the performance of plasma, gradually increases and then reaches about unity as shown in Fig.2. It takes longer than 30 s to become constant. This characteristic time scale is one of the longest time scale required to become steady state. This shows that the duration of longer than 30 sec is necessary to obtain the steady state condition in the view of the performance of the plasma.

Steady-state operation in high density region ($\overline{n_e}$ is more than 1×10^{19} m^{-3}) has been executed. The 8.2 GHz LHCD is utilized for the sustainment of the plasma current. The line-averaged electron density reaches up to ~2×10^{19} m^{-3} and the duration of the discharge in the high density region exceeds 1 min. The termination of the discharge may be mainly caused by the wall saturation, that is the recycling ratio is excess of unity. The electron density abruptly increases without the gas feed in the end of discharge. The density control does not work well just before the termination of the discharge. The recycling ratio of high density discharge increases gradually and it approaches to unity as shown in Fig.2. It takes about 30 s to become constant in both low and high density plasma.

In the low density discharge, the recycling ratio is also close to unity after 30 s from the start of the discharge, although the absolute value of recycling ratio is slightly lower than that of high density discharge. However, the wall saturation phenomena does not take place [12]. A typical example can be shown in Fig. 3. The pumping and fueling stops at the timing of the arrow. The neutral pressure monitored by an ion gage after the stop of pumping and fueling increases up to two times and subsequently its value keeps constant. This shows that the outflux and influx of fuel particles are balanced and the recycling ratio is completely unity for 30 s. This clearly shows that the wall saturation can be avoided in low density region. From this experimental data, the abrupt wall saturation may be caused by the large outflux of the particles, because outflux of the high density

plasma (~ 2×10^{20} particles/s) is about 4 times in magnitude larger than that of the low density plasma. The wall saturation may become a crucial issue for steady state operation in the high density region.

The most important and difficult problem during steady state discharge is the control of the wall condition, because temperature of the wall and the limiter increases and consequently the wall condition gradually changes during the discharge. In the 2-hour discharge, the time evolutions of the temperature of the wall and the limiter are shown in Fig. 4. The characteristic time scale is about 30 minutes. In order to investigate the performance of the steady state plasma, 1-hour discharge is necessary from the viewpoint of the wall condition.

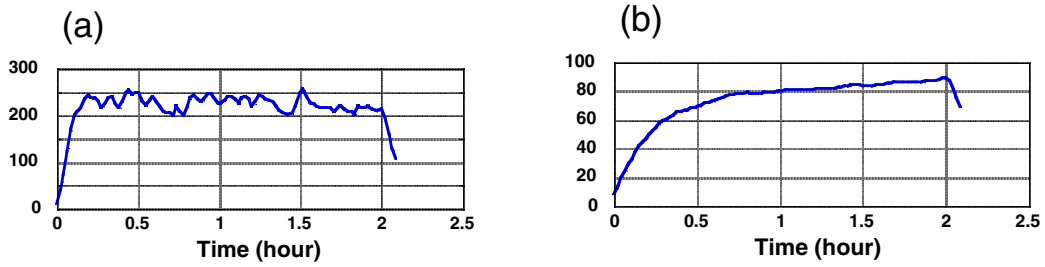

FIG. 4. Time evolutions of the temperature of (a) the limiter and (b) the wall in the case of the 2-hour discharges.

2.3. Long sustainment of high k discharge

Establishment of technique to maintain long single-null configuration with high elongation, k, has been desired for the future reactor both to remove the huge heat load and to improve the plasma performance. Figure 5 shows the summary of the achieved k plotted as a function of discharge duration in various tokamaks in the world. This figure clearly shows the difficulty of the long duration discharge with high k. Generally speaking, main reasons of the difficulty are vertical displacement event (VDE) and power handling on the divertor plate. Although discharge in circular limiter configuration was successfully maintained for longer than 2 hours using Hall generators without drift problem of integrator, VDE cannot be avoided in the single null configuration because of the slow time response of Hall generators. Vertical position control system was improved to aim at the long duration sustainment of the single null divertor configuration by LHCD and the control as fast as the skin time of the vacuum wall was tried. Although the present duration time is limited by both V^2t value of the power supply for vertical position control and the drift of the integrator, where V and t show the voltage and the duration of power supply and the value of V^2t corresponds to the calorific power of the power supply, the single null configuration with k ~1.5 for 1min by 2.45 GHz LHCD only; P_{RF} = 22 kW, B_t = 6 T, n_e = 2 x 10^{18} m^{-3}, T_e = 600 eV, I_p = 23 kA was successfully achieved. This result indicates that the steady state discharge of high k in the single null configuration is possible by developing quick-responsible and long-time-measurable magnetic sensor.

The total energy input of 200 MJ has been injected into the plasma in the limiter configuration, although the heat flux (~1MW/m^2) on the limiter is not so much. In the high density discharge, the heat flux on the limiter reaches ~5MW/m^2, if all input power is put in the limiter. The hot spot and the intense sputtering sometimes appears during the long discharge due to the huge heat load. While, the hot spot and the intense sputtering does not occur in the single null configuration. This shows the better power handling in the single null configuration can be achieved than that in the limiter configuration. The input energy to the divertor plate has been measured with the temperature rise of the cooling water of the divertor plate. At first, the plasma is produced in limiter configuration. Subsequently, the plasma configuration is drastically changed to the single null configuration by the change in the coil current. After the formation of single null configuration, the thermal input to the

divertor plate increases linearly with the discharge duration. From this slope, the input power is estimated to be 10 kW, which is about 30 % of the energy lost from the plasma. This result indicates that a part of the input energy flows to the divertor plate instead of the limiter, and consequently the hot spot is difficult to be formed.

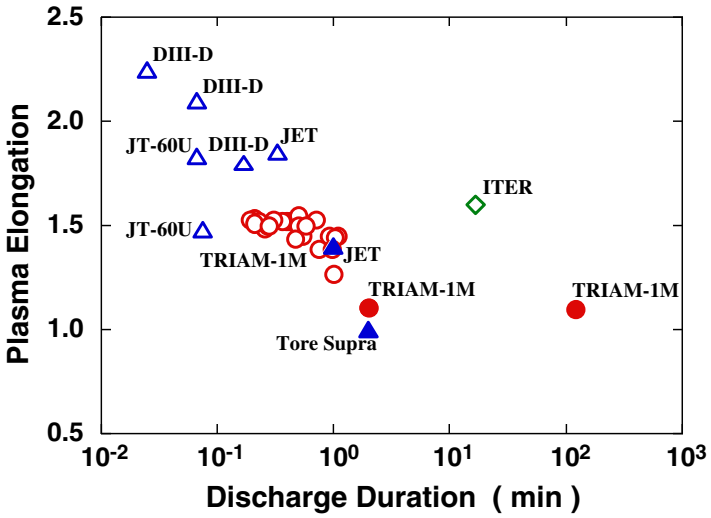

FIG. 5. Plasma elongation, k, as a function of the discharge duration in various tokamaks. The data on the single null configuration in TRIAM-1M (open circles) and in other tokamak (open triangles), on the limiter configuration in TRIAM-1M (close circles) and in other tokamak (close triangles) are plotted in the figure.

3. Achievement of high performance plasma and its long sustainment

3.1. Characteristics of high ion temperature (HIT) discharges

Recently a long duration discharge with the HIT mode has been obtained using 2.45GHz LHCD on both the limiter and the single null configuration. The ion temperatures $T_{i//}$ and T_i have been measured with two kinds of neutral particle analyzer (NEA), NEAP (q~90) and NEAT(~ 36) respectively, here q is the angle between the line of sight and toroidal direction. The HIT mode is obtained under the following conditions; 1.4×10^{18} m^{-3} $\overline{n_e}$ 2.0×10^{18} m^{-3} and -2.5cm DR(=R-R_0) -0.5cm in the limiter configuration, where R means the horizontal plasma position. However, as the horizontal position of the plasma must be controlled tightly in the single null configuration, and the position can not be scanned. The density window is the similar both in the limiter and single null configurations. The HIT mode has been successfully maintained for 1 min by accurate control of DR and n_e as shown in Fig.6.

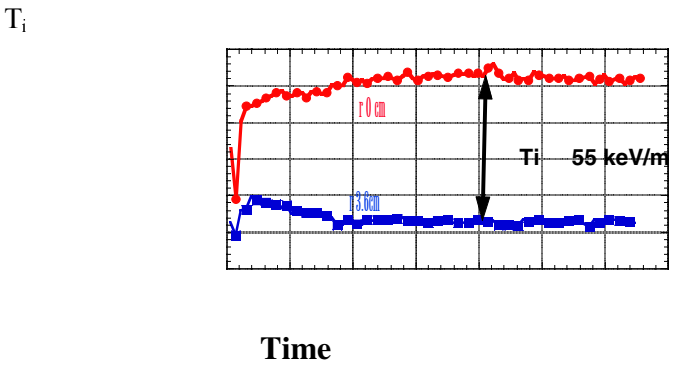

FIG. 6. Time evolutions of T_i at r~0cm (closed circles) and r ~ 3.6cm (closed squares) in long sustained HIT discharge.

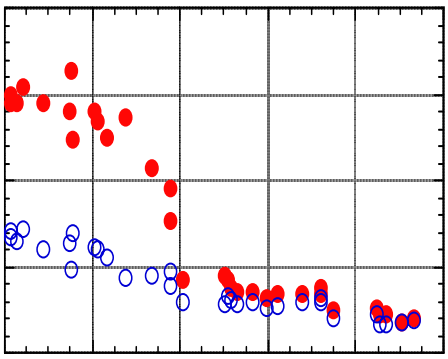

FIG. 7. Radial Profiles of T_i at r ~ 0cm in the HIT mode (closed circles) and the LIT mode (open circles).

The HIT mode is characterized by the steep temperature gradient formed around half of the minor radius as shown in Fig. 7. This suggests that a transport barrier is formed in the middle of the plasma. A transition from low ion temperature (LIT) to HIT sometimes takes place in the fast time scale (10ms). At the transition, T_i measured with NEAP sometimes changes faster than $T_{i//}$ measured with NEAT. This indicates that ions heat in the perpendicular direction and after that T_i becomes almost isotropic via pitch angle scattering process. The energetic ions with small $v_{//}$ are well confined at least during the estimated value of pitch angle scattering time (~8 ms for q = 36).

3.2. Discussion for HIT discharge

These experimental results indicate that 1) effective ion heating takes place in the pure LHCD plasma, 2) energetic ions are confined well by the weak poloidal field. In HIT region, ion heating does not occur by direct heating via linear mode conversion process of LHW. Moreover the power via the slowing down process almost flows from energetic electrons to bulk electrons. Mechanism of ion heating may be that the wave excited by the energetic electrons accelerated by LHW interacts with ions. In low density region of TRIAM-1M, the accessibility condition of LHW is significantly better than the other machine. The LHW of $N_{//}$ of 1.05 is accessible in the center of the plasma. In this situation, the energetic electrons may be produced in the core region. The HXR profile is sometimes peaked in HIT discharge, and this may support it.

The electromagnetic (EM) wave emitted from the plasma are detected by a horn antenna through a quartz vacuum window. Main part of the EM wave corresponds to the wave with the frequency of the 2.45 GHz. This is clearly originated from the injected microwave of 2.45 GHz LHW. The EM wave at the frequency of 2.450.4 GHz is sometimes observed. This sideband wave is coming from the scattering process of the waves of 2.45 GHz and 0.4 GHz, therefore, the signal of sideband wave shows that the wave with the frequency of 0.4 GHz exists in the plasma. It should be noted that the frequency of 0.4 GHz corresponds to ion plasma frequency at the core region of plasma. This wave of 0.4 GHz may have a relation to the ion heating, because the time evolution of the power of the EM wave correlates with that of the ion temperature as shown in Fig. 8. Around 6 s, T_i is clearly higher than T_e and ion heating takes place. At that time, the amplitude of the EM wave of the sideband increases and the abrupt decrease in both T_i and amplitude of EM wave occurs at 7.5 s.

As for the confinement of energetic ions, decay of energetic ions are investigated after the termination of LHW. Although the plasma current gradually decreases with the current diffusion time

(~200ms) after the termination of LHW, the decay time of energetic ions (~10keV) is about 20 ms, which is significantly longer than loss time of energetic ions due to toroidal drift (~10 ms). This clearly shows that the energetic ions are well-confined. This is a significant difference from ion heating scenario based on the linear mode conversion or the parametric decay wave. Although the mechanism of well-confinement is not made clear, the appropriate negative radial electric field shear may work effectively on the confinement of the energetic ions by weak poloidal field.

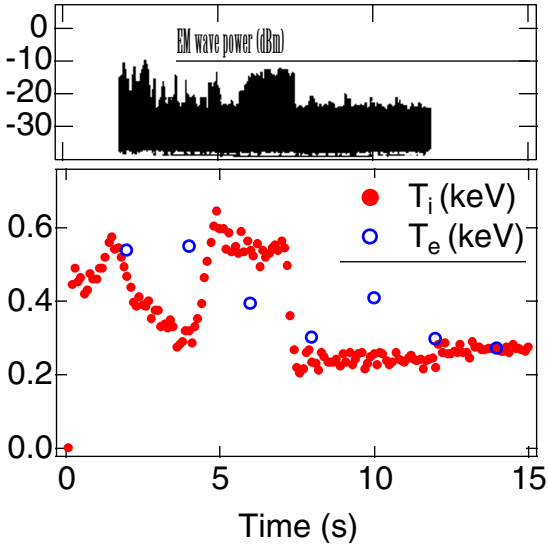

FIG. 8. Top figure shows the time evolution of the amplitude of EM wave at the frequency 2.45 GHz - 0.4 GHz measured with a spectrum analyzer. The amplitude of pump wave (2.45 GHz) is about 30 dBm. Bottom figure shows the time evolution of T_i at the plasma center.

The maximum values of T_i and T_i seem to be limited in the HIT discharge as shown in Fig. 9, although the maintenance of the HIT mode does not depend on duration of the discharge. The maximum value of T_i reaches up to 85 keV/m, which is comparable to T_i in the internal transport barrier on the large tokamaks. As the MHD instabilities are not observed just before the transition from HIT to LIT, the direct cause of the termination of the HIT mode is not made clear.

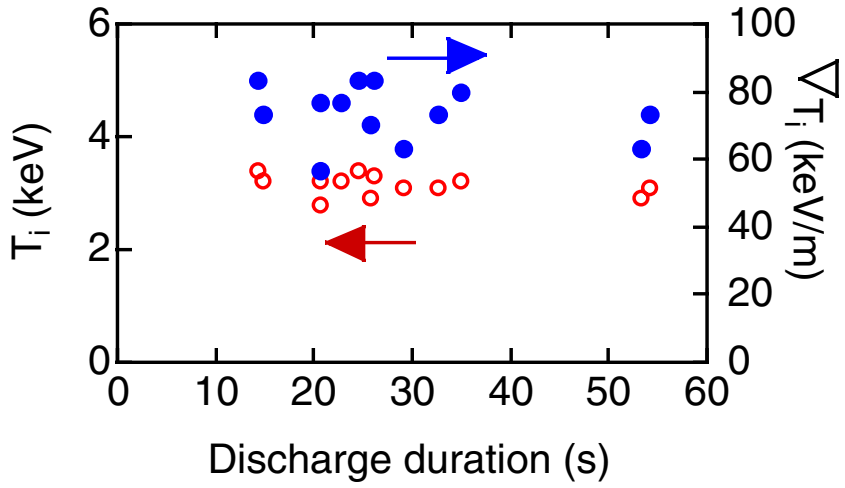

FIG. 9 The values of T_i (open circles) and T_i (solid circles) just before the transition from HIT to LIT as the function of the discharge duration.

As a part of input energy flows to the divertor plate, the heat load to limiter is reduced and consequently the hot spot and intense sputtering is difficult to take place on the single null configuration, compared with the limiter one. The improved thermal insulation between the wall and the plasma on single null configuration brings to higher performance plasma as shown in Fig. 10. The maximum ion temperature reaches at more than 5 keV.

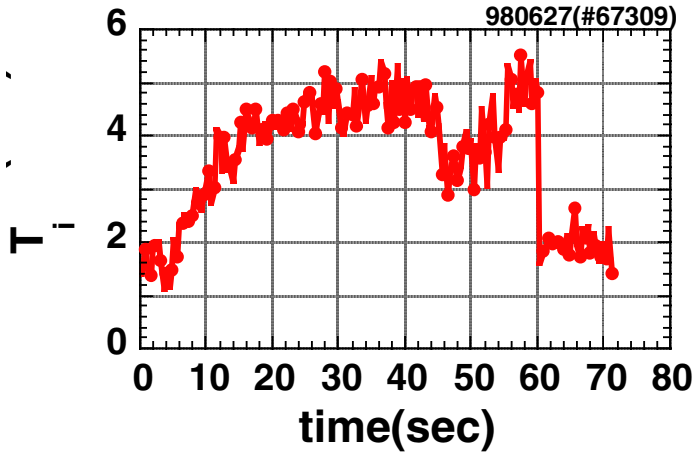

FIG. 10. Time evolution of T_i (keV). The configuration is changed gradually from 4 s to 6s and at 6 s, the single null configuration is formed completely.

4. Summary

Wall saturation and difficulty of avoidance of VDE in long tokamak discharges are pointed out as the main issues for approach to steady state fusion reactor through the experience of the achievement of super ultra long discharge (SULD).

High performance plasmas with high ion temperature up to 5keV and steep temperature gradient up to 85 keV/m can be sustained for longer than 30 sec by 2.45 GHz LHCD on single null divertor configuration. A candidate of the mechanism for ion heating and well-confinement is proposed. Energetic electrons may play an essential role in HIT discharge.

REFERENCES

[1] KOIDE, Y., et al., Phys. Plasmas 4, (1997) 1623.
[2] SOLDNER, F.X., et al., Plasma Phys. Control. Fusion 39, (1997) B353.
[3] LEVINTON, F.M., et al., Phys. Rev. Lett. 75, (1995) 4417.
[4] RICE, B.W., Phys. Plasmas 3, (1996) 1983.
[5] Equipe Tore Supra, in Fusion Energy 1996 (Proc. 16th Int. Conference on Fusion Energy., Montreal, 1996), Vol. 1, IAEA, Vienna (1997) 141.
[6] ITOH, S., et al., in Fusion Energy 1996 (Proc. 16th Int. Conference on Fusion Energy, Montreal, 1996), Vol. 3, IAEA, Vienna (1997) 351.
[7] ITOH, S., et al., in Plasma Physics and Controlled Nuclear Fusion Research 1986 (Proc. 11th Int. Conf., Kyoto, 1986), Vol. 3, IAEA, Vienna (1987) 321.
[8] JOTAKI, E and ITOH, S., Fusion Technology, 27 (1995) 171.
[9] JOTAKI, E and ITOH, S., Fusion Technology, 32 (1997) 487.
[10] NAGAO, A., et al., Jpn. J. Appl. Phys., 28 (1989) 1479.
[11] ITOH, S., et al., in Plasma Physics and Controlled Nuclear Fusion Research 1990 (Proc. 13th Int. Conf., Washington DC, 1990), Vol. 1, IAEA, Vienna (1991) 733.
[12] SAKAMOTO, M., et al. Proc. 24th Int. Europe. Conf. on Controlled Fusion and Plasma Physics, (Berchtesgarden), Vol. 21A, PartII (1997) 721.

SUPERCONDUCTING MAGNETS AND CRYOGENICS FOR THE STEADY STATE SUPERCONDUCTING TOKAMAK SST-1

Y.C. SAXENA, SST-1 TEAM
Institute for Plasma Research,
Bhat, Gandhinagar, India

Abstract

SST-1 is a steady state superconducting tokamak for studying the physics of the plasma processes in tokamak under steady state conditions and to learn technologies related to the steady state operation of the tokamak. SST-1 will have superconducting magnets made from NbTi based conductors operating at 4.5 K temperature. The design of the superconducting magnets and the cryogenic system of SST-1 tokamak are described.

1. Introduction

A steady state superconducting tokamak SST-1 is being designed at the Institute for Plasma Research, with the objectives of studying the physics of the plasma processes in tokamak under steady state conditions and to learn technologies related to the steady state operation of the tokamak. These studies are expected to contribute to the tokamak physics database for very long pulse operations. SST-1 [1] is a large aspect ratio tokamak, configured to run double null diverted plasmas with significant elongation (κ) and triangularity (δ). Superconducting magnets will be used for both the toroidal field (TF) and the poloidal field (PF) coils of SST-1. These coils will operate at 4.5 K. In the following we give a brief description of SST-1 tokamak and discuss the design of the superconducting (SC) coils followed by the description of cryogenic system requirements for these coils.

2. SST-1 Machine

The SST-1 tokamak comprises of superconducting TF coils, a UHV compatible vacuum vessel in the bore of the TF coils and having plasma facing components inside, the superconducting PF coils placed around the TF coils, the support structure for the PF and TF coils, the cryostat enclosing the TF, the PF coils and the vacuum vessel. A liquid nitrogen cooled radiation shield is provided between the SC coils and the vacuum vessel, as well as between the cryostat and the SC coils. A resistive Ohmic transformer system is provided to initiate the plasma and sustain the current for initial period. The overall support system of the machine is derived from 8 pillars grouted to the ground and a central support having four pillars. The vacuum vessel is supported on the cryostat while the TF and PF coils are supported on a cold mass support that transfers the load to the main machine support. Other subsystems include RF systems for pre-ionization, auxiliary current drive and heating, neutral beam injection (NBI) system for supplementary heating, cryogenic systems at LHe and LN_2 temperatures, chilled water system for heat removal from various subsystems. A 3-d view of the SST-1 tokamak is shown in Figure 1. The machine has a major radius of 1.1 m, minor radius of 0.20 m, a toroidal field of 3.0 T at plasma center and a plasma current of 220 kA. Elongated plasma with elongation in the range of 1.7 to 1.9 and triangularity in the range of 0.4 to 0.7 can be produced. Hydrogen gas will be used and plasma discharge duration will be 1000 s. Auxiliary current drive will be based on 1.0 MW of Lower Hybrid current drive (LHCD) at 3.7 GHz. Auxiliary heating systems include 1 MW of Ion Cyclotron Resonance Heating (ICRH) at 22 MHz to 91 MHz, 0.2 MW of Electron Cyclotron Resonance heating (ECRH) at 84 GHz and a Neutral Beam Injection (NBI) with peak power of 0.8 MW with variable beam energy in range of 10-80 keV. A large number of diagnostics for plasma and machine monitoring will be deployed along with a distributed data acquisition and control system. The power for operating various subsystems will be derived from 132 kV grid. A cross-section of SST-1 is shown in Figure 1. In the following the magnet system and cryogenic system for SST-1 tokamak are described in detail.

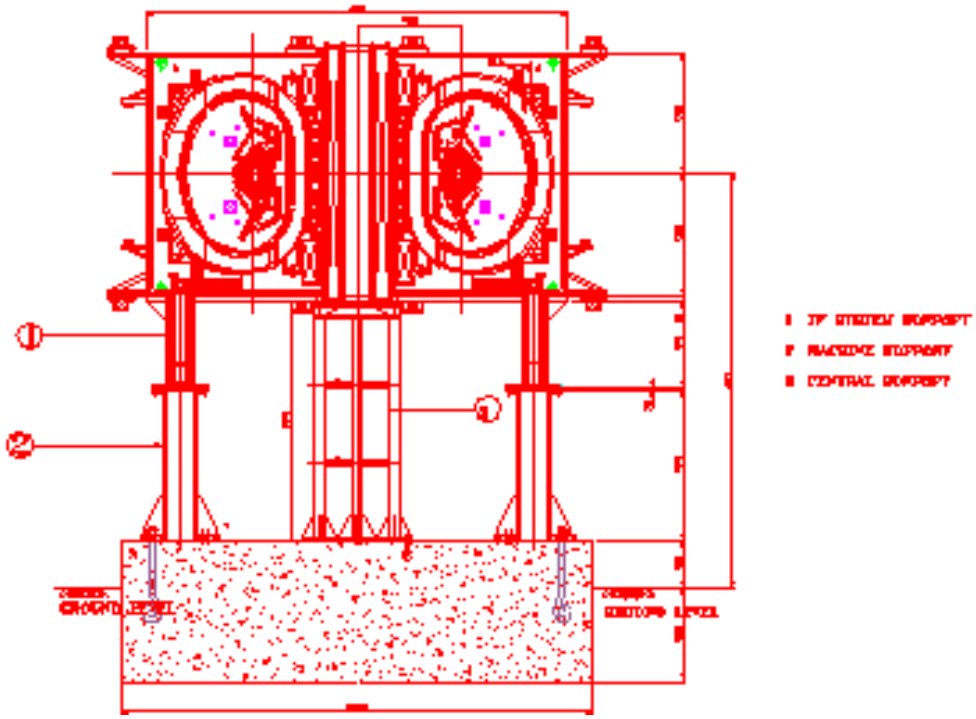

FIG. 1: A cross-section of SST-1 Tokamak.

3. Magnet system

The magnet system comprises of TF system, PF system, Ohmic and vertical field coils, & vertical position control coils.

3.1. Toroidal field system

The TF system design requirements include the production of 3.0 T magnetic field at plasma axis with ripple < 2% within plasma volume. The TF assembly should be capable of providing steady state operation and should withstand the plasma disruptions and vertical displacement events (VDE) without quenching. The assembly shall be capable of being cooled down and warmed up in less than 15 days.

The TF system consists of 16 numbers of modified D shaped TF coils arranged symmetrically around the major axis spaced 22.5° apart. Each of the TF coils will be made up of six double pancakes, each pancake having nine turns. There are 108 turns in each of the coils. A total of 17.28 MAT at a peak current of 10 kA per turn will produce a field of 3.0 T at plasma center and a maximum field of 5.1 T at the TF conductor. The winding pack of 6 double pancakes will be shrunk fitted into a stainless steel (SS316L) casing which supports most of the electromagnetic loads. The contour of D-shaped TF coil consists of a straight leg and 5 arcs. The overall dimensions of the TF coils are dictated by the need to have ≤ 2% field ripple at plasma edge, large enough radial ports on the vacuum vessel so as to allow radial access for NBI, human access inside the vacuum vessel for assembly of in-vessel components.

All coils are connected in series and are protected against the quench by suitable dump resistance, switching and sensing system. The main parameters of TF coils are summarized in Table I.

3.2. The poloidal field system

The SST-1 PF system [2] comprises of nine superconducting coils and two resistive coils. These coils allow for a wide range of elongation and triangularity and support a large range of plasma equilibria.

TABLE I. TOROIDAL FIELD SYSTEM

Number of Coils	16
Shape	Modified D
Turn per Coil	108
Double Pancakes per Coil	6
Rated current	10 kA
Field at Plasma axis	3.0 T
Maximum Field	5.1 T
Maximum Field Ripple	< 0.35%
Bore Dimensions (Radial)	1190 mm
Bore Dimensions (Vertical)	1746 mm
Outer Dimensions (Radial)	1560 mm
Outer Dimensions (Vertical)	2120 mm
Average turn length	5500 mm
Weight of One Coil with casing	1100 Kg
Total weight of TF system	1920 Kg
Centering force per coil	2.73 MN
Tension in the coil	90 – 110 MPa
Total inductance	1.12 H
Total stored energy	56 MJ
Dump time constant	12 s
Peak dump voltage	± 600 V

Feasibility of limiter operation during plasma current ramp-up, double and single null operation at plasma current of 220 kA, double null operation at plasma current of 330 kA and various start-up scenario are the design drivers for PF system. A free boundary, axisymmetric, ideal MHD equilibrium model based code has been used for designing and optimizing the PF system. Table II summarizes the characteristics of the PF coils. The designed PF system allows flexibility in elongation of the plasma in range of 1.7-1.9, triangularity in range of 0.4-0.7, plasma inductance in range of 0.75-1.4, poloidal β in range of 0.01-0.85 and slot divertor configuration.

TABLE II. POLOIDAL FIELD COILS

Coil type	Number of coils	Coil Radius (m)	Vertical Location (m)	Winding Cross-section (mm^2)	Number of turns
PF1	1	0.45	0.0	71x320	80
PF2	2	0.45	±0.43	71x163	40
PF3	2	0.50	±0.93	136x380	192
PF4	2	1.72	±1.03	85x136	40
PF5	2	2.01	±0.65	85x136	40
PF6	2	1.35	±0.35	100x100	16

3.3. Conductor for superconducting coils

All superconducting coils will be made using a cable-in-conduit conductor (CICC) based on NbTi+Copper. The choice of the NbTi is based on the fact that the operating fields in TF and PF coils are moderate. The CICC will be made up of 135 strands cabled in a 3x3x3x5 cabling pattern and conduited inside a SS304L conduit. The characteristics of the CICC are summarized in table III. The CICC is designed for an operational current of 10 kA at 5 T and 4.5 K with a critical current of 36 kA. The nominal critical current for each strand at 5T and 4.5K is 272 A.

The CICC design has been carried out by Institute for Plasma Research in consultation with National High Magnetic Field Laboratory, Florida State University, Tallahassee, USA. In the design and optimization of the CICC various operational constraints have been met. The optimum design was finalized in March 1997 and M/S Hitachi Cables Ltd. were awarded the contract for manufacturing of the cable. Results on pre-qualification trials on virgin strands and strands extracted from sample CICC are summarized in table IV. The tests carried out include critical current measurements at 5T and 4.2K, determination of superconductor to normal state transition index 'n' & RRR, measurement of hysteresis losses, Cu to Sc ratio, sharp bend tests and spring back tests. One strand each from the first stage triplets were taken for the test on extracted strands. Void fraction and conduit thickness measurements were carried out on CICC. The results indicate that degradation in strands due to cabling and jacketing is less than 5% and critical current ≥35 kA at 5T, 4.2K is ensured. A 600m test piece has been fabricated and detailed tests on model coil fabricated from the test piece are in progress at Kurchatov Institute, Moscow. Preliminary results indicate that CICC is able to carry ≥40 kA current at 1.5 T, 4.5k without quenching.

3.4. Support system for superconducting magnets [3]

The straight legs of TF coils are wedged to form the inner vault. The outer vault is formed by connecting inter coil structures between the TF coils. These vaults resist the centering force and overturning torque experienced by the TF system. There is insulation break between each of the TF coils.

TABLE III. CHARACTERISTICS OF CICC

SC material	NbTi + Copper
Filament diameter	≅10 μm
Strand Diameter	0.86 mm
# of filaments per strand	≅1272
Cabling pattern	3×3×3×5
Copper area per strand	≥ 0.482 mm^2
Copper RRR	≥100
CICC Dimensions	14.8 x 14.8 mm^2
Conduit Material	SS304L
Conduit thickness	1.5 mm
Copper Cross-section A_{cu}	0.6769 cm^2
Superconductor Cross-section A_{sc}	0.1386 cm^2
Helium Cross-section A_{He}	0.5484 cm^2
Conductor Cross-section A_{cs}	1.40 cm^2
Void fraction	≥ 36%
Hydraulic diameter	≅0.62 mm
Hysteresis losses	< 100 mJ cm^{-3}

TABLE IV. RESULTS OF CONDUCTOR PRE-QUALIFICATION TESTS

Parameter	Virgin strands	Extracted strands
I_c @ 5T, 4.2K	273 A	262 A
'n' at 5T	46	45
Hysteresis loss (mJ/cm^3)	36.5	32.7
RRR of Cu	108	92
Cu: Sc Ratio	4.98	4.98
Filament breakage %	0	0

The superconducting PF coils are supported on the TF coils' casings and the inter-coil structures, with the coils and structures forming a rigid cold mass of about 30 tons at 4.5 K. The TF coils are further supported on a base support system consisting of a ring with 16 cantilevered beams. The ring rests on eight columns that are inside the cryostat and have liquid nitrogen intercepts to minimize the conduction loss at 4.5 K as the cold mass load is transferred from these columns to main machine support. The main machine support comprises of 16 columns, supporting the base frame of the cryostat and the cold mass, which are firmly grouted to ground.

3.5. Ohmic transformer, vertical field coils and control coils

The SC PF coils cannot be ramped at a very fast rate required for plasma breakdown and initial current rampup. An Ohmic transformer [4], comprising of a central solenoid and two pairs of compensation coils, and made from hollow copper conductor, will, therefore, be used for this purpose in a pulsed mode. The transformer has a storage capacity of 1.4 Vs and can be used for producing circular plasma with current up to 100 kA for almost one second. A pair of vertical field coils will keep this circular plasma in equilibrium during the initial phase till the current drive is taken over by the LHCD and the PF coils are ramped up at slow rate to provide the divertor configuration for elongated triangular plasma. The PF coils' currents will be ramped up to their respective current values in about 2-3 s in pre-programmed way so as to achieve the desired plasma equilibrium.

Passive stabilizer plates are provided inside the vacuum vessel to slow down the vertical instability and a pair of control coils is provided inside the vacuum vessel for active control of plasma position. The coils are made of copper conductor.

3.6. Present status of the superconducting magnets

The engineering design of the SST-1 superconducting magnets has been completed. The cable-in-conduit-conductors for the TF and PF magnets are also presently being manufactured. A 600m long test piece is being used for full scale testing of CICC in form of a model solenoid. Efforts on identifying a suitable vendor from amongst Indian industry for manufacturing the magnets are on. The actual winding activities are expected to begin by mid 1999.

4. Cryogenic system for SST-1

The superconducting magnet system (SCMS), consisting of TF and PF coils, in SST-1 has to be maintained at 4.5 K in presence of steady state heat loads. In addition the pulsed heat loads during the plasma operation have to be taken care of by the cooling system so as to maintain the magnets in superconducting state. The magnets will be cooled using forced flow of supercritical helium (SHe) through the void space in the CICC. Further the magnets have to be energized from power supplies at room temperature using vapor cooled current leads, which evaporate liquid He at cold end to gas He at $\cong$ 300 K at the warm end of the lead. A Helium refrigerator/liquifier with cold circulation system for SHe is, therefore, required for this purpose. In order to minimize the heat loads on magnets and support system at 4.5 K, liquid nitrogen (LN_2) shields are provided between the cold mass at 4.5 K and warmer surfaces, e.g. vacuum vessel and cryostat, at $\geq$ 300 K. A LN_2 storage and distribution system is provided for this purpose.

The different heat loads experienced by the SCMS can be classified into the steady state heat loads (including radiation losses from LN2 shields and residual gas conduction) and the losses during operation, which include the joule heating and ac losses in the joints, and the ac losses in CICC due to the current ramp up/down in the coils and current changes in the feedback coils. In addition to these loads from the SCMS there are heat loads arising from the conduction from supports, eddy currents induced in the magnets casings and structures, losses in the transfer lines and bus ducts, heat loads from cryogenic valves, bayonets and diagnostics inserts. Table V shows the estimates of these heat loads. A total steady state heat load $\cong$ 180W is expected. In addition the SCMS is subjected to pulsed loads during the plasma operation. Typical energy deposited in the SCMS during a plasma pulse is

given in table VI. Most of the contribution to these pulsed loads comes from the ac losses in the CICC, which strongly depend on the coupling time constant of the cable. The coupling time constant cannot be estimated accurately and have to be measured experimentally.

The numbers given in the table are based on a time constant of 200 ms for the cable, though the expected time constant is of the order of few tens of ms. The pulsed loads are, therefore, expected to be smaller than those shown in the table. A total pulsed load of ≅ 125 kJ is expected during one plasma pulse. Such pulses will be repeated every 5000 sec with a total of six pulses per day. The exact time constant, and hence the more accurate estimates of the ac losses, will be available from the results of the experiments which are planned to be conducted on a test solenoid using the actual CICC. The magnets will be energized using 20 pairs of current leads. The TF coils will be energized for about 10 h per day, while PF coils will carry current on the average of about two hours per day. This load would on the average evaporate ≅ 150L/h of LHe to He gas at ≅ 300K, in the current leads of the magnets.

4.1. Flow requirements for she

The heat in the SCMS is to be removed by forced flow of SHe through the void space in CICC. For this purpose the entire magnet system is divided in several parallel paths. The flow requirements for each of the paths is estimated based on the requirement of stability of the SC in presence of pulsed loads ac losses superimposed on the steady state heat loads. The details of the flow paths and flow rates are given in table VII. A total flow ≅ 0.3kg/s is required to keep the SC temperature well below the current sharing temperature in presence of peak pulsed loads.

TABLE V. STEADY STATE HEAT LOADS

Radiation losses	40 W
Residual gas conduction	6 W
Conduction from Support	34 W
Transfer line Losses	20 W
Losses in bus duct	10 W
Losses through Valves	30 W
Losses through Diagnostics Inserts	20 W
Joint Losses in TF coils	20 W

TABLE VI. TRANSIENT HEAT LOADS IN SCMS IN ONE PLASMA PULSE (1006 s)

Coil type	Ramp up/down 3s (kJ)	flat top (kJ)	Joints (kJ)	Total (kJ)
TF	2.11	10.3	48.3	62.82
PF1	0.41	0.70	0.25	1.77
PF2	0.52	1.00	0.50	2.54
PF3	21.4	4.16	0.50	47.46
PF4	0.19	0.72	5.03	6.05
PF5	0.16	0.46	5.03	5.81
Total heat load per pulse			126.45	

4.2. The liquid helium plant

A closed cycle LHe plant is required to cater to both the steady state and transient heat loads in SCMS. Taking into account the steady and transient loads and considering the uncertainties in the estimates a LHe plant with a capacity of 400 W refrigeration at 4.5 K and 200L/h liquefaction at the pressure

1.2 bar(a) is to be installed. The plant will, in additional, also provide the refrigeration capacity of around 250W for the heat dissipation in the cold circulation pump. The above total capacity will be achieved with liquid nitrogen pre-cooling. The total capacity of the plant, (both, refrigeration as well as liquefaction) would be variable from 50-100%. It will also be possible to operate the plant without LN_2 pre-cooling at the reduced capacity.

A cold circulation system, for the flow of SHe through the SCMS in a closed cycle, forms part of the LHe plant. The system will comprise of a cold pump, heat exchangers and valves. The system will be designed for a nominal flow rate of 0.3kg/s with a variability of 50-120% of the nominal value. The heat exchangers of the pump circuit will ensure the maximum supply temperature of SHe to the SCMS to be ≅ 4.5K. The heat exchanger located on the return side will dissipate the steady state as well as transient heat loads into a buffer dewier.

TABLE VII. FLOW PATHS AND FLOW RATES FOR SCMS

Coil type	Number of coils	Flow paths/coil	Path length (m)	Flow per path (g/s)	Total flow (g/s)
TF	16	12	48	1.45	278.4
PF1	1	2	109	0.90	1.75
			117	0.85	
PF2	2	1	113	0.85	1.70
PF3	2	4	136	0.70	5.20
			146	0.65	
			155	0.65	
			164	0.60	
PF4	2	4	98	1.00	8.00
PF5	2	4	117	0.85	6.80

An external dual bed, full flow, on-line purifier with automatic regeneration is provided to remove impurities such as water vapor, N2 and hydrocarbons to <1 ppm level. In order to confirm the purity of the processed He gas, the purifier will be equipped with the impurity monitor to detect the above impurities at <1 ppm level. A buffer dewar (MCD) is provided in the plant. The purpose of the buffer dewar is to absorb the heat loads generated within the SCMS and return cold helium vapors to the cold box at a constant temperature and pressure. The SHe coming from the SCMS delivers heat to the buffer dewar through a suitably designed heat exchanger before returning to the cold pump. The buffer dewar also serves as a reservoir for supplying LHe to the current leads. The capacity of the Dewar will be 2500L with maximum operating pressure ≅ 1.2 bar(a).

The refrigerator will be fully automatic with necessary instrumentation and controls. A provision will be made to interface the monitoring and controls to main control system for the remote monitoring, exchange of data and emergency signals. The control system would be capable of handling the variations in the application load. A suitable heater of wattage equivalent to the total capacity of the plant shall be incorporated in the plant. This will ensure an independent testing of the plant before connecting to the SCMS.

4.3. LN_2 distribution system

As mentioned above, liquid nitrogen cooled radiation shields (LN_2 shields) are provided between the SC coils and vacuum vessel as well as between the cryostat and SC coils. While the cryostat walls will be at room temperature, the vacuum vessel walls will have different temperatures under different operating conditions. During baking the walls will be at 525K, during wall conditioning the temperature will be 425K while during plasma operation the temperature will be 325K. The LN_2 consumption during these three phases will be ≅1200L/h , ≅600L/h and ≅300L/h respectively. In addition, LN_2 @150L/h is required for pre-cooler and purifier of the LHe plant and @200L/h for NBI system. LN_2 storage tanks of 105 m^3 has been provided for with a flow rate of 1500L/h . The LN_2 will

be purchased commercially and filled in these tanks to replenish the consumed liquid. The gas/vapors from the applications will be released to atmosphere. Appropriate distribution systems with valves, transfer lines and phase separators are being provided.

5. Summary

The Superconducting Magnet System design meets the SST-1 objectives. The engineering design of the magnet system has been completed. The CICC to be used in the magnet windings are presently being manufactured. The winding of the magnets will begin by mid 1999. The cryogenic system requirements have been detailed out and liquid Helium plant and other cryogenic systems are being procured. The SST-1 tokamak is expected to be operational by year 2002.

REFERENCES

[1] The SST Team, ″Conceptual Design of SST-1 Tokamak″, 16th IEEE/NPSS Symposium on Fusion Engineering, University of Illinois, Urbana-Champaign, 1, (1995) 481; Deshpande, S.P., and SST-1 Team, ″SST-1: an Overview″, Proc. 17th IEEE/NPSS Symposium on Fusion Engineering, San Diego Vol. 1 (1997) 227.

[2] Pradhan, S., et al., ″SST-1 Poloidal Field Magnets″, Proc. 17th IEEE/NPSS Symposium on Fusion Engineering, San Diego Vol. 2 (1997) 665.

[3] Bedakihale, V.M., et al., ″Support structure of TF magnet System″, Proc.17th IEEE/NPSS Symposium on Fusion Engineering, San Diego Vol. 2, (1997) 657.

[4] Bahl, R., et al., ″Design of Ohmic System for SST-1″, Proc. 17th IEEE/NPSS Symposium on Fusion Engineering, San Diego Vol.2, (1997) 661.

SUPERCONDUCTING TOKAMAK RESEARCH PROGRAMME IN ASIPP

Y.X. WAN
Institute of Plasma Physics, Chinese Academy of Sciences,
Hefei, Anhui, China

Abstract

Founded in September of 1978, the Institute of Plasma Physics, Academia Sinica (ASIPP) is directed in the research and development in the fields of high temperature plasma physics, magnetically confined fusion and the related advanced technology. The main facilities in ASIPP include the first Chinese superconducting tokamak HT-7, a conventional tokamak HT-6M, 2MW ion cyclotron resonant heating system, 2MW lower hybrid current drive system, a.c. and d.c. fly wheel generators with total power output of 200MW, a cryogenic liquid helium system, 20 Tesla static hybrid magnet and an advanced computer control and data acquisition *system.* A new superconducting tokamak project HT-7U has been approved by China Government; it is scheduled to be built as the next generation tokamak of ASIPP and to begin its first operation in 2003. The major parameters of the device are R = 1.7 m, a = 0.4 m, B_t = 3.5T, I = 1MA together with flexible large or small elongation and triangularity of the magnetic surfaces. The mission of HT-7U is to develop scientific basis for a continuously operating tokamak fusion reactor.

NON-INDUCTIVE CURRENT DRIVE AND RF HEATING IN SST-1 TOKAMAK

RF GROUP[1]

Institute for Plasma Research,
Bhat, Gandhinagar, India

Abstract

Steady state superconducting tokamak (SST-1) machine is being developed for 1000 sec operation at different operating parameters [1]. Radio Frequency (RF) and neutral beam injection (NBI) methods are planned in SST-1 for noninductive current drive and heating. In this paper, we describe the non inductive current drive and RF heating methods that are being developed for this purpose. SST-1 is a large aspect ratio tokamak configured to run double-null divertor plasmas with significant elongation (κ = 1.7-1.9) and triangularity (δ = 0.4-0.7). SST-1 has a major radius of 1.1 m and minor radius of 0.2 m. Circular and shaped plasma experiments would be conducted at 1.5 and 3 T toroidal magnetic field in three different phases with I_p = 110kA & 220kA. Two main factors have been considered during the development of auxiliary systems, namely, high heat flux (1 MW/m^2) incident on the plasma facing antennae components and fast feedback for constant power input due to small energy confinement time (~10 ms).

1. Lower hybrid current drive (LHCD)

LHCD system would be used as the prime method of steady state plasma current in a circular as well as an elongated plasma. The system has been optimized for efficient current drive for 1.5 T and 3.0 T operation, for different plasma elongation within 1.7 - 1.9 and triangularity of 0.4 - 0.7 for plasma inductance value of 0.75 to 1.4. Lower hybrid waves with asymmetric spectrum ($N_{||}$~ 1.8 - 4.0) would be launched by changing the phase between adjacent waveguides from 40 to 160 degrees using high power phase shifters through a radial port at 3.7 GHz to drive plasma current during different operating scenarios. Computational analysis using LSC [2] and WDFP [3] codes show that 220 kA plasma current would be driven with available power of 1.1 MW for circular plasma at 2 ´ 10^{13}cm^{-3} average density and 3T toroidal magnetic field. For the same machine and plasma parameters and plasma current, 860 kW of power is sufficient if the plasma is heated by auxiliary ICRH power of 650 kW. Since the launcher is made of two rows of narrow waveguides, they could be fed with equal power and independently phased at different angles so as to radiate different spectra. Under similar conditions it is possible to drive the same plasma current at a total input power of 600 kW. Current driven for a shaped plasma is being estimated with the help of ACCOME [4] code. 1 MW of CW power would be supplied from two klystrons to feed a grill consisting of 64 narrow waveguides in two rows placed on the equatorial plane of LFS radial port. Power and other parameters required to drive 100 kA of plasma current is given in Table I.

TABLE I

Mag. Field (Tesla)	Avg n_e ($*$ 10^{20} m^{3})	N//	T_e (keV)	$\eta * 10^{19}$ (m^{-2}MA/MW)	Current (kA)	Power reqd. (kW)
1.5	0.10	1.8	0.513	0.199	100	527
	0.09	1.8	0.521	0.211	100	448
	0.08	1.7	0.528	0.225	100	374
	0.07	1.7	0.538	0.241	100	305
3.0	0.13	1.4	0.459	0.265	100	514
	0.10	1.4	0.483	0.297	100	354
	0.09	1.3	0.493	0.310	100	305
	0.08	1.3	0.505	0.325	100	259

[1] See the Appendix.

Power and other parameters required to drive 100 kA of plasma current with additional auxiliary power of 650 kW is shown in Table II.

TABLE II

Mag. Field (Tesla)	Avg n_e (* 10^{20} m^{3})	N//	T_e (keV)	$\eta * 10^{19}$ (m^{-2}MA/MW)	Current (kA)	Power reqd. (kW)
3.0	0.13	1.437	0.646	0.373	100	366
	0.10	1.378	0.759	0.466	100	225

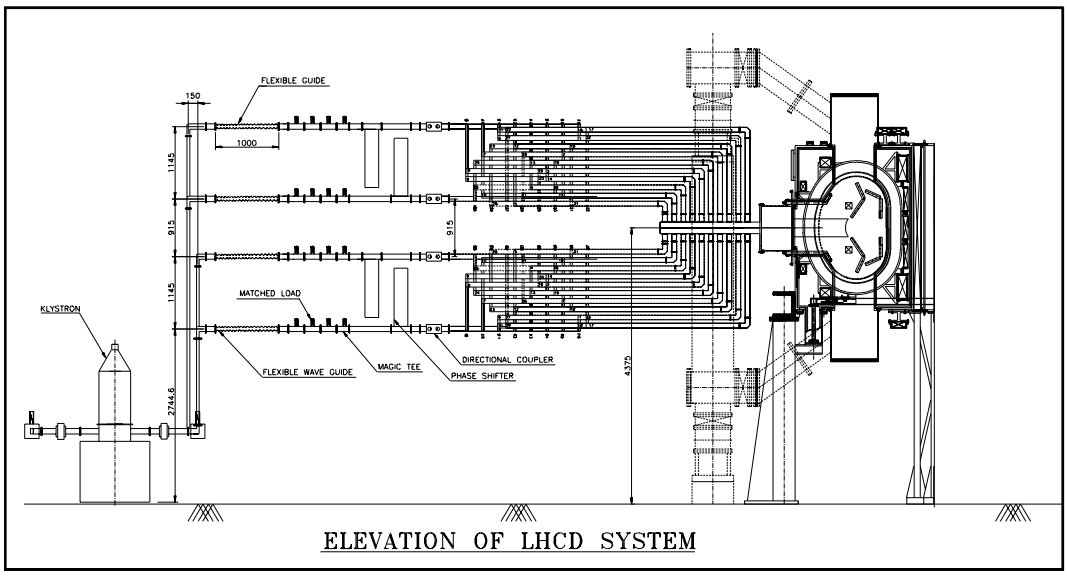

FIG.1. Elevation view of LHCD system.

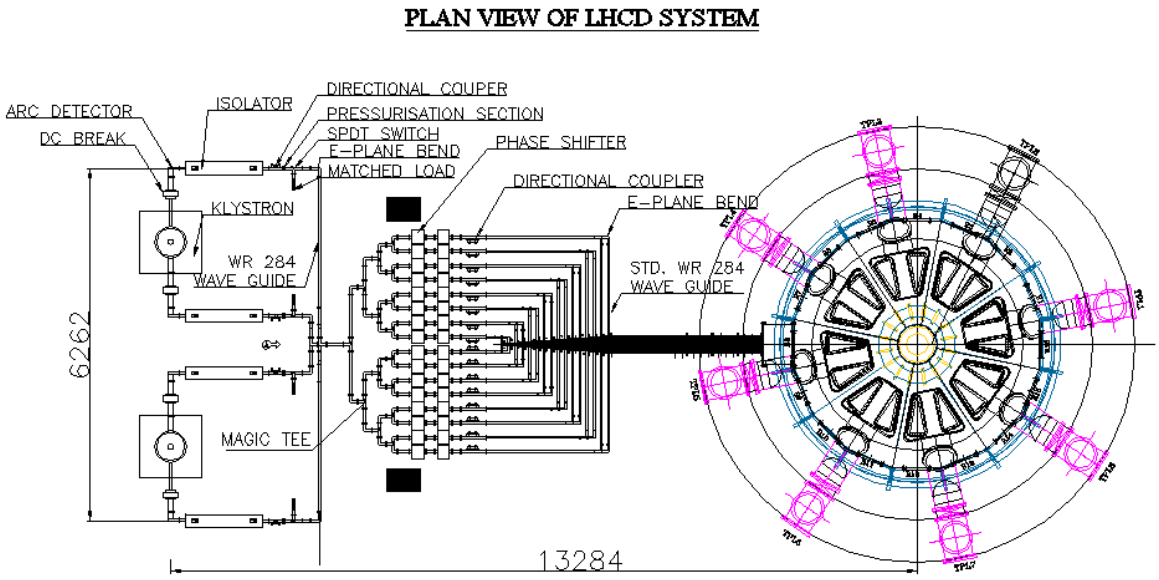

FIG. 2. Plan view of LHCD system.

The typical layout of LHCD system is shown in Figure 1 and Figure 2. The main components of the system are low power section, high power amplifier (klystrons), high power transmission line, high power phase shifter (to vary the launched spectrum), high power directional coupler (to monitor forward and reflected power), vacuum window and grill. Each Thomson CSF klystron (TH2103D) operates at 3.7 GHz and delivers 250 kW each in two arms of WR284 waveguide for 1000 sec. Power from each of these outputs would be divided to sixteen channels of transmission line consisting of the above mentioned components. It is to be noted that the power level in each of the channel is around 15 kW and is definitely easy to handle. Finally the power will be coupled to the plasma through the grill interfaced by a vacuum window assembly. The RF power is coupled through the grill which comprises of two rows, each having 32 narrow waveguides of dimension 7mm $\times$ 76 mm with a periodicity of 9 mm. Four dummy waveguides of quarter wavelength are at the four corners to reduce fringe field effect. A protection limiter is placed around the grill to protect the launcher from direct particle load. It is positioned behind the LCFS. Calculation based on Brambilla theory shows that a power with N_{II} at 2.25 with 90 degree phasing with FWHM ~ 0.28 would be launched. The grill will be placed in a hostile environment of continuous heat load for 1000 seconds. Two major sources of heat would affect the grill. One is the RF ohmic loss in the narrow waveguide while the other is the radiation heatload which is falling on the plasma facing surface. The conducted heat load is ~120 W/cm^2 while the radiated heat load is ~ 20 W/cm^2 . The RF loss accounts for a loss of ~ 8 kW. Hence the total heat flux would be ~ 3 kW/cm^2 at full power. The protection tiles made of graphite would also encounter these two sources of heat dissipation. It is proposed that the grill would be positioned at 1.3 λ_n (or equivalently at 3.25 λ_Q behind the LCFS). Due to the heat load on the tiles and under constant cooling the temperature rise of the tiles are envisaged to be about ~ 310 degree.

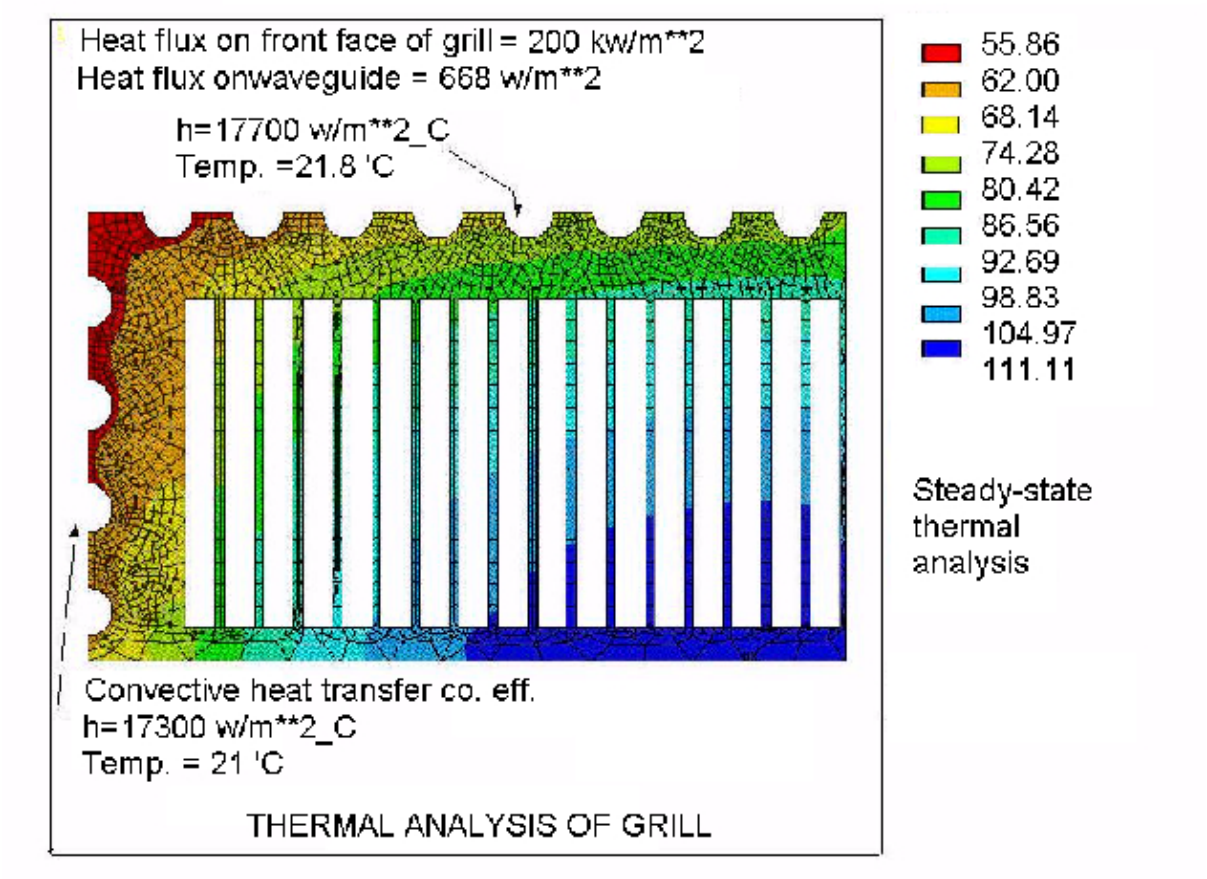

FIG. 3. Thermal analysis for the grill.

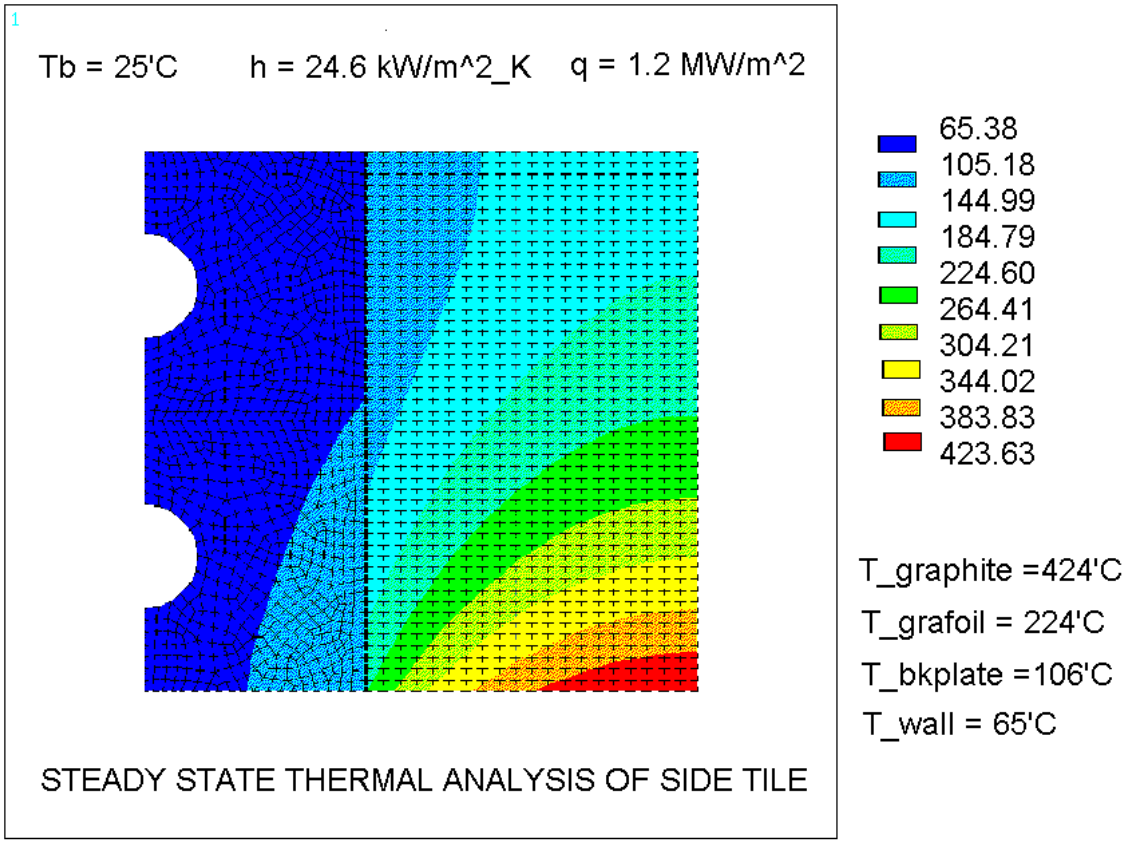

FIG. 4. Thermal analysis for the side tile.

Zirconium-chromium-copper, with high thermal conductivity and high tensile strength has been chosen for the fabrication of the grill to withstand the thermal stresses developed due to the above discussed heat loads. Analytical calculation shows a maximum bulk temperature rise of about 30^{o}C with water flow rate of ~ 5 m/s, for a tube diameter of 1 cm. For conducted heat load, bolted tiles will be used with active cooling. Large flow rates (~6.6 m/s) will be required and the estimated rise in the surface temperature of the tile is ~313 ^{o}C. Since the grill will be actively cooled at the top and bottom of the surfaces, the maximum temperature rise will be at the midplane of the grill. Calculation shows that the estimated peak temperature rise of the copper grill is ~ 116^{o}C producing a thermal stress of ~ 220 MPa which is below the yield stress for Zr-Cr copper. Finite element ANSYS analysis confirms the analytic calculations. Figure 3 and Figure 4 show two such cases of the grill and the graphite tile. Disruption stress analysis shows that a maximum of ~ 13 kN force will be generated on the grill. The calculation is based on a simple model which assumes that 220 kA plasma current disrupts within 0.1 ms (decay rate ~ 2.2 GA/ sec). Similar results are obtained with SPARK code (Eddy current) analysis.

The vacuum window which accommodates 64 narrow waveguides would be made out of 99.9% Alumina and the frame will be made out of 6242 Titanium alloy to avoid thermal cracks and microcracks due to differential thermal expansion. Both the materials have similar coefficient of thermal expansion. The brazing material will be Ag-Al (instead cusil) to have better performance during long pulse rf injection. Other transmission line components like E/H bend, transformer, narrow waveguide are being designed and performance being evaluated on 3D microwave component design software, using FEM techniques.

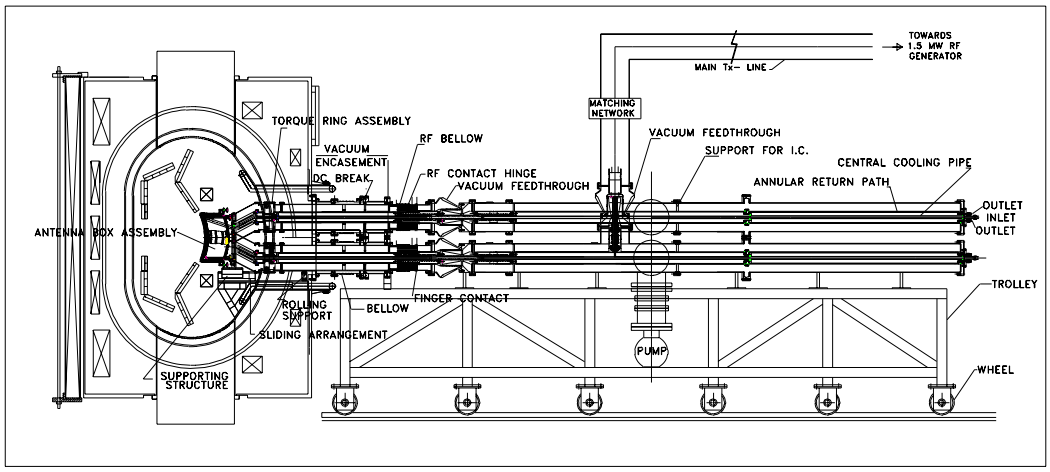

FIG. 5. *Elevation view of ICRH antennae mounted in radial port.*

2. Ion cyclotron resonance frequency (ICRF)

Ion cyclotron heating is chosen to heat the plasma to 1.0 keV, during pulse length of 1000 s. A 1.5 MW ICRF system would operate at different frequencies between 20-92 MHz for different heating scenarios at 1.5 T and at 3.0 T operation. Fig.5 is an elevation view of the tokamak showing ICRH antennae mounted in one of the radial ports.

Conventional design criteria have been implemented in developing the 1.5MW, 1000 s RF system. Various efficient heating scenarios (e.g. 2^{nd} harmonic of majority species at 1.5T and 3.0T, minority D in H-plasma) would be implemented. The generator is tetrode based and modular. For the last high power stage, tetrode TH526 has been selected which has wider frequency bandwidth. All the components used in designing generator have high frequency performance. RF generator will be placed in the generator room about 90 m away. Coolant requirement for the tube is demineralised water at 800 LPM/5 bar.

A 90 m long pressurised 9", 50 ohm transmission line would feed the antennae. RF power is divided by 3 dB hybrid coupler and then by two Tees to obtain equal power at each antenna. The entire Tx-line will be pressurized at 3 bar to avoid breakdown. Estimated power losses are 0.6kW/m and 0.25kW/m in the inner and outer conductor respectively increasing the temperature by 116^0C (max.). Hence cooling is mandatory. Forced dry air flow pressurised at 3 bar with 24 m/sec flow velocity, through annular section of 9 inch Tx-line or water flow through inner conductor would be selected as the most suitable method after prototype testing. Slow stub matching (in seconds and 20-30 ms) as well as fast frequency (~2 ms) matching techniques would be used to optimize matching during the discharge. Reflected power would be replenished by increasing the RF input power as per the feedback signal till slow matching is achieved. Impurity generation by the ICRH antenna is not so severe. Interface would be made of SS304L for better mechanical strength and coated with copper (~100μ) for better rf transmission. For 1000 s pulse operation interface will be actively cooled (full length of inner conductor and a narrow portion of outer conductor). Antennae are designed using two powerful codes BRACC [5] and SWHAP [6]. Code results for the SST-1 antennae are given in table III below.

Four antennae (each carrying 375 kW of power), placed on low field side (out of beam sight) at $3.5\lambda_q$ behind the last closed surface, will heat plasma to 1 keV during 1000 s. Design goal for power density is 1.2 kW/cm^2. Assembled view of the antenna box viewing from the plasma side is shown in Fig 6.

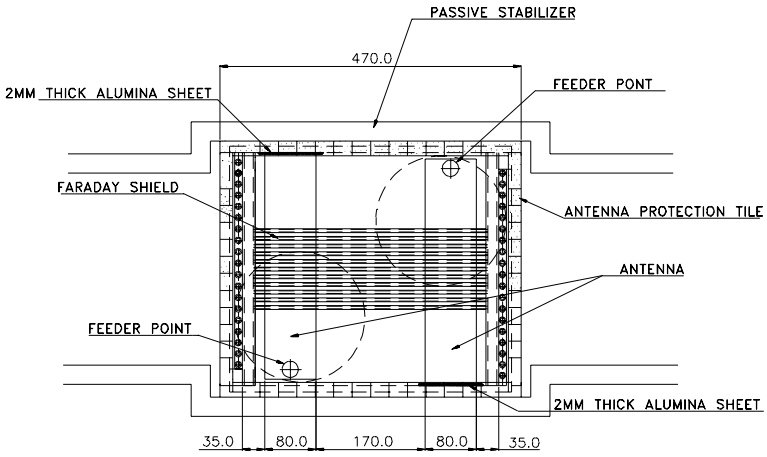

FIG. 6. Assembled view of antenna box.

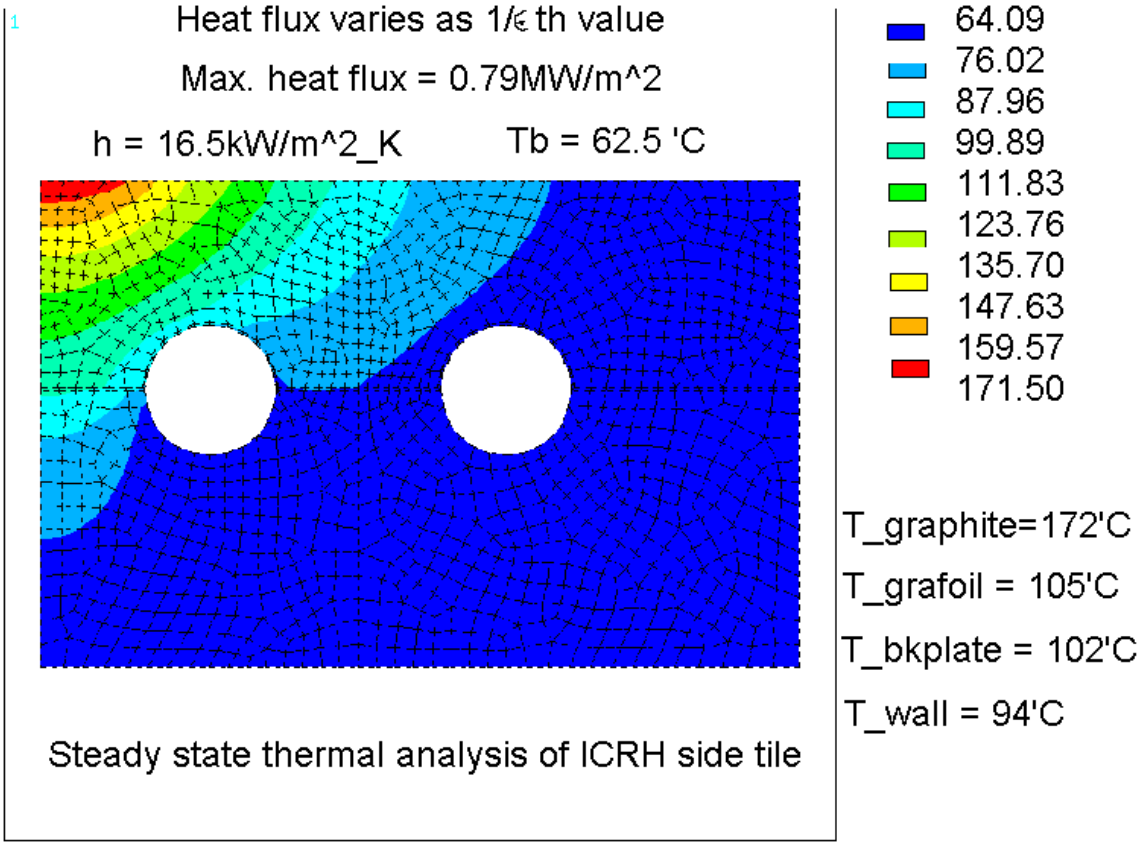

FIG. 7. Thermal analysis for side tile.

Antenna is shielded from the plasma by 30 no. of Faraday shields in a single row. Antenna assembly is made of SS304L. Graphite tiles will form the protection limiters around the antenna box. Expected heat load on the antenna assembly is 80 W/cm^2. Required flow velocity for the antenna is 4.5 m/s through 3 cooling channels of I.D. 4 mm. Flow rate through hollow Faraday shields (I.D. 4 mm) will be 2.5 m/s and 2.7 m/s for tiles. Maximum temperature at the tiles would be 211^{0}C. Thermal analysis has been conducted with the help of ANSYS for all the plasma facing components. Maximum thermal

stress on the antenna and on protection tiles are 330 MPa and 25 MPa respectively. Thermal distribution on one of the side tiles is shown in Fig 7. Disruption stress analysis shows that a maximum of 1.4 kNm of torque will be generated on the antenna structure. Impurities generated due to physical sputtering of shield material limits the power density. Analytical calculation shows that acceleration of ions in the rf sheath does not produce significant sputtered SS ions. Sputtering due to charge exchange neutral from plasma and NBI rendered Z_{eff}~ 0.0083 due to SS impurity. Plasma will not be diluted over 1000 s pulse.

3. Electron cyclotron resonance frequency (ECRF)

ECRF system at 200 kW, 84 GHz will be used initially to preionize and startup of SST-1 discharges. A Gyrotron source capable of delivering 200 kW CW has been chosen. Second harmonic 'X' & 'O' mode launching would be used during 1.5 T operation. Provision for low as well as high field sidelaunch have been made. The output mode of the gyrotron with internal mode converter is HE_{11}. A transmission line consisting of d.c.break, bellows, miter bend, polarizer and corrugated waveguide terminating with a barrier window will be used to transmit power from the gyrotron to the tokamak (Fig. 8). The total attenuation of the line is 1.1 dB. Quasi optical reflecting mirror system has been designed to steer the microwave beam toroidally[7]. The launcher design for ECRF system is basically

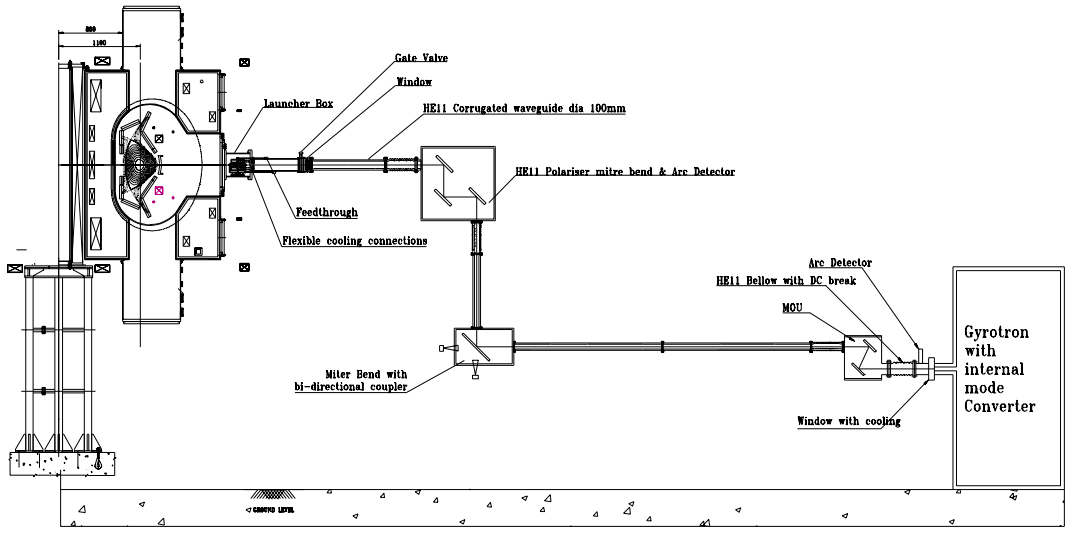

FIG. 8. Schematic of ECRH LFS launching system.

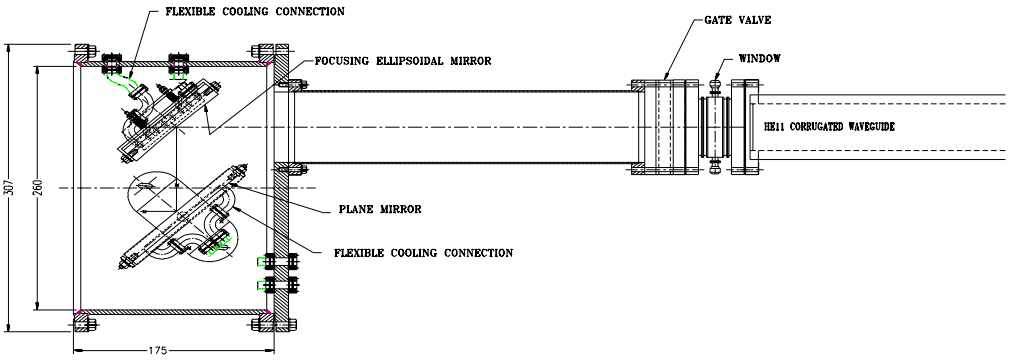

FIG.9. ECRH LFS launcher for SST-1.

TABLE III

f (MHz)	Mode	R (Ω)	L (nH)	C (nF)	η (%)	El. length
45.6	Ia, (0,0)	1.55	111.7	0.52	84.3	λ/8.2
45.6	Ia,(π,0)	1.78	93.5	0.52	86.2	λ/8.9
45.6	Ib, (0,0)	1.8	112.6	0.52	86.2	λ/8.1
45.6	Ib,(π,0)	1.07	87.2	0.52	78.9	λ/9.25
22.8	II, (0,0)	1.0	112.4	0.52	83.0	λ/16.3
22.8	II,(π,0)	1.14	87.9	0.52	84.8	λ/18.4
24.4	II, (0,0)	1.22	112.6	0.52	85.6	λ/15.2
24.4	II,(π,0)	1.12	88.0	0.52	84.6	λ/17.2
91.2	II, (0,0)	3.37	119.5	0.52	89.1	λ/3.95
91.2	II,(π,0)	4.4	92.7	0.52	91.5	λ/4.48

determined by the available space , required beam width and cross-section in the plasma. Over moded waveguide is used to transmit the power which follows quasi optical transmission with gaussian pattern. Low Field Side launcher consists two reflectors: one focusing mirror and a plane mirror. For long pulse operation the reflectors require effective cooling.. A separate mirror box is attached to the radial port flange to accommodate the reflectors along with their cooling arrangement (fig. 9). The designed reflector has a focal length of 819 mm and a size of 202 × 148 mm. It is inclined at 45 degrees with respect to the beam axis. A plane mirror is inserted in the path of the beam to steer the beam into the plasma volume as well as to steer it toroidally. The plane mirror is 180mm apart from focusing mirror. In this design, maximum possible steering of the beam is $\pm 15^0$. Similarly in top launch scheme, two mirrors (one focusing and one plane) is used to focus the beam. The distance between focusing reflector and baffle is 1150 mm. Radius of beam waist at the baffle is selected to be 18mm. 14.5% power is lost at the baffle. The size of focusing reflector is 205mm × 145mm. The temperature rise of the smallest reflector is around 350^0C, taking 1% absorption of microwave on the reflector for 1000 second operation. Demineralised cold water is used as coolant with a flow velocity of 0.75 m/s and mass flow rate of 0.048 kg/sec through the tubes attached at the back surface. Negligible part of EM power is absorbed during O-mode launch in its first pass. After reflection from the vessel wall beam is absorbed in the centre. The beam waist radius at the wall is 29 mm and corresponding rise in temperature of wall for 1% absorption is approximately 700^0C. During plasma disruption the EM forces experienced by the box and its support is 2kN. Force on the plane reflector due to toroidal field component is ≅ 20 N/m while the force on the support and reflector due to B_R component is≅ 40 N/m. The force on the plane reflector due to toroidal field component ≅ 120 N.

4. Conclusion

Design issues of SST-1 RF systems for long pulse operation are described which primarily relate to continuous heat removal mechanisms. Thermal, electromagnetic and mechanical stresses have been analyzed and critically studied for efficient thermal management, for it plays a key role in a high power 1000 second system.

REFERENCES

[1] Deshpande S.P. and the SST-1 Team, SST-1: An Overview, *17th Symposium on Fusion Engineering*, 1997.

[2] Ignat D.W., et al., Nucl. Fusion, 34, 837, 1994.

[3] Kupfer K., et. al., Phys. Fluids, B5, 4391, 1993.

[4] Tani K., et. al., J. Comput. Phys., 98, 332, 1992.
[5] Koch R., Bhatnagar, V.P., Messiaen, A.M. and VanEester, D., *Computer Phys. Communication*, 40, pp. 1-22, 1986.
[6] Van Eester D. and R. Koch, "SWHAP: a code for modeling ICRH heating of non-maxwellian populations", *Europhysics conference Abstracts*, 16E, pp 129-132, 1992.
[7] Vinogradov,D.V., *Int.Journal of Infrared and Millimetre waves,* 16 (11), pp 1945-1963, 1995.

APPENDIX

RF Group

D. Bora, A. Mukherjee, P.K. Sharma, K. Sathyanarayana, J.P. Singh, K.K. Samanta, B.K. Shukla, S. Gangopadhyay, S. Kumar, L. Rao, Y.S.S. Srinivas, P. Khilar, M. Kushwah, B. Pal, A. Bhardwaj, P. Gupta, Raj Singh, S.V. KulkArni, Sai Kumar.

PRESENT DESIGN OF THE HT-7U TOKAMAK DEVICE

S.T. WU, W.Y. WU, Y.F. BI, P.D. WENG, Y.N. PAN, Z.M. CHEN,
B.Z. LI, D.M. GAO, J. WANG, Z.Y. LIAO, D.M. YAO, Y.H. ZHU,
J. YE, Y. WU, J.D. LI, D. WU, W.J. PAN, D.J. GAO,
X.B. WU, Y.T. SONG, Y.L. LI, Y.M. XI
Institute of Plasma Physics,
Chinese Academy of Sciences,
Hefei, Anhui, China

Abstract

The HT-7U superconducting tokamak is an advanced steady-state plasma physics experimental device to be built at the Institute of Plasma Physics, the Chinese Academy of Sciences (CASIPP). The preliminary engineering design incorporates the superconducting toroidal field (TF) and poloidal field (PF) magnets, the vacuum vessel, the radiation shields, the cryostat and the current leads. The general mechanical structure of the HT-7U tokamak device with the detail structure of main parts is in design phase. The stability calculation and analysis of superconductors and coils have been done initially. The maximum field on the TF and PF coils and the maximum stress on the cases of coils, vacuum vessel and cryostat are evaluated. The R&D programs on the HT-7U tokamak device have been planed and in progress, which are focused on the design and development of conductors and model coils both in bath-cooling and force-cooling, test facility, winding machine, prototype of one 1/16 segment of vacuum vessel, and some key technologies.

Introduction

The HT-7U superconducting tokamak, which is approved by Chinese government, is an advanced steady- state plasma physics experimental device to be built at the Institute of Plasma Physics, the Chinese Academy of Sciences (ASIPP). The scientific mission of the HT-7U project is to study physical issues on the sustainment of a non-burning plasma scenario for the steady-state operation of next generation advanced tokamak devices. The engineering mission of the HT-7U project is to establish technology basis of full superconducting tokamaks to support future reactors. HT-7U will have a long pulse (60-1000s) capability, a flexible PF system, and auxiliary heating and current drive systems, and will be able to accommodate divertor heat loads that make it an attractive test for the development of advanced tokamak operating modes [1].

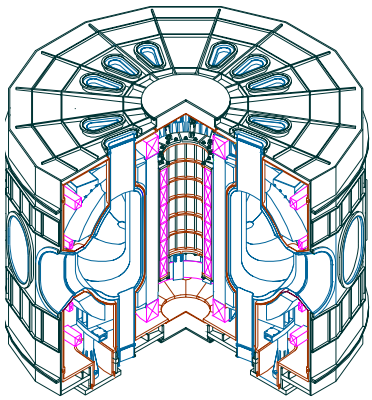

Fig. 1. The HT-7U tokamak device.

The preliminary engineering design incorporates the superconducting toroidal field (TF) and poloidal field (PF) magnets, the vacuum vessel, the radiation shields, the cryostat and the current leads. The general mechanical structure of the HT-7U tokamak device with the detail structure of main parts is in design phase. The overview structure of HT-7U is shown in Fig. 1. The main parameters of the HT-7U device are summarized in Table I.

TABLE I. MAIN PARAMETERS OF HT-7U

Toroidal field, B_o	3.5 T
Plasma current, I_P	1 MA
Major radius, R_o	1.7 m
Minor radius, a	0.4 m
Aspect ratio, R/a	4.25
Elongation, K_x	1.6 - 2
Triangularity, d_x	0.6 - 0.8
Heating and driving:	
ICRH	3-3.5MW
LHCD	3.5 MW
ECRH	0.5 MW
Pulse length	1- 1000 s
Configuration:	double-null divertor
	single null divertor
	pump limiter

The considerations on the choice of the device parameters are:

- Based on the criterion and scaling law of experiment results of tokamaks in the world.
- To ensure the advanced status of the HT-7U device and its physical experiment in the world.
- To reusethe existing HT-7 facilities as possible as we can, including the high power supplies, the cryogenic system, ICRH, LHCD, ECRF, vacuum pumping and gas puffing system, etc..
- To take advantage of the tokamak design experience and fabrication ability accumulated in past years in the world and in ASIPP. The design of HT-7U features sixteen superconducting TF coils and twelve superconducting PF coils, symmetrically located about the plasma mid-plane. Six inner PF coils constitute the CS assembly. A vacuum vessel with race-shaped horizontal ports and bathtub-shaped vertical ports are located in the bore of the TF coil. Two thermal shields of about 80 K cover all of the superconducting magnet system. A cryostat encloses all of the superconducting coils with radiation shields, the vacuum vessel and support structures. The superconducting magnets system, the vacuum vessel and the thermal shields are supported on the cryostat independently [2].

Superconducting Magnet System

Design of the PF System: The PF system consists of twelve coils located symmetrically about the vertical mid-plane and the equatorial plane. Six inner PF coils form a central solenoid assembly. The PF coils will provide about 10 V-s for inducing 1 MA plasma current ohmically and ensure plasma equilibrium by controlling the vertical field amplitude and curvature index. All the PF coils are capable of steady-state operation. The operational current of PF is less than 14 kA. The maximum field on the PF coils is less than 4.2 T and the maximum ramp during plasma startup is about 7 T/s in 60 ms [3].

NbTi cable-in-conduit conductor (CICC) cooled by supercritical helium at 4.5 K is used as superconductor for all of the PF coils. To minimize A.C. losses, all wires in the PF conductor will be

TABLE II. MAIN PARAMETERS OF PF CONDUCTOR

Conductor	NbTi/Cu
Type of conductor	CICC, Forced-flow
Cabling configuration	(2NbTi+1Cu)×3×3×(6+ 1Tube)
No. of NbTi strands	108
No. of Cu strands	54
Conduit: Material of conduit	316 L
Wall thickness of conduit	1.5 mm
Conduit outer dimensions	17.4×17.4 mm × mm
Operating current	14 kA
Rated magnetic field	4.5 T
Cooling condition	SHe, 4.5K, 4bar
Temperature margin	2.14 K
Stability margin	700 mJ/cm^3

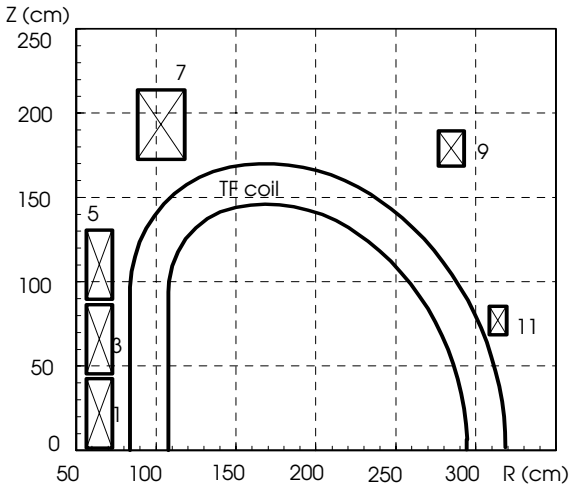

Fig. 2. The HT-7U PF Location and TF coil shape overview.

electroplated with 2 μm chromium (Cr) and the second stage cable will be 80% wrapped with a stainless steel strip of 0.05 mm thickness. The main parameters of the PF conductor are summarized in Table II and the PF location is shown in Fig. 2.

All of the PF coils will be attached to the TF assembly. The CS sub-assembly will be hung and bolted inside the inner bore formed by squeezed cases along the straight legs. The other six PF coils will be cramped and bolted on the TF assembly.

Design of the TF System: The superconducting TF magnet system of HT-7U is consisting of a toroidally arrayed sixteen coils which produce 3.5 T toroidal field at plasma major radius of 1.7 m and about 5.8 T peak field at the TF coils with ripple of less than 1% within the plasma volume. The TF magnets are designed to withstand the magnetic centering force by wedges at their inner legs and to withstand overturning torque by wedges between their outer arc segments. Two TF coils are encased in a TF module case from two sides and assembled in one coil module. Two modules are then jointed into a quadrant. Four quadrants form a TF assembly. Through thermal insulation bearings, the TF assembly with twelve PF coils is mounted on a circular structure supported by eight pillar assemblies.

TABLE III MAIN PARAMETERS OF TF CICC

Dimension (mm×mm)	22.0×22.0
Length of CICC in a double-pancake (m)	174
Thickness of the conduit (mm)	1.7
Dimension of the central channel (mm)	∅7.5×1
Diameter of SC strands (mm)	∅0.85
Number of SC strands	192
Ratio of Cu/NbTi in SC strands	1.38:1
Diameter of copper strands (mm)	∅0.65
Number of copper strands	192
RRR of the copper	100
Fraction of Iop to Ic	0.306
Void fraction in CICC	0.356
Final Cu/NbTi	2.77:1

TABLE IV. PARAMETERS OF TF COIL (Based on CICC)

Central field in major plasma radius	3.5 T
Peak field in the windings	5.8 T
Ampere turns	30 MAt
Operation current of the cables	15.5 kA
Operation system pressure of helium	4.5 bar
Operation temperature of helium Number of turns in a coil	4.5 K 120
Dump resistance	0.1 ohm × 2
Inductance of half of the TF magnets	1.06 henry

TABLE V. MAIN CALCULATION RESULTS OF TF CICC

Stability margin	14.6 kW/m (301 mj/cm^3)
Quench calculation time	20 s
Protection lagging time when quenched detected	1 s
Dump residual time	10.8 s
Peak helium pressure when quenched	10 bar
Peak temperature of the conductor when quenched	75 K
Peak voltage v (v = IR) when quenched	3.4 V
Peak resistance of the conductor when quenched	0.63 mΩ
Operation system pressure of helium	4.5 bar
Pressure drop (Pin-Pout)	0.5 bar

TABLE VI. MAIN PARAMETERS OF TF BCC
(Based on the SSC Inner Cable)

Maximum field	5.8 to 6.6 T
Operation current	5234 A
Operation temperature	4.3 K
RRR of Cu	> 150
Critical current(at 4.3K, 6.6T)	10307 A
Recovery current	5584 A
Conductor dimension	6.9 × 16.7 mm × mm
Solder material	Sn 95% + Ag 5%
Roughened surface: Depth of fins Angle of fins Pitch of fins Number of fins	 0.9 mm 62° 1.2 mm 10
Wetted perimeter	42 mm
Total length of SSC	64.2 km

TABLE VII. MAIN PARAMETERS OF TF COIL (based on BCC)

Magnet field in the center of plasma	3.5 to 4.0 T
Number of coils	16
Number of turns in a coil	406
Turn-to-turn insulation thickness	0.3 mm
Pancake-to-pancake insulation thickness	2.7 mm
Ground insulation thickness	6 mm
Inductance of ¼ TF coils	8.7 H
Paris of current leads	4
Total Ampere-turns	30 to 34 MAt

Each pillar assembly is cooled by cold helium gas evaporated from a liquid helium container connected to the interface of the TF supports.

NbTi CICC and bath-cooling conductor (BCC) are candidates to be the superconductor of the coils. Up to now, several versions of the TF conductor design have been done. The configuration of 15.5 kA CICC is (2SC + 2Cu) × 4 × 4 × (6 + 1 tube). The stability calculation of the 15.5 kA CICC has been finished. The parameters of CICC, the TF coils and the stability calculation results are shown in Table III, IV, and V respectively. The voltage evolution, temperature distribution, helium pressure and helium velocity during a quench in the middle of one conductor are shown in Fig. 3, 4, 5 and 6 respectively [4]. The main parameters of one of the design of BCC and its coil based on the SSC cable are shown in Table VI and VII.

The maximum stress on the TF cases is less than 350 MPa [5], shown in Fig. 7. Through thermal insulation bearings, the TF assembly with twelve PF coils is mounted on a circular structure supported by eight pillar assemblies.

Preliminary calculation of the heat loads to the TF and PF systems: The radiation from the thermal shields (QES-TF, QIS-TF), the heat flux caused by a residual gas (QP), and that of mechanical supports (QSUP) have been considered in the calculation of the stationary heat load (QTOT) to the TF and PF systems. To reduce QSUP from 310 W to 90 W, the nitrogen cooling pipes on the support pillar assemblies are needed. At $\varepsilon = 0.2$ and T = 300 K of the vacuum vessel, the total stationary heat

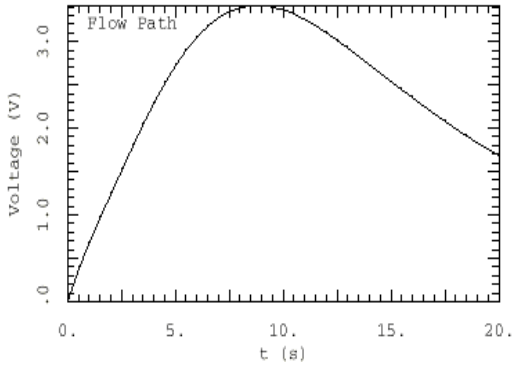

Fig. 3. Voltage (V = IR) Evolution.

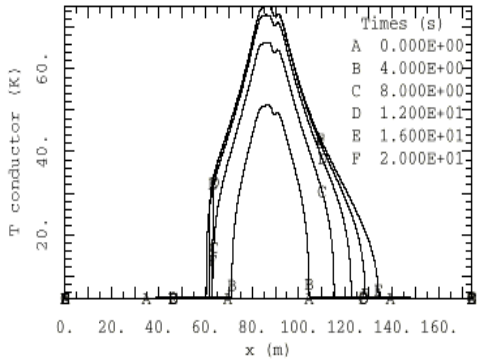

Fig. 4. The conductor temperature distribution along the length at different periods.

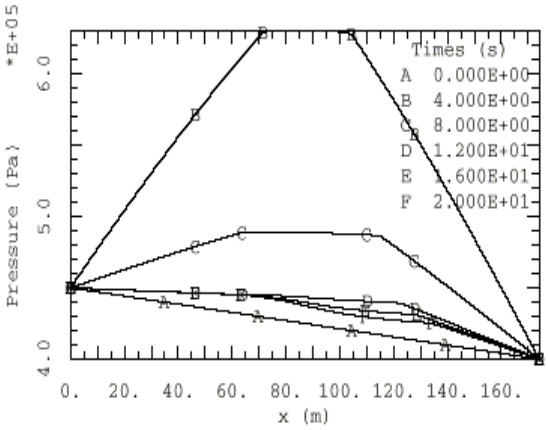

Fig. 5. The helium pressure distributions.

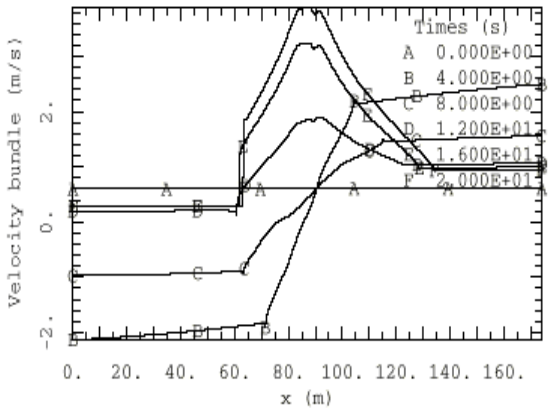

FIG. 6. The distributions of helium velocity along the length at different periods in the bundles along the length at different periods.

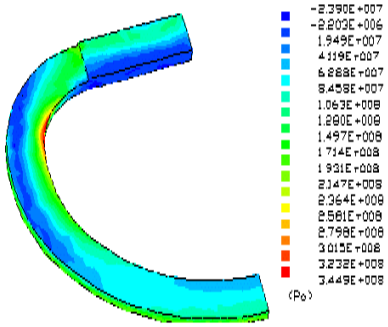

Fig. 7. The result of stress analysis of the TF case.

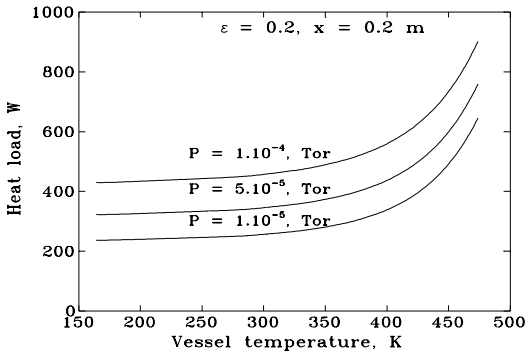

FIG. 8. Total stationary heat load to TF and PF systems at different pressures in cryostat depend on vacuum vessel temperature.

load of TF and PF is changed from 260 W up to 460 W based on the pressure range p = 1×10^{-5} to 1×10^{-4} torr [6], shown in Fig. 8. The resistive heat loads will be 8 to 40 W based on a joint resistance of 1 to 5×10^{-9} ohm. The liquid helium consumption of current leads will be 96.5 l/h at zero currents and 266 l/h at maximal operational currents based on 4×10^{-4} W/A at zero current and1.1×10^{-3} W/A at the operational current respectively. The total helium consumption for 1000s operation will be about 266 l.

Vacuum vessel and other components

Design of the vacuum vessel: The vacuum vessel of HT-7U is a completely welded toroidal structure with noncircular cross-section nested in the bore of the TF coils. Double-wall configuration design is considered for neutron shield. The preliminary finite element analysis of stress load on the body of the vacuum vessel has been conducted. The loads considered in the analyses were dead weight, atmospheric pressure, electromagnetic force caused by the disruption of a 1.5MA plasma current and a 3.5 T magnetic field and thermal stress caused by bake-out. Fig.9 shows the Von Misses stress distribution on Vacuum Vessel. The Maximum stress is 816 kgf/cm^2 (about 80 MPa). The concept of plasma facing components (PFC) has been considered which includes a divertor, passive plates, feedback control coils and limiter. The draft calculation and design of the vessel baking system has been done, in which heaters disposed on the inner surface of the vacuum vessel are used, as shown in Fig.10. The results of calculation show that required baking power is changed from 60 kW for $\varepsilon = 0.1$ up to 160 kW for $\varepsilon = 0.3$, shown in Fig. 11 [7]. Preliminary calculation of the water cooling system of the vessel has been based on design scheme of PFC. The results show that the total mass flow is about 154 kg/s with the maximum temperature of less than 5000C on the graphite, are depicted in Fig. 12 and Fig. 13 [8].

Design of the thermal shield: An internal shield and an external shield of about 75 to 80 K which are made of sandwich structure with square tubes welded to enclose the whole superconducting magnets of HT-7U. The internal shield is polygon shaped from 16 wedged of noncircular cross-section with sectors of 22.5^0 toroidal angle each. The external shield is polygon shape cylinder consisting of three parts including an upper structure, a polygon ring and a lower structure with four support structures. The internal shield and the external shield are strongly linked by ducts surrounding the ports of the vacuum vessel to form a rigid tour that is supported by four grounded supports down on the cryostat base through insulators. The total heat load to the thermal shields cooled by nitrogen determined by radiation from the cryostat, the vacuum vessel and the heat conduction of mechanical supports is about 40 kW based on $\varepsilon = 0.2$ and the vacuum vessel temperature of 300K, as seen in Fig. 14.

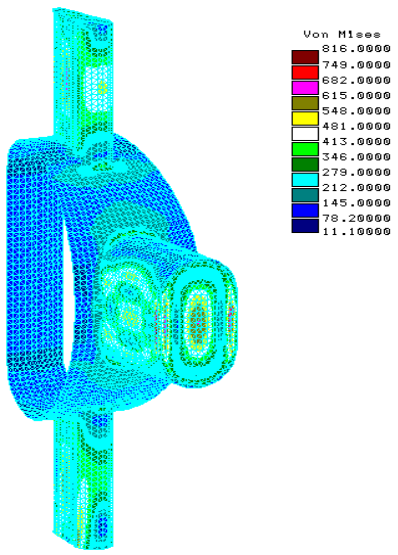

Fig. 9. Von Misses stress distribution on vacuum vessel inside the vacuum vessel.

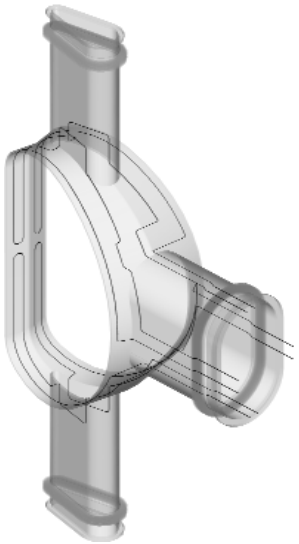

Fig. 10. The heater cables layout.

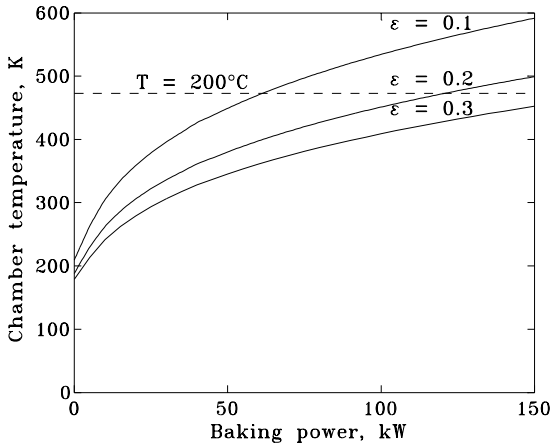

Fig. 11. The chamber temperature dependence for different elements vs. water temperature.

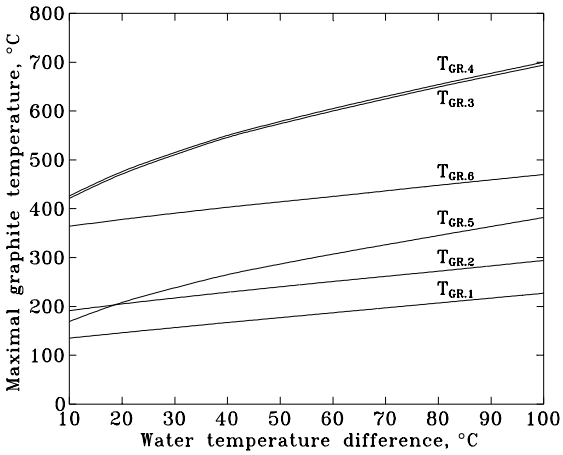

Fig. 12. Maximal graphite temperature dependencies via baking power for different ε values.

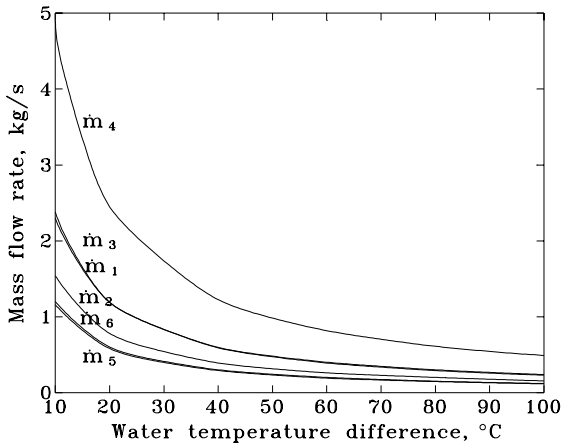

Fig. 13. Mass flow rate dependencies for different PFC elements vs. water temperature shields at different vacuum vessel temperature.

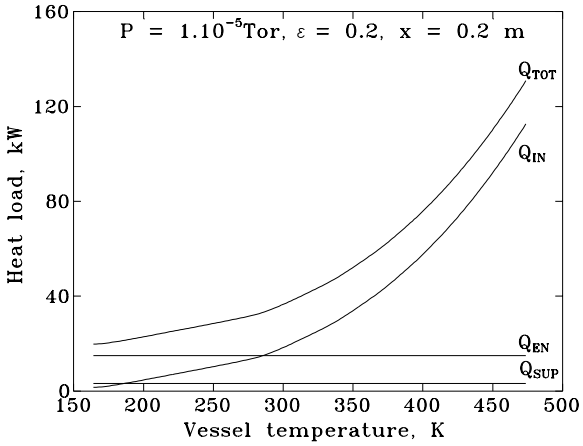

Fig. 14. Total heat load to nitrogen radiation.

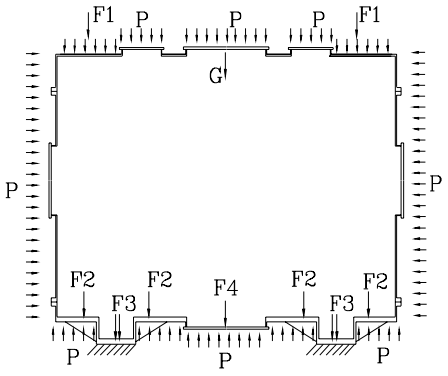

Fig. 15. Loads considered in cryostat analyses.

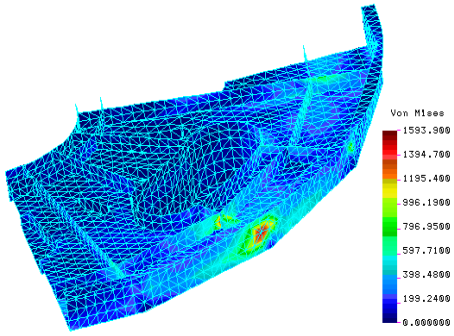

FIG. 16. Von Misses stress distribution on the base of the Cryostat (kgf/cm^2): Progress of the R&D programs.

Design of the cryostat: The cryostat of HT-7U is a polygon cylindrical vacuum vessel with ambient operating temperature, which consists of a cap structure, a middle ring and a base structure. The cryostat will house the TF and PF assembly with the vacuum vessel, the radiation shields and will support all loads from them. The preliminary calculations of finite element analysis show that the former structure design should be modified. Fig. 15 shows the load considerations during analysis. The stress distribution on the cryostat is shown in Fig. 16.

Design and fabrication of test conductors: Two types of CICC and one type of BCC were chosen as the test conductors for R&D purposes [9]. With the cooperation of Chinese industries, three pieces of test CICC including one dummy CICC have been fabricated and delivered to ASIPP. The configuration of the test CICC is 3 × 3 × 3 × (6 + 1 tube). In the first stage of the cable, a pure copper strand is added to increase the ratio of copper to superconductor [10]. A spiral tube made of stainless steel strap is in the center of the conductor to relieve the inner pressure of the conductor during quenches. In the test CICC of PF, Cr coating on the surface of every strand is required, and a stainless steel foil of 0.05mm thickness is wrapped on the third stage of the cable to reduce A. C. losses. The final cable is wrapped by a stainless steel strap of 0.1 mm thickness for cable protection during jacketing. The conduit is made by continuous tube milling and seam tungsten-inert-gas (TIG) welding with the cable inside. 316L is selected as the conduit material in the test CICC. 316 LN will be the conduit material in real CICC of HT-7U. The designed cross-section size of the PF test CICC is 17.3 mm × 17.3 mm. In order to gain experience at different steps of test CICC fabrication such as Cr coating, cabling and jacketing, a dummy CICC of 350 m with the same configuration, strand diameter and size as the test CICC, but with all copper strands inside, was fabricated prior to the test CICC fabrication. To test the process of jacketing, several empty tubes had been fabricated and formed to required size. During the jacketing of the dummy CICC, the temperature of TIG welding had been measured and adjusted carefully to a suitable value. The PF test CICC of 375 m and the TF test CICC of 275 m were fabricated following the fabrication of the dummy CICC. In the third stage of cabling for the TF and PF test CICC, a voltage sensor wire of 0.4 mm diameter was added.

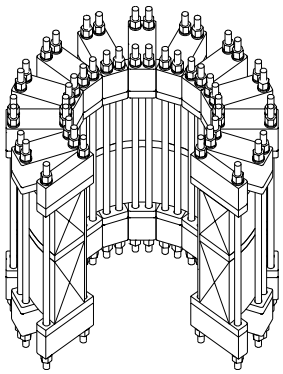

Fig. 17. Overview of central solenoid model coil.

TABLE VIII. MAIN PARAMETERS OF CSMC

Inner diameter	574 mm
Outer diameter	1140 mm
Height	485 mm
Number of turns	216
Operation current	18 kA
Maximum field	6.3 T (with 18 kA)
Total length of CICC	650 m
Inductance	36 mH
Stored energy	5.83 MJ
Test ramping rate	7 T/s

One type of test BCC has been designed. A transposed cable is housed in and soldered with a copper matrix. The surface of the copper matrix is roughened to increase the effect of heat exchange with liquid helium. Now, a 20 m BCC with copper cable has been developed in ASIPP to verify the technical processes. The test BCC of 10 m length using SSC cable is planned to be fabricated.

Design of CSMC and TFDC: To define design criteria and ensure fabrication processes, a central solenoidal model coil (CSMC) is designed and will be fabricated in ASIPP [11], as seen in Fig. 17. The designed maximum field on the coil is 6.3T with the operation current of 18kA. The main parameters of CSMC are shown in Table VIII. The test of mechanical and electrical performances, including stress and strain in the conductor, deformations on the winding, critical current at different temperature and self-fields are planned to be done. To determine the requirements of equipment and processes for D-shape bending and forming using an automated system to support continuous winding, a TF dummy coil (TFDC) of a 2/3 scale of the TF coil is designed and will be fabricated in ASIPP using the dummy CICC. Now, a double pancake of 1/10 scale of the TF coil of HT-7U has been fabricated using a copper conductor of rectangular cross-section of 8 mm × 10 mm to confirm the transition design.

Development of voltage sensors: The consideration of adopting co-winding sensors inside the conduit is based on avoiding compromise of the electrical insulation system of the conductor and obtaining better signal to noise ratio [9]. During cabling of the test CICC, a high-strength enamel-insulated copper wire of 0.4 mm diameter was co-wound inside the third stage of the cables as voltage sensor. Unfortunately, some local insulation had been damaged after jacketing. Now, a type of armored copper cable covered by stainless steel of 0.1 mm thickness and filled with polymer between cable and jacket is being developed successfully.

Development of helium isolators: High-voltage isolators at inlet and outlet of each helium channel of superconducting magnets are required. Two types of isolators made of ceramics and composite are the candidates. The composite one is in priority to be developed for its more secured properties. Labyrinth structure has been adopted in the design of the composite isolators. Six pieces of isolators have been fabricated with different processes and using modified insulation materials. All these isolators have been tested under pressure of 10MPa and electric voltage of 15kV between stubs from room temperature to liquid nitrogen temperature and liquid helium temperature. The test results show that some modifications should be done for the structure, insulation materials and fabrication processes.

Development of cooling stubs: In the manufacture of the HT-7U superconducting magnets of CICC, the method of continuous pancake winding will be adopted to reduce slices inside the coils. To reduce the cooling channel length and cool the coils more effectively, each CICC coil will be divided into several cooling channels. Each channel has an inlet stub and an outlet stub attached to the conductor surface. To avoid the damage of cables and degradation of superconductor performances, following considerations have been taken during installation of helium cooling stubs:

- to avoid the damage of cables during conduit and foil penetration, a special and extreme care processes should be adopted;
- to control the temperature inside cables, TIG welding of intermittent process will be helpful. And the region of the cable immediately under the stub must be cooled in an effective way.

At present the empty conduits are being used for penetration and welding trials in ASIPP. Important examination for stubs should be the leak test after thermal cycling between room temperature and liquid helium temperature.

Separable joint for CICC: A type of separable joint for the CSMC has been designed and is under fabrication in ASIPP. The joint consists of two copper conjunctions and two copper lids. After two terminals of the cable being soldered with the joints, two joints will be soldered and connected by bolts. Because of the requirement of separability, the separable and massive conjunctions are needed. The A.C. losses of the separable joint may be higher, but the resistance may be low. A compact joint used in the TF and PF systems will be developed.

Test of strands and sub-cables: To ensure feasibility, the superconducting strands and sub-cables need to be tested. Up to now, the $I_c(B)$ of strand samples has been tested in different background fields from 5 T to 7 T. The test results indicate that $I_c(B)$ of most strands tally with the values provided by the vendor. In the primary test of the first stage of sub-cables, no significant degradation of the critical current of strands has been shown. The second stage and the third stage of sub-cables are planned to be tested in the future. The test of A. C. losses of strands is in progress. The strands will be wound on a spool and located in a background field of less than 6 T with a verifying field.

Development of winding machine for CICC coils: To fabricate PF or TF coils in pre-bending and continuous pancake winding way, a winding machine has been designed and fabricated in ASIPP. To understand the bending/forming behavior of CICC and formulate the specifications of the machine and manufacturing procedures, principle tests have been demonstrated by bending/forming a short piece of the dummy CICC. Now, trials and tests are being done using the empty conduits and the dummy CICC to determine the elastic range of the conduit and the relationship between deflection and deformation of the conduit after it is removed from the machine.

Development of the test facility: A full size TF coil is planned to be fabricated and tested and essential test on every TF coil and eight PF coils must be done to ensure coil qualification before they are installed in the device. So, a test facility is being designed. The test facility consists of a cryostat with a nitrogen shield, a vacuum pumping system, a power supply system, a quench detection and protection system, support structures and current leads. The support structure for test magnets inside the cryostat is similar to the support designed for the magnets of HT-7U. One section of the nitrogen shield will be designed in a similar structure as the radiation shields of HT-7U to see if it works properly. A pair of 18kA current leads will also be designed for test magnets. The vacuum pumping system, the power supply system and the quench detection and protection system not only will be used in the test facility system, but also may be reused in the HT-7U system after modification and upgrade.

Design of prototype segment of vacuum vessel: A prototype 1/16 segment of the vacuum vessel is required to obtain design and fabrication experience which will benefit final design and subsequent fabrication of the vacuum vessel. A prototype segment of the vacuum vessel is planned to be designed. It consists of two 11.25° segments of the vacuum vessel body, one radial port, two vertical ports and a support assembly. The arrangement of heating elements and cooling channels will be designed, too. The prototype segment of the vacuum vessel will be used to test deformations and stress with the simulation forces on it and test temperature distribution during simulation bake-out. The assembly processes of PFC will also be simulated inside the prototype segment.

Conclusions

The preliminary engineering design has begun, which incorporates superconducting magnet systems of TF and PF, vacuum vessel, thermal shields, cryostat and current leads. The R&D programs on the HT-7U tokamak device are in progress, which focuses on the design and development of conductors and model coils, test facility , winding machine, prototype of one 1/16 segment of the vacuum vessel, and some key technologies. Because the detail physics design related to the device has not finished, some improvements on the engineering design may be required and even significant changes in configuration may be required in the near future. The future thermal and stress analysis for each component of the device shall be performed in detail. The R & D program will also be continued further in the future.

ACKNOWLEDGEMENTS

All works mentioned above are the efforts of the HT-7U Project Team.

REFERENCES

[1] T.Wu, et al., “The Project of HT-7U and its Progress”, MT-15, 20-24, Oct., 1997, Beijing.
[2] T.Wu, et al., “The HT-7U Project and its Preliminary Engineering Design”, Fusion Engineering, Proc. Symp. San Diego, 1997, Vol. 1, 249-252.
[3] Y.Wu, et al., “New Results of PF Calculation”, personal communication, 1998.
[4] J.Xiao, et al. “Preliminary Results of 15.5 kA CICC Calculation and Analyses”, personal communication, 1998.
[5] Wang, “Static Structural Analyses of Some Key Parts for the HT-7U Device”, Fusion Technology, Proc. Symp. Marseille,1998, Vol. 2, 1741-1744.
[6] P.Khvostenko, I.A.Posadsky, “Calculations of Heat Load on the HT-7U Cryogenic System”, ASIPP report, 1998.
[7] V.Alexandrov, “Calculation and Draft Design of the Chamber Baking System”, ASIPP report, 1998.
[8] V.Alexandrov, “ Calculation and Designing of the Water Cooling System for Steady-state Operation”, ASIPP report, 1998.
[9] T.Wu, et al., “Present Status of the R&D Programs on the HT-7U Tokamak Device”, Fusion Technology, Proc. Symp. Marseille,1998, Vol. 2, 1679-1682.
[10] D.Weng, et al., “Conductor Fabrication for the HT-7U Model Coil”, Fusion Technology, Proc. Symp. Marseille,1998, Vol. 2, 891-894.
[11] Z.Li, et al., “The HT-7U Superconducting Tokamak Model Coils”, Fusion Technology, Proc. Symp. Marseille,1998, Vol. 2, 775-778.

DESIGN OF PLASMA FACING COMPONENTS FOR THE SST-1 TOKAMAK

S. JACOB, D. CHENNA REDDY, P. CHOUDHURY, S. KHIRWADKAR,
R. PRAGASH, P. SANTRA, Y.C. SAXENA, P. SINHA
Institute for Plasma Research,
Bhat, Gandhinagar, India

Abstract

Steady state Superconducting Tokamak, SST-1, is a medium sized tokamak with major and minor radii of 1.10 m and 0.20 m respectively. Elongated plasma operation with double null poloidal divertor is planned with a maximum input power of 1 MW. The Plasma Facing Components (PFC) like Divertors & Baffles, Poloidal limiters and Passive stabilizers form the first material boundary around the plasma and hence receive high heat and particle fluxes. The PFC design should ensure efficient heat and particle removal during steady state tokamak operation. A closed divertor geometry is adopted to ensure high neutral pressure in the divertor region (and hence high recycling) and less impurity influx into the core plasma. A set of poloidal limiters are provided to assist break down, current ramp-up and current ramp down phases and for the protection of the in-vessel components. Two pairs of Passive stabilizers, one on the inboard and the other on the outboard side of the plasma are provided to slow down the vertical instability growth rates of the shaped plasma column. All PFCs are actively cooled to keep the plasma facing surface temperature within the design limits. The PFCs have been shaped/profiled so that maximum steady state heat flux on the surface is less than 1 MW/m^2.

1. Introduction

A Superconducting Steady state Tokamak, SST-1, is being designed to address some of the physics and technological issues related to steady state tokamak operation. The proposed tokamak is a medium sized device with major radius of 1.10 m and minor radius of 0.20 m. Machine parameters of SST-1 are given in Table 1. Elongated plasma operation with double null poloidal divertor and a maximum steady state input power of 1 MW is planned. Plasma facing components of SST-1, comprising of Divertors & Baffles, Poloidal limiters and Passive stabilizers are to be designed to accommodate the envelope of equilibria defined by elongation, κ = 1.7 to 1.9, triangularity, δ = 0.4 to 0.7 and plasma internal inductance, l_i = 0.75 to 1.40. In long pulse (quasi-steady state) discharges, like the one in SST1, the design of plasma facing components have to ensure steady state heat removal capability. Particle removal in steady state is also a major concern. The latter requires the divertor to be compatible with high pumping speed requirement.

TABLE 1. BASIC MACHINE PARAMETERS OF SST-1

Major radius, R_o	=	1.10 m
Minor radius, a	=	0.20 m
Elongation, κ	=	1.7-1.9
Triangularity, δ	=	0.4-0.7
Internal inductance, l_i	=	0.75-1.40
Toroidal field at R_o , B_0	=	3 T
Plasma current, I_p	=	220 kA
Pulse duration	~	1000 s
Plasma species		Hydrogen and Limited Deuterium
Configuration		Elongated/D-shaped, SN/DN divertor Plasma

The poloidal limiter, divertor, and passive stabilizer in SST-1 are actively cooled so as to keep the surface temperature of the plasma facing components less than 1000^{o}C. In the present design, the steady state heat removal capability is limited to a maximum of 1 MW/m^2 due to mechanical attachment scheme adopted for actively cooled of PFCs. The plasma facing component surfaces have been profiled/shaped so that the maximum steady state heat flux on the surface is less than 1 MW/m^2. The PFCs are designed for baking at 350^{o}C.
The plasma facing components will be experiencing large electromagnetic forces during VDEs and disruptions due to induced eddy currents and also due to halo currents. The PFCs and their support structure have to be designed to handle these large electromagnetic loads. At the same time the supports have to be flexible enough to keep thermal stresses within acceptable limits during baking and/or during steady state operation. The support structure is being designed to meet these conflicting requirements. Here we discuss the requirements and the design adopted to meet these requirements on the plasma facing components for steady state operation.

2. Design requirements

2.1. Operational and configurational requirements

Divertors are to be designed for worst possible heat load when 80% of input power is conducted across the separatrix. The inboard and outboard divertors are designed to receive 0.15 MW and 0.35 MW of power respectively. The divertor geometry should be such that neutral pressure in the divertor region should be high for efficient pumping of the divertor region and reduction of electron temperature due to high recycling. A closed divertor geometry will be the ideal choice where the recycled particles are directed away from the plasma. To ensure a closed divertor configuration a set of baffles are required.
A set of poloidal limiters are required to assist the plasma breakdown, current ramp-up and current ramp-down and for the protection of RF antennae and other in-vessel components during steady state operation and during VDEs and disruption. The outboard limiter is to be made movable to offer effective protection to the antennae that are movable. The inboard and outboard set of limiters are to be designed to take about 4% of the input power during steady state operation and up to 50% of the input power during plasma current ramp-up and ramp-down phases (up to about 4 seconds) and during short duration circular plasma operation (in the initial phase of SST-1 operation).
A set of passive stabilizers are required for SST-1 to slow down the vertical instability growth rate to ensure the feasibility of active feedback control of the vertical instability. The passive stabilizers are toroidally continuous and in saddle configuration forming a conducting shell around the plasma. The passive stabilizer should be made of high electrical conductivity material (≥93%IACS) and possess good mechanical properties to withstand electro-magnetic forces generated during VDEs and disruptions due to induced currents.
Plasma facing surfaces of the PFCs are to be kept below 1000^{o}C during steady state operation. The stabilizer plates are to be kept below 150^{o}C to ensure good electrical conductivity of the material. Hence active cooling of PFCs are essential. The PFCs may need to be baked up to 350^{o}C for about 48-72 hours to reduce impurities into the plasma and to have good density control. The systems are to be designed to satisfy this requirement. The plasma facing components will be experiencing large electro-magnetic forces during VDEs and disruptions due to induced eddy currents and due to halo currents. The PFCs and their supports have to be designed to handle such high electro-magnetic loads. At the same time the supports have to be flexible enough to keep thermal stresses within acceptable limits during baking and/or during steady state operation. The PFC designs should be modular for easy maneuverability and maintenance inside the vessel and should offer enough flexibility to align the components with respect to the magnetic fields. The module joints of passive stabilizers should ensure the required electrical conductivity for passive stabilization.

2.2. Requirements onm materials

Very high thermal conductivity and good thermo-mechanical properties etc. are essential requirements for candidate materials of SST-1 plasma facing armor material. Since tolerance level of low-Z

impurities in plasma is significantly higher than for high-Z impurities, low-Z material like Beryllium or Carbon based materials are preferred over high-Z materials like Tungsten or Molybdenum as the armor material. Though Beryllium has certain advantages over Carbon based materials, Carbon based materials are chosen as PFC-armor due to their wide operational experience and due to non toxicity. Isostatically pressed fine grained graphite will be the base line armor material for PFCs of SST-1 tokamak.
Good thermal conductivity and good mechanical behavior at elevated temperatures and after exposure to high temperatures for long duration is required for actively cooled substrate of divertor and limiter assemblies. In addition to the above properties passive stabilizer material requires high electrical conductivity at elevated temperatures. Copper based alloys like Copper-Zirconium or Copper-Chromium-Zirconium will be the most suitable materials because of their good electrical and thermal conductivities and good thermo-mechanical properties and relatively less degradation of mechanical properties after exposure to high temperatures for long duration. Stainless steel (SS-304) and to a certain extent Inconel are the baseline materials for PFC support structure and fasteners.

3. Design description

3.1. Divertor & baffle

The elevation view of divertors along with other PFCs are shown in Figure 1. The inboard and outboard divertor plates are designed for the worst possible heat loads by assuming in-out asymmetry of 1:2 (SN) for the inboard divertor and 1:4 (DN) asymmetry for outboard divertor. The up-down

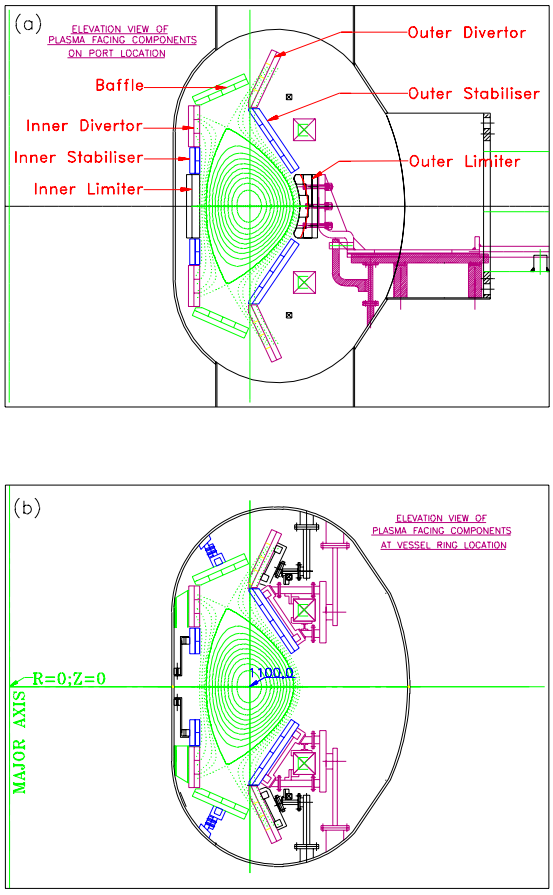

FIG. 1. Elevation view of the Plasma facing components (a) at the port location with limiter supports and (b) at the vessel ring location with supports of divertor and passive stabilizers.

asymmetry of 1:1.2 has been assumed for taking into account the relatively higher power loads on the divertor plates facing the ∇B drift direction for ions. The normal incident peak heat flux (calculated by assuming SOL width of 5 mm for heat flux, λ_q, at the outboard mid-plane) on inboard and outboard strike point is 1.6 MW/m^2 and 5.6 MW/m^2 respectively. The poloidal inclination of the outboard divertor plates is adjusted so as to have the heat flux averaged over 50 mm poloidal length (typical width of a graphite tile) at the strike point to be less than 0.75 MW/m^2. However, the inboard divertor is not inclined to the optimum requirements but are kept parallel to the vacuum vessel due to space constraints. Still, the average heat flux is in the tolerable limits. The target points of inboard as well as outboard divertor plates have been chosen at a distance as large as practicable from the null point. This reduces the electron temperature at the target plate and decreases the impurity influx from divertor region into the core plasma region. A baffle has been incorporated in the design so as to form a closed divertor configuration, which helps in increasing the neutral pressure in the divertor region thus improving the neutral particle recycling. The baffle is designed assuming an average heat flux of about 0.6 MW/m^2.

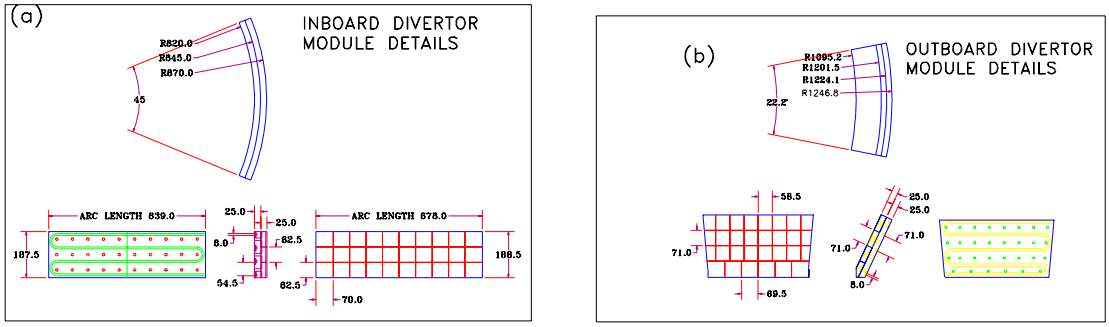

FIG. 2. Module dimension Details of (a) inboard divertor and (b) outboard divertor.

In the proposed design, the divertor assembly consists of graphite tiles mechanically mounted on a 25 mm thick back plate made up of copper alloy with a 0.2 to 0.5 mm thick flexible graphite foil used as a compliant layer for improving the contact conductance. The inner and outer divertors are in modular form for easy handling. The inner one consists of 8 modules each on top and bottom and the outer one consists of 16 each on top and bottom. The dimensions of the modules are shown in Figure 2. The top and bottom baffles consist of 8 modules each.

3.2. Poloidal limiter

There are two outboard limiters placed 180^o apart (on port numbers 3 and 11) and two inboard limiters are placed at the same toroidal location.

A set of limiters to accommodate various plasma equilibrium configurations, from circular to highly D-shaped plasmas, is designed. The plasma configuration with κ=*1.8* and l_i=*1.4* is taken as the reference equilibrium for the outboard poloidal limiter design. On the inboard side, a safety limiter is placed 30 mm away from the separatrix. The front face of the limiter is flush with inner passive stabilizers and divertors. The height of the set of limiters is restricted to ±0.145 m, so as to fill the vertical opening between the top and bottom passive stabilizers, and to allow thermal expansion and other required clearances. The horizon of the outboard poloidal limiter plasma facing surface conforms to a circular arc of radius 0.30 m centered at the major radius of 1.03 m on the midplane up to a height of ± 0.125 m. From ± 0.125 m to ± 0.145 m vertically, appropriate poloidal curvature is made to avoid interference with divertor operation at high κ and l_i equilibria. For the reference equilibrium, the front edge of the limiter closely approximates the +3 cm flux surface. For this configuration, a peak heat load of 6.4 MW/m^2 is expected for normal incidence. As we limit the steady state heat removal capability to less than 1 MW/m^2, the limiter surface is shaped/profiled in the toroidal direction. We opted for a semicircular shape with the front edge having a radius of curvature of 1.095 m in the toroidal direction. The toroidal width of the limiter is 0.37 m with appropriate curvature at the ends. Figure 3.(a) shows the outboard limiter dimensions.

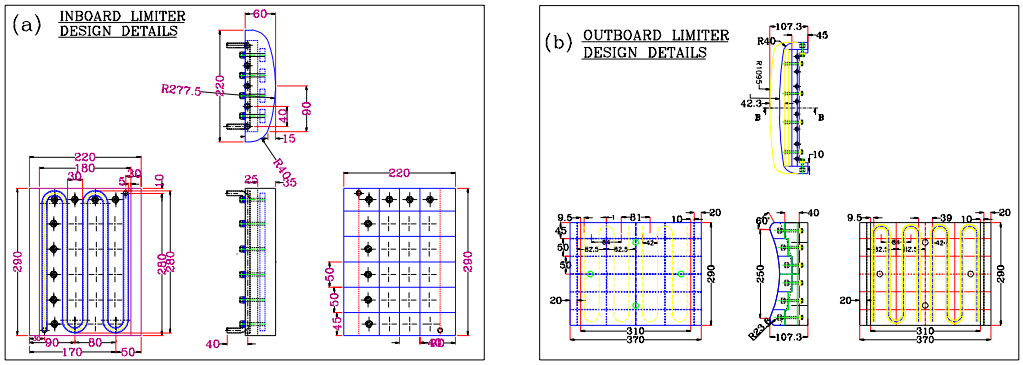

FIG. 3. Design details of (a) Inboard limiter and (b) Outboard limiter.

For the inboard limiter also, the peak heat load for normal incidence is estimated to be 6.4 MW/m^2. To reduce the heat flux to less than 1 MW/m^2, this limiter is also toroidally profiled. As mentioned above, a semicircular shape with the front curvature of 0.278 m in the toroidal direction has been adopted. The toroidal width of the inboard limiter is 0.22 m with optimum curvature at the edges. The design details are shown in Figure 3.(b).

3.3. Passive stabilizers

There are two pairs of stabilizers one on the inboard and the other on the outboard side of the plasma, placed above and below the midplane. At one toroidal location the top and bottom plates are connected with current bridges to make a saddle configuration. The heat loads during normal operation on the stabilizers are very low. However, the passive stabilizers have been designed to accommodate heat flux up to 0.25 MW/m^2. On 25 mm thick copper alloy stabilizer plate, 20 mm thick graphite tiles of suitable dimensions will be mechanically attached with 0.2 mm flexible graphite compliant layer. With the active cooling, the plate temperature will be about 150^{o}C and the graphite surface will be below 300^{o}C.

The passive stabilizers will be made by joining a number of modules *in-situ* with very low contact resistance (mechanical) joints. Each of the inner top & bottom stabilizer will consist of 8 modules, weighing about 20 kg each. Each of the outer top & bottom stabilizers will be made of 16 modules, weighing about 45 kg each. Figure 4 shows the dimensions of the inboard and outboard stabilizer modules.

The inner and the outer current bridges will be of 'Radial Lap' type with appropriate geometry and cross-sections of the vertical straps to withstand the forces and meeting the least possible resistance in the saddle path and to minimize the error fields. To prevent flow of induced toroidal currents in stabilizer loops through the supports, during VDEs and disruptions, the support structures of stabilizers are electrically insulated from the vacuum vessel and shunt resistances of appropriate values are provided across the electrical breaks and across the current bridges.

3.4. Cooling and baking of PFCs

All PFCs are cooled and baked by channels embedded in the copper-alloy back plates. De-ionized water at about 35^{o}C will be used for cooling of the PFCs and Nitrogen gas at about 400^{o}C will be used for baking. All PFC modules, except Outboard limiter will have one micro-circuit each. The outboard limiter will have two microcircuits, to optimize the flow parameters. Initial flow parameters for cooling is arrived through analytical calculations. Since the same channels are being used for cooling and baking, the compatibility of the layout for both is checked and the channel layout is finalized suiting the requirement of the each subsystem for baking and cooling. The flow parameters thus

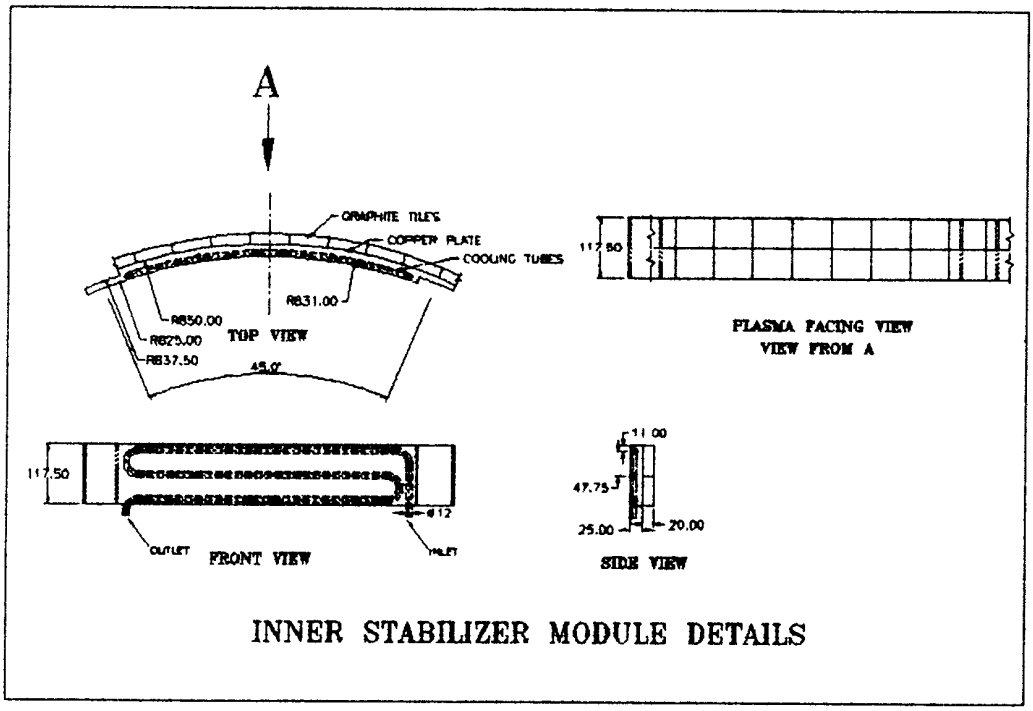

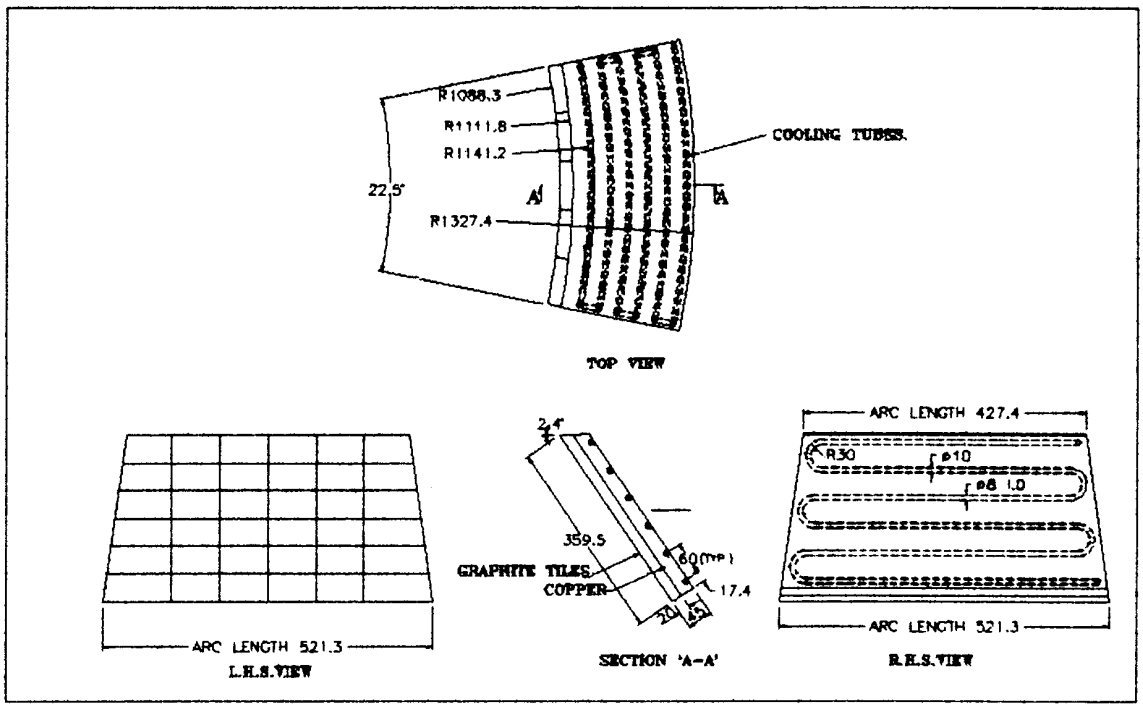

FIG. 4. Module dimension details of (a) Inboard and (b) Outboard passive stabilizer.

derived are used in finite element calculations to check the temperatures of various materials in steady state and transient events. Finite element analysis is carried out using ANSYS®, assuming the worst case scenarios for each component. Figure 5.(a) shows finite analysis results for a typical case of inboard divertor plate where the heat flux is falling exponentially and Figure 5.(b) shows a typical case with uniform heat flux of 0.25 MW/m^2 on the passive plates. The flow parameters for SST-1 plasma facing components are shown in table 2 and table 3.

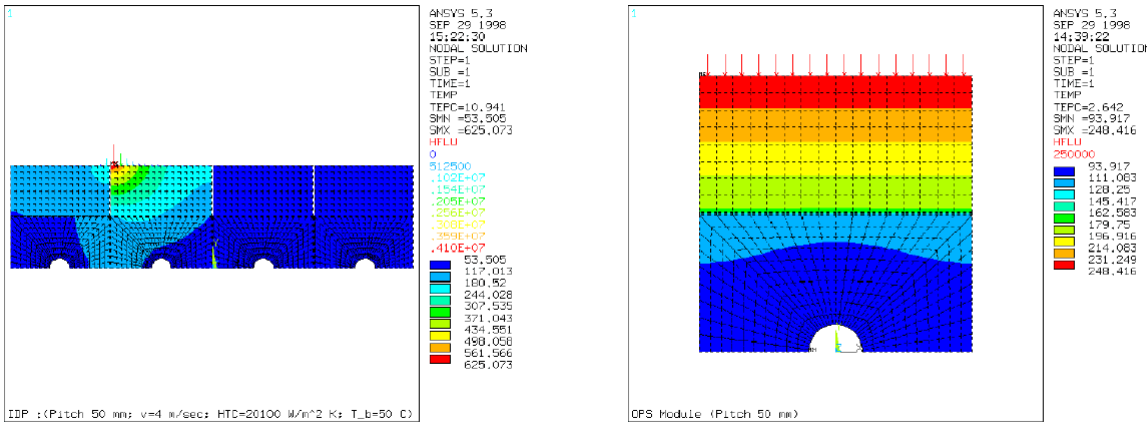

FIG. 5. Finite element analysis for (a) exponential heat flux profile as in divertor and (b) uniform heat flux of 0.25 MW/m^2 as in passive plates.

TABLE 2. COOLING PARAMETERS OF THE PFCs

	IDP	*ODP*	*IPS*	*OPS*	*IL*	*OL*
Diameter (mm)	10	10	10	10	8	8
Mass flow rate (kg/s)	0.310	0.310	0.271	0.271	0.223	0.223
Velocity (m/s)	4	4	3.5	3.5	4.5	4.5
Heat tranf. coeff. (W/m^2)	20,000	20,000	18,000	18,000	22,000	22,000
In-out temperature (^{o}C)	35/85	35/85	35/85	35/85	35/85	35/75
Pressure drop (bar)	1.81	1.92	1.21	1.75	1.96	1.30
Cu plate surf. temp. (^{o}C)	164	194	110	116	152	206
Compl. Layer temp. (^{o}C)	172	342	172	178	158	443
Graphite surf. temp. (^{o}C)	641	766	241	248	846	881

TABLE 3. BAKING PARAMETERS OF THE PFCs

	IDP	*ODP*	*IPS*	*OPS*	*IL*	*OL*
Diameter (mm)	10	10	10	10	8	8
Mass flow rate ($\times 10^{-3}$ kg/s)	5.27	3.91	6.52	7.13	6.93	7.54
Velocity (m/s)	40	30	32	35	34	37
Heat tranf. coeff. (W/m^2)	413	342	332	380	369	390
Out temperature (^{o}C)	361	364	359	352	353	356
Pressure drop (bar)	0.48	0.23	0.30	0.52	0.43	0.47
Graphite surf. temp. (^{o}C)	350	350	350	350	350	350

3.5. Tile design and mounting

One of the major constraints of PFC design is the tile attachment scheme. Though graphite tiles that are brazed to copper back plate are preferred for high heat transfer, we opted for mechanically attached tile system in the initial phase of operation. Hence heat removal capability is limited to less than 1 MW/m^2. The design adopted for the PFCs is shown in Figure 6 with typical dimensions. Mechanical stress analysis is carried out using ANSYS®. A more detailed thermo-mechanical analysis is underway. Initial analysis shows that the design can be used for heat fluxes up to about 1 MW/m^2. For Inner and outer divertors 25 mm thick graphite tile is bolted to actively cooled copper back plate with 0.5 mm thick flexible graphite compliant layer. In the case of limiter, the tile thickness varies from

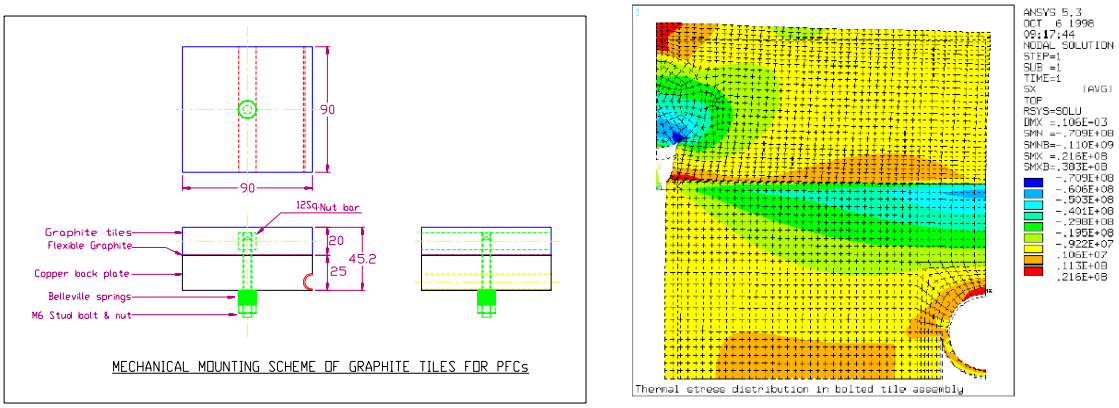

FIG. 6. (a) Tile attachment scheme of PFCs with typical dimensions. (b) Finite element analysis result showing the thermal stresses with bolting.

40 to 22 mm, as it is profiled toroidally. Passive plates are covered by 20 mm graphite tiles. The design ensures graphite surface temperature to be less than 1000^{o}C.

3.6. Forces on the PFCs

SST-1 tokamak will operate plasmas of D-shaped cross-section and such plasmas are inherently unstable for motion in vertical direction. Because of good inductive coupling of the PFCs with the plasma, the movements of the plasma or the alterations in the plasma current cause eddy currents to be induced in these structures. Interaction of these currents and fields generates significant electro-magnetic loads on the PFCs. Additional forces arise from the development of the '*halo*' plasma. This forms when the shifted plasma has physically touched the metallic structures like divertor or baffle, with a concomitant decay in plasma current. The halo plasma causes halo currents to flow poloidally in the PFCs and vessel and leads to additional forces. The loads on the PFCs have been calculated for these events. A typical scenario modeled is an upward VDE up to Zp=0.25 m, followed by disruption of full plasma current in 1 ms. The plasma position and current are given an ad-hoc but typical wave form for calculating eddy currents. The loads are calculated using a finite element code, EFFI, where the PFCs are modeled as toroidal filaments with appropriate cross-section. There are large forces on passive stabilizers due to toroidal eddy currents. The outboard divertors and baffles do not form a toroidal loop and there is shielding of the PFCs from the inner vessel post. The worst-case halo current forces have been estimated by assuming 0.4 times plasma current with a toroidal peaking factor of 2 on the halo current, and the halo current traversing the full poloidal length of the PFCs.

3.7. PFC support structure

The support structures of divertors and passive stabilizers are designed as per the requirements of modularity of the components for easy handling during assembly and disassembly of modules inside the vacuum vessel within the limited space. The supports are also designed to withstand the static (dead) weights of the PFCs and impulsive electromagnetic forces during VDEs, disruptions and due to halo currents. The supports are designed to allow thermal expansion of the components (by deflecting the support structure elements) during baking to limit thermal stresses within acceptable limits. Differential thermal expansions of the vessel, the PFCs and the support itself, during baking and during normal (steady state) operation are taken care of in the design. The elevation view of supports of Divertors and Passive stabilizers is shown in Figure 1.(a). The Outboard limiter is mounted on a movable support structure attached on radial port with suitable vacuum interfaces.

4. Conclusion

The design of the plasma facing components for the SST-1 tokamak is completed. The steady state operational requirements put stringent constraints on materials, heat removal systems and the design options. Carbon based materials are chosen as plasma facing material while copper based alloys are opted for the heat sinks as well as passive stabilizers. Thermal hydraulic calculations were done which gave reasonable flow parameters ensuring the design requirements on the surface temperatures of PFCs. The design of the divertor and baffle ensures the maximum heat flux is less than 1 MW/m^2 and provides a closed divertor configuration. This in turn enhances the neutral pressure and increases recycling. The limiters are designed to protect the RF antennae and at the same time to assist the various start-up scenarios. The design of the passive stabilizers ensures the feasibility of active feedback control of the vertical instability by slowing down the growth rates. The engineering design of various PFCs and their supports is currently underway.

STEADY STATE NEUTRAL BEAM INJECTOR

S.K. MATTOO, M. BANDYOPADHYAY, U.K. BARUAH, N. BISAI,
A.K. CHAKRABORTY, CH. CHAKRAPANI, M.R. JANA, M. BAJPAI,
P.K. JAYKUMAR, D. PATEL, G. PATEL, P.J. PATEL, V. PRAHLAD,
N.V.M. RAO, C. ROTTI, N.P. SINGH, B. SRIDHAR
Institute for Plasma Research,
Bhat, Gandhinagar, India

Abstract

Learning from operational reliability of neutral beam injectors in particular and various heating schemes including RF in general on TFTR, JET, JT-60, it has become clear that neutral beam injectors may find a greater role assigned to them for maintaining the plasma in steady state devices under construction. Many technological solutions, integrated in the present day generation of injectors have given rise to capability of producing multimegawatt power at many tens of kV. They have already operated for integrated time $>10^5$ S without deterioration in the performance. However, a new generation of injectors for steady state devices have to address to some basic issues. They stem from material erosion under particle bombardment, heat transfer > 10MW/m^2 , frequent regeneration of cryopanels, inertial power supplies, data acquisition and control of large volume of data. Some of these engineering issues have been addressed to in the proposed neutral beam injector for SST-1 at our institute; the remaining shall have to wait for the inputs of the database generated from the actual experience with steady state injectors.

1. Introduction

Neutral beam injection have demonstrated their capability in providing novel plasma configurations in short pulse confinement devices. These plasmas have demonstrated improved stability and confinements. The role of neutral beam injection as a sustaining device for thermal, particle and momentum influx to the plasma have therefore assumed prominence among all the options available for heating systems in steady state machines. The experimental objectives are simulation of ITER relevant experimental regimes.

To minimize the design efforts on all the components, this injector system design has relied on the existing database on the operating systems. The technological complications associated with the design of a neutral beam injector system however intensifies when long pulse operation is considered. The complications are component based and they are summarized in Table I below.

TABLE I. STEADY STATE ISSUES

Component	Issues
Back plate	Fatigue induced damages
Grids	Material erosion induced beam property degradation
Cryopumps	Requirement of frequent regeneration
Magnet	Inadequate space charge compensation
Heat removal system	Material erosion
Duct	Uncertain duct conditions at long operational pulses
Data acquisition system	Management of large volume of data accumulated during a shot
Power supply system	Steady state transmission of multimegawatts of power

These issues have been studied and recommendations have emerged on the design, fabrication and operation of specific systems for long pulse compatibility. Some of these recommendations have been incorporated in the design, while others shall have to wait until a data base on the performance is generated. These have been discussed in this paper.

The paper begins with a basic description of the system in Section 2, the problems associated with the beam formation system, transportation system and with the transmission and supply of multimegawatt of power and the management of a large volume of data are discussed in Section 3 . The concluding Section 4, presents a summary of the long pulse issues and ends with a discussion of the physics objectives that this technology mission is expected to make.

2. System description

For the SST-1 machine with parameters listed in Table II, the power required in neutral beam injection in the low and high density phases are 0.5 MW and 1.7 MW respectively. As shown in Fig.1, this requirement is accommodated through a tangential injection of the beam corresponding to a maximum absorption at the .98 m radius of tangency in the plasma. The beam parameters and its effect on the plasma have been modeled using the 1D transport code BALDUR, these have been summarized in Table III. The injection is expected to raise the ion temperature to ~1 keV, contribute to a fueling of ~ 4 torr lit/sec, impart a toroidal momentum of ~ 10^5 m/sec, drive a current of ~ 40 kA at the core of the plasma.

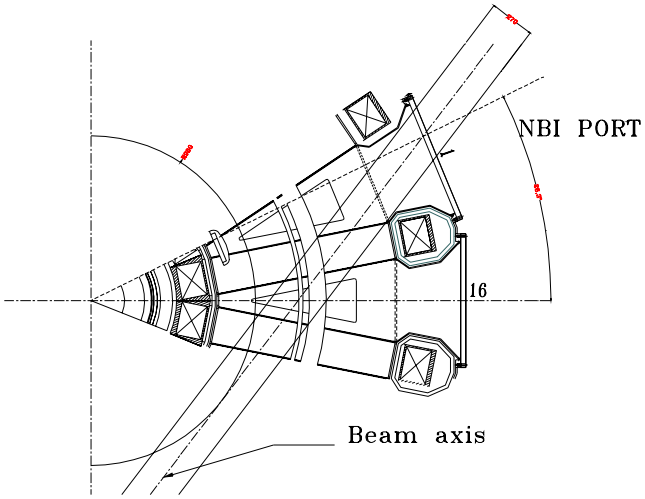

FIG.1. Tangential injection of the beam.

The beam-formation system in the injector is based a multipole bucket type plasma source where option of both checkerboard and supercusp magnetic geometry can be exercised. The extractor system is based on a shaped circular aperture geometry. The grid system is supported on the grid holders and the whole assembly is electrically isolated and mechanically supported by a set of three post insulators. The ion source is mounted on a ion source flange on the injector box with an isolation valve in between. The neutralizer is equipped with a provision of feeding gas up to 50 Torr lit/sec. The magnet system qualifies in its uniqueness through a short pathlength design. The field in the iron circuit is high ~2 T. The ion dump, scraper and the V-target assembly is based on the modular concept of a heat removal system elements. The V-target also acts as a preduct scraper in the synchronous mode of operation.

The vacuum system is designed for a reionization loss of < 5 % along the total path length. The data acquisition and control system for the injector system handles data from 600 channels and the data management system acquires, stores, displays and archives about 1 GB of data per shot.

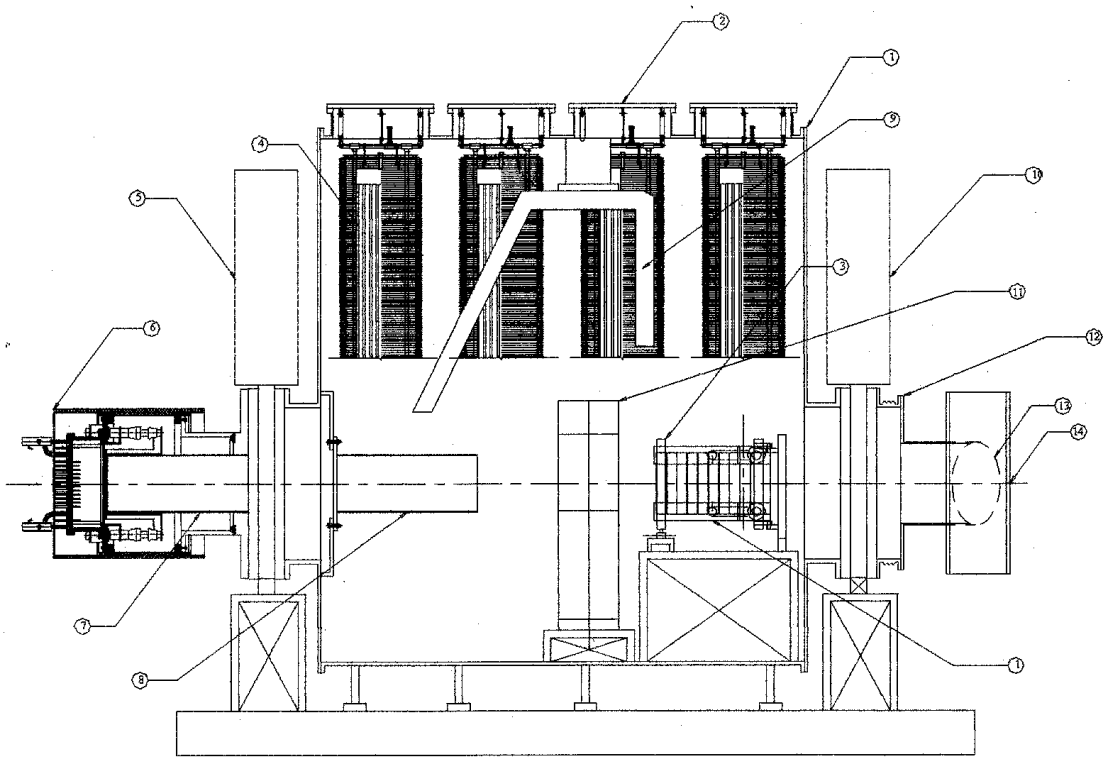

COMPONENTS:

1.INJECTOR BOX VACUUM VESSEL	5.ISOLATION VALVE-1	10.ISOLATION VALVE-2
2.CRYOPUMP SUPPORT FLANGE	6.ION SOURCE ASSEMBLY	11.MAGNET
3.MAGNET AND V-TARGET PLACEMENT PORT	7.NEUTRALISER FIRST STAGE	12.BELLOW
4.CRYOPUMP	8.NEUTRALISER SECOND STAGE	13.TOKAMAK CONNECTIONG PIPE
	9.ION DUMP	14.TOKAMAK COUPLING FLANGE

FIG. 2. Elevation view of injector system.

TABLE II. PARAMETERS OF SST-1

R (m)	A(m)	n_e (m^{-3})	κ	δ	T_e(keV)	I_p(kA)	$\tau_{E(}$ms)	T_p(S)
1.10	.20	2 x 10^{7}	1.7	0.67	1.0	220	14	1000

TABLE III. PARAMETERS OF NEUTRAL BEAM

Species	Energy(keV)	Power(MW)	Power density to plasma(MW/m^2)	% shine through	Focal lengths (m)	Diverg--ence
H, D	30–80	0.5–1.7	15–40	<5	7.1(h),5.4(v)	$<1^{o}$

TABLE IV. PARAMETERS OF THE INJECTOR SYSTEM

Component	**Description**
Plasma source	Multipole bucket. 24 filaments independently controlled. Density ~10^{12} cm^{-3}
Extractor system	Circular multi-aperture system. Extraction current density 230 mA/cm^2.
Neutralizer	2 stages. Length 2 m. ∫ndl ~10^{20} mol/m^2
Ion deflection magnet	Transmission typr. Maximum field 0.3 T in air & ~2.0 T in iron. Liner dissipation ~200 kW.
V-target	Movable. Designed to dissipate 2.5 MW of neutral beam power, at maximum flux of 10 MW/m^2.
Duct	Designed for a transportation current of ~100 A.
Vacuum system	Based on cryopumps. ~15 m^2 of active pumping area at 3.8 K.
Power supply system	Solid state modular supplies based on PSM. Filament supply independently controlled for the 24 sets.
Data acquisition system	Designed to handle 2 GB of Data over 500 channels. Real time display incorporated.

The power shall be delivered from a single beamline and the dynamic range of voltage shall be accommodated in a single source[1]. An elevation view of the beam line is shown in Fig. 2. The summary of the system design elements and the components therein are listed in Table IV.

3. Steady state issues

Steady state in the thermal effects are said to have been established in the actively cooled components of the injector systems operating in the range ~10-20 sec as these pulse lengths are two orders of magnitude greater than the thermal diffusion time scales. The real challenge in the steady state operation stems from the degradation in the material properties over long pulse lengths of ~1000 s. The important effects are erosion, fatigue induced creep, transition of the material into the plastic domain etc. Effect of these degradation on the material properties have been studied for the different components of the injector system. They are discussed below.

3.1. Beam formation system:

The back plate, the extractor system and the first stage of the neutralizer cell are the critical elements in the beam forming system.

3.1.1. Backplate

The backplate in the present design is based on the concept of the system operating in the JET PINI's [2]. However, there have been reports of failure of this component whenever there is an attempt to increase the power extracted from the ion source. The failures have been ascribed to a rise in the temperature of the copper surface under higher heat fluxes. This issue has been examined and its impact on the long pulse operation of this component have been assessed. The results of a 2D finite element analysis using ANSYS shows that surface temperature enhancement can be arrested with an enhancement in the flow rates by ~20% from the existing 8 gm/s along with a modification in the configuration of the flow channel where mixing of coolant is allowed [3]. The results of this analysis is presented in Fig. 3.

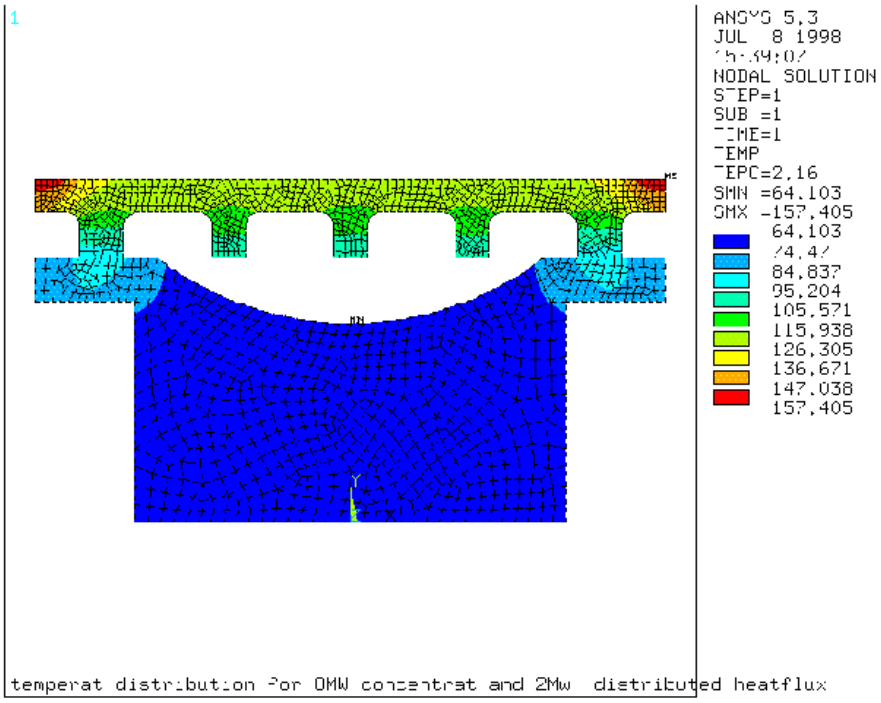

FIG. 3. Flow channel configuration of back plate (ANSYS Analysis).

3.1.2. Extractor grids

Material erosion induced degradation in the beam properties have been studied in relation to the performance of the grids. As evident from Fig 4, OFHC grids shows that beam divergence degrades by ~ 30% from an original value of 1^{o} after 10^{6} seconds of operation in Deuterium, when ~100 μm of material has eroded from the surface due to the incidence of 100 eV ion beams on the accelerator grid. The situation does not improve when Molybdenum grids are used, since the sputtering database predicts erosion rates comparable to that of copper at lower energies. The erosion effects are significantly reduced for both copper and molybdenum at lower voltages of the ion beam incident from the plasma source. This however, is accompanied by an increase in the divergence of the beam, the effect is represented in Fig. 5. Incorporating the recommendations of this study, for the long pulse operation of the grids, the beam line components have been designed to accommodate higher values of beam divergence.

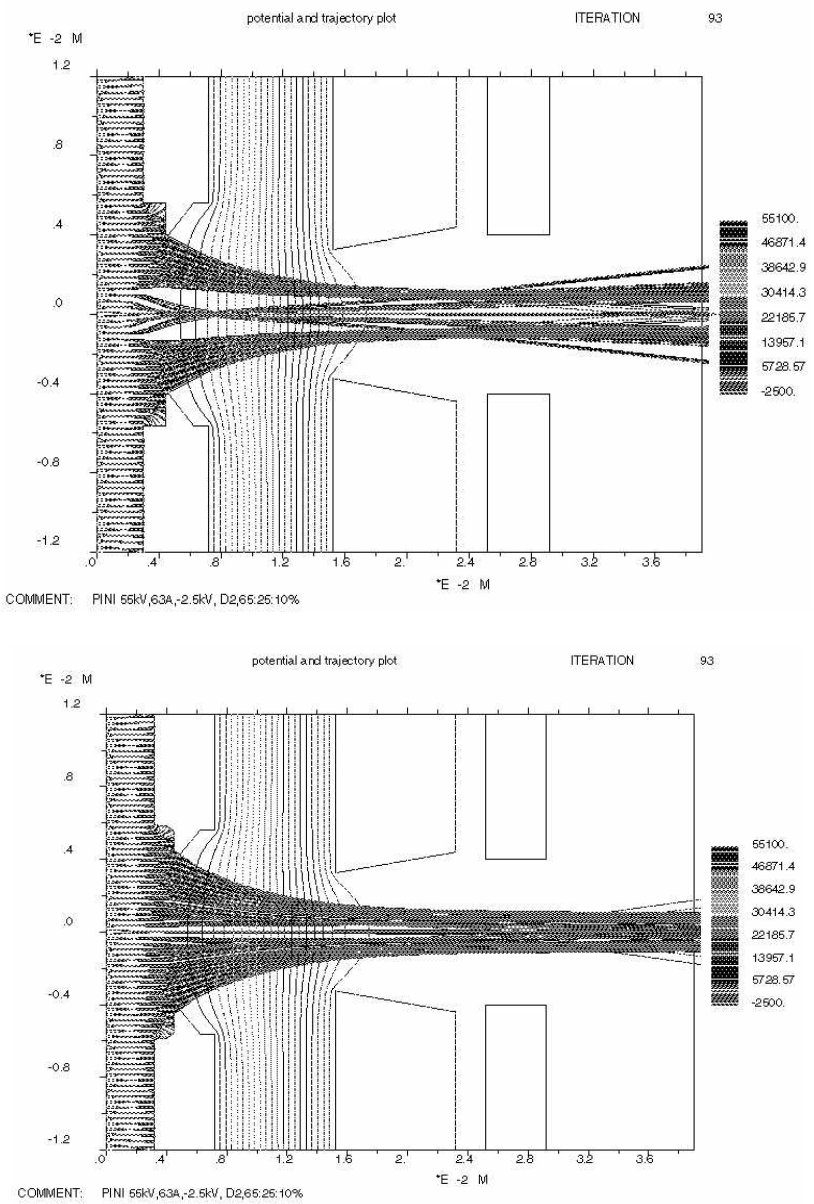

Fig. 4. Erosion effects in Extractor grid system.

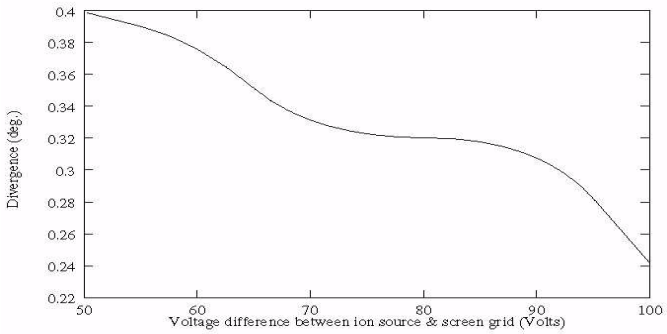

FIG. 5. Divergence as a function of voltage.

3.1.3. First stage of neutralizer

The first stage of the neutralizer, housed inside the earth grid holder has an access limitation for accommodating cooling provisions. However power dissipation estimates show ~70 kW of heat may be dissipated in this inaccessible section. This thin walled inertial structure has therefore been cooled through a set of embedded channels on this structure to dissipate ~100 kW of heat, this is shown in Fig 6.

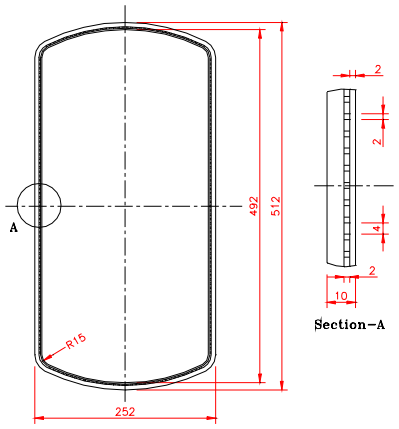

FIG. 6. Embedded cooling channels for neutralizer.

3.2. Beam transportation system

The magnet in the ion removal system, the heat transfer elements, the duct and the supporting vacuum system are the critical elements of the beam transportation system. The transportation system has been designed with the primary objective of compactness in its dimensions [4]. This objective has been met under the constraints of minimization of power density on the scrapers and the beam intercepting elements and minimization of the power loss inside the duct. The system design has utilized three numerical codes on beam transmission, magnetic fields and Monte Carlo simulation of the pressure profile.

3.2.1. Ion deflection magnet

The performance database on the magnet indicates that there is considerable reduction in the power dissipation on the magnet liner for a short path length magnet. The magnet design accommodates this need through a compact ~ 45 cm length. The ion beam traversing the magnet shall however be

subjected to space charge expansion of the beam, which is proportional to the operation of the beam. Experimental database does indicate a reduction in this loading when excess gas is made to flow within the pole pieces [5]. The long pulse design of the magnet has included these additional features of active liner cooling to dissipate up to 120 kW, and provision of additional gas feed up to 10 torr lit/sec within the magnet. In addition, to prevent excess loading on the LN_2 panels due to an estimated 26 kW of power in the devious particles, provisions of a high conductance ~10^6 l/s protection baffle the region between the magnet exit and the cryopump has been made in the beam line design.

3.2.2. Heat transfer elements

The limits of operation of the heat dissipation system are imposed by considerations of material erosion. Estimates suggests that ~ 2 mm of the beam facing surface erodes in 10^6 s which implies that these elements shall be replaced within a year of its operation. The operational experience with Hypervapotron in JET and their projected use during the initial phase of TPX corroborates this apprehension. Use of molybdenum or its copper alloy on the other hand enhances the lifetime of the panels by a factor of 8. Though molybdenum should have been a natural choice for the heat transfer elements, the present design is based on Cu-Cr-Zr alloy as it is felt that its reliability in long pulse operation, and cyclic loading conditions have not been established. Molybdenum is also associated with the problem of oxygen induced embrittlement. The water quality and the operating vacuum environment demand additional stringency. A database in this matter is necessary. Fabrication difficulty in molybdenum is another deterrent.

3.2.3. Duct

Duct design is one of the most critical areas of system design for tangential injection geometry. The pressure profile and therefore the possibility of reionized power loading on the duct walls enhanced by the focusing due to the vertical field poses serious hurdles for long pulse injection. In the present system an unique concept has been incorporated in the design of the duct where the tokamak port wall has itself been lined with a thin walled heat transfer system made of OFHC to dissipate the incident power flux and increase the conductance. The pressure profiles shown in Fig. 7 clearly indicate the reduction in the background pressure with the incorporation of this geometry. The scraping of the beam for the purpose of injection is carried out by the in-situ V-target in its partially open configuration.

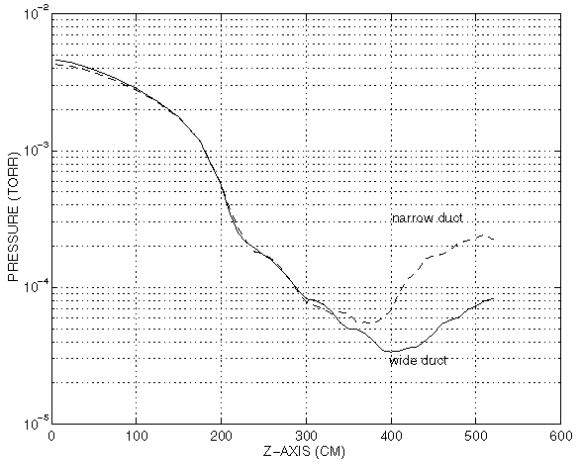

FIG. 7. Background pressure in duct.

3.2.4. Vacuum system

The vacuum system is based on cryocondensation pumping with the panels operating at 3.8K. Safety requirements for operation in hydrogen which limits the maximum pressure build up to 12 torr of partial pressure for hydrogen gas. This limits the accommodation of gas for a maximum of 4 shots of 1000 S in hydrogen or 5 shots of 1000 S in deuterium before the panels need to be regenerated. During

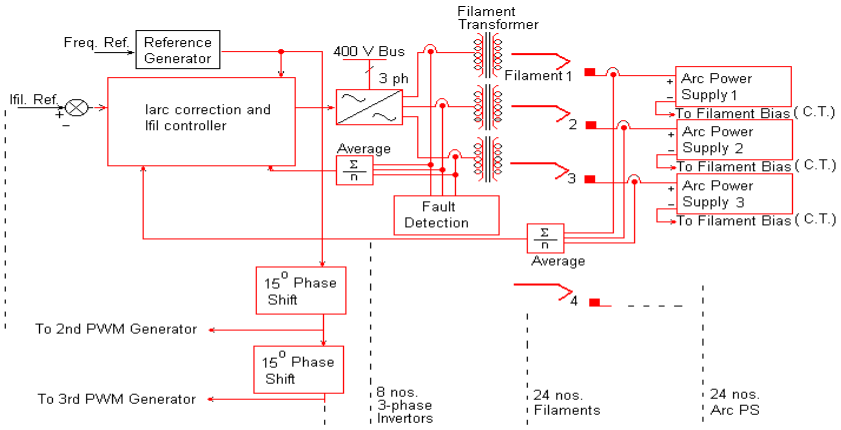

FIG. 8. Integrated arc and filament power system.

regeneration the panels are cycled to 77 K from 3.8 K. The flow channels in the LHe panel have therefore been optimized to accommodate a minimum quantity of LHe. Another related issue is the effect of hydrogen ice on the pumping performance of hydrogen. A prototype experiment designed to study these effects is expected to yield the desired data.

3.3. Power supply system

The HV regulated DC power supply for extraction is a wide dynamic range (4-80kV) and fast transient response (~20μS voltage rise time and ~5μS turn off time). The solid state power supply uses high frequency pulse step modulated switching [6]. Technical problems that are resolved are: transient free fast switching, efficient heat dissipation from semiconductors and low stored energy in the load side of the system. The multisecondary transformers are designed for very low stray capacitance of the secondary windings. The transmission line (~50m long) stores about 30 J energy, which is removed by a passive snubber on occurrence of grid sparkover. The arc and filament system is a closed loop system (Fig. 8) for controlling the discharge current by control of the actual heating current of each filament. The focus is on obtaining steady plasma density with temporal and spatial homogeneity.

3.4. Control and data acquisition system

For acquisition of about 600 data channels for each 1000 S injection shot, a data acquisition and control system based on VXI is used. Logical subsystems (e.g., vacuum, power supply, diagnostics, etc.) has been defined to build a structured distributed system where part of the system can run independent of the others. The volume of data acquired per shot is ~1GB. The data base manager is written with postgre.

4. Conclusions

The long pulse operational issues have been presented in this paper. Material erosion is one of the main concern. The design has incorporated some of the modifications necessary in the magnet and the cryopumps, as the indicators from the present database could be extrapolated over long pulse lengths. In the case of other components where predictions have emerged sufficient support from the database is not available. The present injector in its test stand operational mode is expected to generate the necessary database. The injector in is installation on the SST-1 machine is expected to yield a considerable database not only on the heating and fueling of a long pulse plasma but also on the

experiments on locked modes, hot ion H modes, high beta plasma, neutral beam injection controlled post Greenwald density limits, which shall be useful for deciding on the ITER relevant regimes.

REFERENCES

[1] CHAKRABORTY, A.K., et al., "Neutral Beam injector for Steady state super conducting tokamak" (Proc. Symp. on Fusion Technology, 1996), Lisbon.

[2] DUESING, et al., Neutral beam injector system, Fusion Technology, 11(1987)163-202.

[3] JAYAKUMAR, P.K., et al., "Engineering issues of a 1000 S ion source", Plasma Heating and Current Drive (Proc. Symp. Fusion Technology, 1998), Marseille, France.

[4] CHAKRABORTY, A.K, et al., "A compact beamline design for the SST-1 neutral beam injector" (Proc. Symp. on Fusion Engg., 1997), San Diego, USA.

[5] KESSLER, et al., "Investigation of collisional effects within the bending magnet region of a DIII-D neutral beam line" (Proc. Symp. on Fusion Engg.,1993), USA.

[6] TOMLJENOVIC, N, et al., "Solid state DC power supply for Gyrotron and NBI sources"(17th Symposium on Fusion Technology,)Rome, Italy.

THE RECONSTRUCTION OF HT-7 SUPERCONDUCTING TOKAMAK AND THE PRESENT STATUS OF HT-7U PROJECT

P.D. WENG
Institute of Plasma physics,
Chinese Academy of Sciences
Heifei, Anhui, China

Abstract

The first Chinese superconducting tokamak HT-7 was reconstructed from T-7. The main purposes of reconstruction are to improve the accessibility of the device and to provide a possibility of long pulse operation with high performance. The reconstruction has been done successfully. The HT-7U project has been approved and funded as a National Project, the engineering design and R & D are on the way.

1. Reconstruction of HT-7

The HT-7 Tokamak that was built at the Institute of Plasma Physics (ASIPP) in 1994 is the first superconducting tokamak in China (Figure 1). The main mission of HT-7 is to study the high plasma performance under the long pulse operation condition. The HT-7 tokamak is reconstructed from Russian Tokamak T-7. The main purposes of the construction are:

- To make the device with good accessibility by increasing new ports large enough to satisfy requirements of different physics experiments and diagnostics
- To provide the capability of long pulse operation with high power of auxiliary heating
- To increase the coil-case intensity for ensuring the magnetic field to reach its design value
- To raise the vertical field for satisfying the requirements of physics experiments.

FIG. 1. The HT-7 Tokamak.

To meet the above purposes, a series of important structural improvements were made during the reconstruction.
The coils of the superconducting magnet system (SMS) were rearranged to provide the possibility of increasing new larger ports on the vacuum vessel. The SMS of HT-7 consists of 24 coils and distributed uniformly around the torus. Two coils of T-7 were merged together to form one coil of HT-7, therefore, the number of coils of SMS reduced from 48 to 24, the angle between two coils increased from 6 degree and 9 degree to 15 degree. Thickness of the coil case was increased from 10 mm to 15 mm, forming a relatively strong vault structure to support the centering force of the coil.

A new vacuum vessel of HT-7 was designed and fabricated, 10 horizontal ports and 16 vertical ports for diagnostics and heating as well as 8 vertical ports for cooling were added. Plus 12 old ports, the new vessel has 46 ports in total. The width of the biggest ports was increased from 100mm to 245mm. Water cooling tubes were welded on the rigid sections of the vacuum vessel to remove the heat load during long pulse operation. Liner plates were installed to protect bellows and wall of the vacuum vessel from bombardment of high-energy particles. Electric heaters, which can bake the liner plates up to 250°C, were installed on the liner plates. Wall of the vacuum vessel can be baked to 150°C.
Corresponding with the above, necessary reforms of nitrogen screen and cryostat were made, the new ducts were added to increase ports of vacuum vessel, the cooling channel on the nitrogen screen as well as their inlets and outlets were rearranged.
Thirty three new ports on cryostat were increased, specially shaped rubber seals were used for the cross seal structure, therefore, the technical difficulty of unreliable cross-seal was solved and the vacuum of the cryostat was much better than the design value.
The superconducting current leads were optimized and reconstructed. As a result, the consumption of liquid helium for current leads is reduced from 63L/h to 20L/h. The new vertical coils were designed and fabricated, the maximum vertical field at the plasma center reach 2.2KG which is two times more than that of the original one of T-7.
Reconstruction of the tokamak has been done successfully. The accessibility of the device is improved significantly. Using optimized current leads, low heat losses cryogenic transfer line, high helium mass flow from injector and overcooled liquid nitrogen cool down the nitrogen screen, the long time stable operation of SMS was ensured under high heat loads due to increasing ports. The maximum field reached 2.5 Tesla. A series of physical experiments have been carried out, plasma current of 220KA and plasma density of $5 \times 10^{13} cm^{-3}$ were obtained. Lower hybrid current drive (LHCD) experiment has been performed, the longest pulse of current drive was 3.5 Sec for 100KA. It is the best experimental result of LHCD in China up to now.

2. Present status of the HT-7U project

The HT-7U project has been approved and funded as a National Science Engineering Project by Chinese government. It has begun in 1998 and will be completed in 2003. The main missions of the project are as follows:

- To construct and operate a non-circular cross-section tokamak with superconducting TF and PF coils.
- To develop advanced tokamak operating modes in steady-state operation.
- To investigate the optimization between high plasma parameters and its confinement performances in continuos operation.

2.1. Tokamak and vacuum system

The main parameters of HT-7U tokamak are as follows:

Major Radius	R	1.7	m
Minor Radius	a/b	0.4/0.8	m
Toroidal Field	B_t	3.5	T
Plasma Current	I_p	1	MA
Elongation	κ	1.6 - 2	
Triangularity	δ	0.4 - 0.8	
Pulse Length	t_{pulse}	60 - 1000	s.
Plasma Shape		Double /Single Null Divertor Limiter	

Current Drive and Heating

ICRF	3.5 (8)	MW
LHCD	4 (8)	MW
ECRH	0.5	MW
NBI	(4)	MW

The device consists of Superconducting TF and PF magnet system, Vacuum vessel, cryostat and the heat radiation shield. The detail structure is described in the paper [1].

The requirements of the inner vacuum chamber are ultimate pressure of $1 \times 10^{-5} P_a$, effective pumping speed 6000L/s (for divertor 40000L/s). 12 Turbo-molecular-pumps(TMP) plus Cryopump or Ti sublimation pump will be used for the divertor pumping, another 8 TMPs will be used for the vacuum vessel itself. The requirements for cryostat and current lead reservoir are ultimate pressure $10^{-3} P_a$, effective pumping speed 4000L/s. 8 TMPs will be used for them. A common primary pumping station including roots pumps and rotary pumps for all of the pumping systems will be adopted. Piezocrystal valves will be used for the gas puffing of vacuum vessel and divertor baffle.

2.2. Cryogenic system

The main cooled components are TF magnets, PF magnets, current leads, superconducting bus line, cryogenic transfer line and coolant control box, TF coil case, support structure and radiation shields.

Estimated heat loads are as follows:

	4.5 K **Operation**		80K **Standby**	
Radiation	240		240	7000
Conduction	115		115	1600
Convection	55		55	80
Joints	190		0	
AC Loss	400		0	100
SC Bus Line	5		5	500
Current Leads	8 g/s		5 g/s	
Transfer Line and valves	45		45	720
Sum	1050 W +8 g/s	+ 5 g/s	460W	10000

1.2-1.5 kW/4.5K plus 9-10 g/s liquefaction rate are required according to the estimation. Two 500 W/4.5 K refrigerators will be used to supply a mass flow rate of 9-10 g/s for all of the current leads.
One refrigerator with capacity of 1.2-1.5 kW will be used to cool the TF and PF magnets and the others. We plan to enhance MG-300 capacity up to 1.2-1.5 kW/4.5 K by adding expanders and increasing the mass flow rate. A set of refrigerator with capacity of 30 kW/80 K. to cool 80 K shields.

2.3. Power supply system

The TF power supply is used to energize TF magnet with maximum energy of 340 MJ. It can deliver 10 kA with the capacity of 500 kVA.
The PF power supply system consists of 6 groups. Three groups supply central solenoid coils, another 3 groups supply out PF coils; they can run simultaneously and will be modulated separately. The maximum current will be 20 kA. 100 MW flywheel motor generator will be used during start-up for

limiting the peak power from the grid. An additional power supply will be used for the fast feed back control coils
The capacity of existing power station will be increased from 8 MW to 63 MW, the grid voltage will be raised from 35 kV to 110 kV.

2.4. LHCD and ICRF systems

The LHCD system will be composed of two subsystems. One of them has an output power of 2 MW at a frequency of 2.45 GHz, another has an output power of 1.5 MW at a frequency of 3.7 GHz. The main parameters are listed as following:

2.45 GHz LHCD system (consists of 20 klystron amplifiers)

Output power	2 MW
Wave pulse	1000 sec
Efficiency	50%
Antennae	2 pieces, each consists of 80 subwaveguides
Spectrum	1.4 $N_{//}{}^{p}$ 3.0, $N_{//}$ 0.4
DC voltage	33 kV, voltage ripple 1%

3.7 GHz LHCD system (consists of 2 klystron amplifiers)

Output power	1.5 MW
Wave pulse	1000 sec
Efficiency	40%
Antennae	1 piece, consisting of 4 × 32 subwaveguides
Wave spectrum	1.35 $N_{//}{}^{p}$ 3.0, $N_{//}$ 0.23
DC voltage	65 kV, voltage ripple 1%

3. HT-7U ICRF heating system

The ICRF heating system for HT-7U superconducting TOKAMAK will consist of two subsystems. One has 2 MW output power, and another has 1.5 MW output power. The frequency range is from 30MHz to 110MHz. The specifications for this system are listed as following.

Output power	2MW & 1.5MW
Frequency range	30MHz~110MHz
Wave pulse duration	CW.
Antenna	4 loop antennas
Matching system	Stub tuner

4. Progress of R & D

The engineering design is on the way now. Part of R& D related with the Superconducting TF and PF magnet is carried out. 600 meters prototype of CICC conductor has been developed and fabricated, a winding machine, which will be used for CICC conductor, has been prepared already.

A model CS coil and a double pancake of dummy model TF coil have been designed and will be wound soon.

The design of test facility for TF & CS coils will be finished soon.

REFERENCE

[1] "Present Design of the HT-7U Tokamak Device" S. T. WU, IAEA Technical Committee meeting Steady-state Operation of Tokamak Oct. 1998

THE ASSEMBLY SIMULATION FOR HT-7U SUPERCONDUCTING TOKAMAK

W.W. XIAO, D.M. GAO
Institute of Plasma Physics,
Heifei, Anhui, China

Abstract

It is well known that the assembly process for Tokamak, especially for superconducting Tokamak is very complicated and difficult since Tokamak has its own structural features. Since the good performance of tokamak mainly depends on its assembly quality, it is very important that all contradictions and problems in assembly process should be found and solved as early as possible. In recent years the VPT (Virtual Prototype Technique) or MSS (mechanical system simulation) and its application has made big progress. It has become an engineering and analysis tool which can be easy to use by scientist and engineer from a complex and special research method. This paper emphasizes on the preliminary results of the digital simulation for assembly process of HT-7U Tokamak after making use of the VPT method.

SOME KEY ISSUES OF SUPERCONDUCTING TOKAMAK DESIGN

D.P. IVANOV

Russian Research Center "Kurchatov Institute",
Moscow, Russian Federation

Abstract

Some comments and recommendations concerning SC-magnet cooling scheme (preference of supplying fresh LHe directly into the inner turns), conductor design optimizations (suggestion of an improved CICC), testing programme (remarks concerning Short Sample tests, the ways to avoid of all coil tests before assembly - design which allows to change any coil without full disassembling of the device), support structure (which allows to adjust the position of magnet with respect to Vacuum Vessel), the need of access for changing of the in-vessel components, Vacuum Vessel baking requirements, approach to nitrogen shield design and some other points of projects under discussion at the meeting along with their basis will be given. In this presentation, I would like to comment on some of the engineering solutions accepted or suggested as possible variants in the projects under discussion as well as to give some recommendations based on the critical analyses of the experience in design, construction and operation of T-7, HT-7 and T-15 as well as of some information from other projects.

1. Cooling Method and Scheme

The values of toroidal field chosen in all the three projects is not too high - Bo=3-4T and Bm=5.7-7.0T. These values allow to use NbTi, so the choice of SC material made by SST-1 and HT-7U designers is quiet reasonable. But it is necessary to take into account that the temperature margin in this case is rather low, $T_c(B) - T_{op}$ ~1-2 K only, even if one takes rather big I_c/I_{op} ~3. That is why, the requirements for magnet cooling becomes more demanding.
It is not too difficult to stay within such low margin of T_{op} if use of bath cooling for the magnet systems is made. The method is in principle acceptable for experimental devices of suggested dimensions as successful operation of TORE-SUPRA, TRIAM-1M as well as LCT results have shown. Especially if the recommendation is accepted to design the device by such a way that each coil will be able to be changed without the full disassembly of the device that will be discussed later.
Due to lack of reliability of electrical insulation as well as mechanical disadvantages of rather crumbly bath cooled coils, most of the designers of projects under discussion prefer to use forced flow cooling and all the experts who have been involved in discussions of SC magnets, support this solution of cooling.

But for the forced cooling scheme, it becomes very important to make the proper choice of the cooling. In T-7 and HT-7 as well as in TPX, HT-7U and KSTAR proposals, both inlet and outlet LHe communications come to the coil from the outer side (low field region). Helium reaches the inner turns (high field region) after passing through one single layer and goes out through the neighboring one.
In T-15 and in SST-1 proposal, fresh LHe flow comes directly to the inner turns and goes to the outer turns through all neighboring single layers in parallel.

This difference which seems to be small and not too important really has drastic consequences in the case if there is some heat generation in the coil which usually always exist for some reason or other.

For instance, in T-15 some heat was generated by residual resistance of Nb_3Sn conductor (10-30W per coil at I_{op}=4 kA). Simple analysis of T-15 magnet behavior shows clearly that it will be impossible to operate at the rated field being cooled by He sent from outside.

In TPX and KSTAR radiation heating increases He temperature along the cooling channel before He flow reaches the inner to a large value of 6K or more in some regimes. Temperature of these turns obtained from calculations is even considerably higher than the T_{outlet} because the outgoing He flow is

again cooled down due to thermal contact with inlet flow in neighboring single pancake (so called "thermal short circuit" effect).

Because of this high temperature in the turns working in the highest magnetic field and subjected to the strongest disturbances from plasma current disruption using of Nb_3Sn becomes necessary. But if to supply fresh He from inside, the use of NbTi becomes possible at least for magnet with KSTAR parameters. This could allow to make SC magnets for that device which are much less expensive, more reliable, easier and faster to construct.

For TPX team the choice of SC material was out of question because their project had to be "ITER relevant". Having the choice of Nb3Sn both cooling schemes were able to satisfy the design criteria. And the first one have been chosen basing on the argument that the doubling of the number of He supplying "stubs" as well as their displacement on inner surface of coil will reduce reliability of coils. But optimal temperature distribution across the coil seems to be incomparably more important for reliable operation of the magnet as a whole. And this is so for any of the SC material which could be used for magnet.

In tokamaks with rather high aspect ratio and strongly elongated plasma some heat generation in the magnet coils is possible due to vertical fluctuations of the plasma column, sweeping of S-point if it would be necessary, due to friction losses of LHe flow etc. without speaking of unpredictable thermal contacts of magnet with warmer parts of the machine which can arise during its assembly. Such "thermal bridges" certainly were present in T-7 , T-15 and it seems they are present in HT-7 as well. Certainly, such kind of incidents could be called easily avoidable "children mistakes" till the time the project is only on paper.

Also it is necessary to mention that installation of supplying stubs inside of the coil considerably reduces the rise of pressure and temperature following the quench as the normal zone would rise in the most loaded and the most disturbed inner turns of inner leg of the coil or at a distance less than the length of one turn from He entrance.

The reduction of cooling channel lengths as well as reduction of temperature difference and hence thermal stresses between neighboring pancakes would allow to reduce the cooling time. Lower hydraulic resistance due to smaller length could allow to get many other advantages like using ejectors for mass flow increase, two phase He cooling etc.

That is why, I would like to insistently recommend to install additional stubs on the inner surface of TFC outer legs and to supply coils by fresh He through it for HT-7U as well as for KSTAR even if the authors of the latter do not want to discuss the SC material which possibly has been chosen for their magnet for any other reasons and even in spite of the fact that using of Nb_3Sn allows formally to satisfy the requirements of design criteria formulated in TPX project for both the cooling schemes.

2. Optimization of cable design

Next point of our consideration will concern cable design optimization. SST-1 will use conventional CICC. First 600m piece of this 10kA cable 15 X 15 mm^2 have been produced by Hitachi, Japan and delivered for tests to Kurchatov RRC last July. Now a model coil from it is almost completed and should be tested soon - in November or December of this year. Preliminary results of short sample tests show that the cable quality could provide acceptable magnet performance.

HT-7U has not yet done the final cable choice. Two versions are under considerations. The first is bath cooled 5kA cable made by soldering of Rutherford type flat cable (originally intended to be used in SSC, US) in a groove of Cu busbar.

This design principally is acceptable though it is in contradiction with recommendations of the international experts. But to confirm its validity it is necessary to organize the tests of a model coil or at least a set in which a number (at least 10 or more) of parallel vertically displaced conductors will be

disturbed simultaneously by fast varying magnetic field. Reference on high stability of such cable design in TRIAM-1M or in LCT coils are not sufficient because high T_c/T_{op} margin in the first and slow ramp up of disturbing field in the last.

The need of testing not one but many conductors is connected with the fact that in contrast to local mechanical disturbances usually considered as a most probable reason of normal phase generation in tokamaks, disturbances from plasma current disruption act on all turns in the coil simultaneously. In this case, each turn can use the He which is in direct contact with it for its recovery. More He is needed for recovering other turns at the same moment. So experiments with recovery of only one turn are not exact representation of the real situation.

The second version of conductor for HT-7U is CICC changed in the way suggested earlier by ITER team - with subcables wrapped by SS foil and with a helical tube inside for reducing the hydraulic resistance of the cable. It seems that this way of CICC improvement is improper. It increases the inherent contradiction in the nature of CICC approach - good cooling and low hydraulic resistance require crumbly (with high void fraction) twisting structure - but this crumbly structure can not provide good mechanical fixation of strands against movement.

Attempts to insert one or a number of perforated or helical tubes inside the conductor cross section gives redistribution of He flow - considerable reduction of He velocity at the strand surface, reduction of heat transfer coefficient and reduction of stability. The surrounding cable still has to be rather crumbly to allow He to go through it.

It is surprising as to why the solution having such inherent contradictions has been accepted by international community for such big and important project like ITER. It seems that a more reasonable way of CICC improvement is just an opposite one. It might be better to twist the subcables as tightly as possible for good fixation of strands, may be even to solder it through by high resistive alloy (if NbTi is used) and to display such subcables at some distance from each other as it was done on conductor for LCT EU coil with wide channels for He passage between them.

In comparison with conventional CICC such a cable will have much lower possibility of strand movement, much lower hydraulic resistance as well as good cooling of strands due to the direct contact with the main He stream especially if the subcables are made in the form of double layer flat cables of Rutherford type wrapped around in a Cu core. The latter also has to be from tightly twisted Cu wires to reduce AC losses . But certainly this suggestion needs careful experimental verification.

3. Test program for SC magnet

The SC cable tests as well as whole program of tests needed for SC magnet should be the next point of our discussion. Most of the experts agree that after the special cable have been designed and some length of it has been produced, a model coil from it should be wound and tested before making full scale magnet. There is also a point that in addition or even instead of this the short sample tests should be done.
It seems to me that short sample tests are reasonable only in the case if this test could be done considerably earlier than a piece needed for coil or if there is a number of cable design versions which should be compared before the final choice like in the case of HT7-U. And it seems that there is no sense to do such tests if short sample has to be cut from a long piece of cable, as it happens in the case of SST-1. I am sure that in this case it would be much more useful to test the joints, insulators and other “critical” points of magnet, which have to be tested in any case. Unfortunately designers of all projects under discussion don’t give enough attention to making such tests though often the workability of magnet is often defined just by such a “small” details.

But, in reality the most important aspect is to discuss the problems of all coil tests before the assembly of the device which has been very hard, long and expensive step in the construction of all previous tokamaks with SC coils. For instance in T-15, it took two years and more then 15% of the whole cost

of the project. Three coils had to be changed when they were integrated based on single coil tests. Without this T-15 magnet would never be able to reach the rated parameters.

But even after testing all coils TORE-SUPRA had to change one of the coils. It took about six months - much less than the time taken for all tests before assembly. It shows that in any case the possibility to change any coil after device assembly is more necessary than to test all of the coils before it. Moreover, analysis of the way the tests of all coils for T-7 and T-15 were performed shows that installation of coils in test facility is not much easier and faster than in the device itself. It will be definitely so if special care to simplify the replacement of coil will be done by device designers. Taking into account all of this it seems reasonable to recommend that tests of all coils before assembly may not be required if the integration and assembly of the device is done in such a way that the faulty coil could be changed without the full disassembling of the device but with minimum disassembling. This is possible if the other neighboring coils and magnet interconnections are done in appropriate manner which is discussed below.

4. Disassembly and ability to repair

This ability is generally one of the most important requirement for any experimental device. Concrete recommendations to improve the projects in this direction could be as follows.

Mechanical structure for magnets, cryostat and vacuum vessel could be recommended to have in many modules - same quantity as the number of toroidal field coils. Direct welding for connection of their thick plates to bigger assembly modules, say quadrants as it has been suggested in TPX is not acceptable because such a design does not allow changing of a coil at all.

It might have been reasonable for TPX because one of the very important goal for that project was to demonstrate reliability of applied SC technology based on previous vast experience from constructing other magnets which was needed to support US participation in ITER. But even there refusing from preliminary tests of the coils and from the ability to change it had raised a lot of doubts and even objections during discussions within the magnet design team as a very risky option. Moreover I doubt that such approach could be valid for the first big SC magnet constructed in India or in China with indigenous effort.

It seems better to connect magnet modules by bolts with insulation while VV and cryostat parts - by thin SS plates welded to flanges and with each other like it was done on T-15 cryostat. Such way of connections allows to open any part of the cryostat (and it was really done) as well as to take off any TFC together with VV sector or the latter one alone.

Mechanical weakness of such connections is not dangerous since the forces acting on each module of VV from VDE and on the cryostat from atmosphere will be accepted inside it by transferring the loads through the ports welded with parts of both toroidal shells.

For direct welding of the ports with VV and Cryostat is acceptable because baking of VV could be restricted at the level $<\sim 200^0$C if taken into account that plasma will be almost completely surrounded by PFC components and will not practically interact with VV unlike usual situation in tokamaks. So thermal expansion compensators, moreover insulation in the connections are not needed.

Certainly for the first assembling, the modules could be combined by the most convenient way. But the ability to change as small a part as possible in case it is required during any repair need seems to be very useful.

5. The support structure

The magnet support structure as well as support of the complete device should not occupy the space under the device. Supporting columns should be moved to outside to allow to open bottom plate of the cryostat - to be able to change any of the lower poloidal coils, to repair inner interconnections etc.

Also this space is very much needed for displacement of plasma diagnostics, RF heating and Current Drive equipment's, pumps and cooling equipment's etc.

Concerning of magnet supports, it is also better do displace them on the lower part of the cryostat and to move them out as far as possible - up to the outer wall of the cryostat.

It is necessary to take into account the needs of magnet position adjustment with respect to VV and in-vessel components needed for the regulation of plasma interaction with them as well as for avoiding of short circuits if they would occur inside the device as it happened in T-7 and T-15 . I think the best and the simplest way of doing this is to suspend by SS tie rods or better by special high heat resistive oriented fiberglass loops. This design can provide very low, few W only heat load as well as very good precise positioning of magnet even when it is cooled.

6. Design approach for nitrogen shield

It is necessary to point out that in all the projects including such well documented one as TPX, LN2 shield has not been presented in details may be because it is usually accepted as a "not too important" part of the project. T-7 and T-15 also have not given enough attention to this part of the project in time. And due to this both had many difficulties during machine construction only with the shield or else much with more with other parts. So I should recommend not to delay the detail design of this part and not to consider the completion of VV or Cryostat design ready without this.

In all previous projects LN2 shield had the form of two separate toroidal shells displaced between magnet and warm parts – VV, cryostat and ports connecting them. Such designs of "many shells" provide many difficulties during assembly. Therefore, it seems better to look through possibility to make it not as a separate structure but in the form of panels carried on other structures. It could allow to reduce the gaps needed for it's displacement as well as to reduce the danger of "short circuits" which was a serious problem in T-7 and T-15.

7. Ability to change in-vessel components

It is necessary to point out that for device intended to get and to study steady state plasma, the most unknown, uncertain as well as less reliable are not SC magnets which we have discussed till now but the plasma facing components. That is why I am sure that any device of such a kind should have the biggest possible access to the plasma and to the inveigles components - to allow for a man to go in to repair or even change and install a new component - without disassembling the device.

From this point it seems that VV design suggested in TPX is certainly not a optimal one. There is lot of unused space (about 0.5m) between VV outer wall and TFC outer legs but only few (about 0.35m) between VV and outer parts of in-vessel components. The latter makes it difficult to do something inside of VV, moreover the ports are long but not too wide and not provided in every intercoil gaps. So for changing of in-vessel components practically whole machine disassembling is required.

I think VV should use all space available inside the magnet. The ports should be displaced in all cross sections between the coils, their walls should go parallel to the side walls of coils as close as possible to them, ports should be as short as possible and all connections of at least horizontal ports with VV and with cryostat should be conical.

VV will be rather the "warm magnets (room temperature) bore" while other parts of the device would be used fully for interaction with the plasma. They will be covered by special materials, baked up to high Temperature (at least 350 C if tile material is Carbon) etc.

Ability to change in-vessel components gives also an attractive possibility concerning project design organization. It becomes possible to split the design process as well as device construction and commissioning into two steps. Magnet, VV and cryostat design and construction in this case need not wait for the completion of the unknown in-vessel components as well as for solution of a lot of

problems connected with them. The last should be ready number of years later then the magnet and even the first plasma.

I am glad to see that some of these recommendations are already accepted in projects under discussion at this meeting. I hope that the discussion of the others will help designers to make further improvement of their projects.

Also, I hope that in the next such meeting more engineers from our devices as well as from US, Japan, France and other countries will be involved to make our discussions more fruitful as the transferring of experience from those who are doing such work for a long time to the teams who have started recently is one of the most important requirements for successful development of Controlled Fusion Programme in the World.

The suggestions given above are the result of many discussions during the long work under T-7 and T-15 projects in Kurchatov Institute. Author would like to acknowledge the members of T-7 and T-15 teams as well as specialists from other organizations taking part in this work.

THE ASSEMBLY SIMULATION FOR HT-7 SUPERCONDUCTING TOKAMAK

W.W. XIAO, D.M. GAO
Institute of Plasma Physics,
Heifei, Anhui, China

Abstract

It is well known that the assembly process for Tokamak, especially for superconducting Tokamak is very complicated and difficult since Tokamak has its own structural features. Since the good performance of tokamak mainly depends on its assembly quality, it is very important that all contradictions and problems in assembly process should be found and solved as early as possible. In recent years the VPT (Virtual Prototype Technique) or MSS (mechanical system simulation) and its application has made big progress. It has become an engineering and analysis tool which can be easy to use by scientist and engineer from a complex and special research method. This paper emphasizes on the preliminary results of the digital simulation for assembly process of HT-7U Tokamak after making use of the VPT method.

HIGH DENSITY LHCD EXPERIMENTS AND RECENT PROGRESS ON HT-7 SUPERCONDUCTING TOKAMAK

HT-7 TEAM
(Presented by Jiangang Li)

Institute of Plasma Physics,
Academia Sinica,
Hefei, China

Abstract

The quasi-steady state ($\tau_H > 10\ \tau_{Eoh}$) H-mode was obtained with very high plasma density by Lower Hybrid Current Drive (LHCD). The line average density during improved confinement phase is about $4.5 \sim 6.0 \times 10^{13}cm^{-3}$ which is very close to the Greenwald density limit (78 ~ 96% of Greenwald density limit). The τ_E is about 1.5 ~ 2.0 times than the L-mode scaling during H-phase. The experimental results show a good agreement with code simulation for the LH off-axis power deposition profile with a reproducible manner. These off-axis hollow current profile and enhanced confinement improvement are attributed to a strong reduction of electron thermal diffusivity in the reversed shear region. Steady state full LH wave current drive has been achieved. The pulse length is 3.5 seconds, which reaches the present limit of PF system. The good plasma condition is obtained by ICRF boronization, which makes Z_{eff} close to 1.0. High density shots are obtained by two different fueling methods: multi pellet injection and supersonic beam injection. The later shows a high fueling efficiency that could be used for steady-state operation and the plasma density excesses the Greenwald density limit. ICRH pre-ionization, start-up, heating and its synergy with LHCD have been tested during recent experiments and some interesting results have been obtained.

1. Introduction

The steady-state tokamak operation and high performance plasma under non-inductive current drive are the most important issues for the tokamak fusion research. The various improved confinement modes are obtained in different machines. How to make these modes work under steady state is unsolved. HT-7 is a mid-size superconducting tokamak. Its main purpose is to explore steady-state tokamak operation with high plasma performance. The redesign parameters of the machine are as follow. B_T = 2.5T, Ip= 100~250kA, R=122cm, a = 30cm , line average density $n_e = 1 \sim 5 \times 10^{19}m^{-3}$, T_e = 1.0 keV, T_i = 0.5 keV, τ_E = 15ms and plasma duration time is about 1~3 seconds. A stainless steel liner was installed in the vacuum chamber. 24 large windows give very good accessibility to the diagnostics and wave systems. 1.2MW Lower Hybrid Current Drive (LHCD) system is tested with 10 second pulse length. The power for the ICRH system is 0.3MW with CW capacity. 1MW ECRH system is still under construction. More than 20 diagnostics were installed on the machine. A few experiments have been carried out in the past few years and some good results were obtained. The outline of HT-7 main experiments is briefly described in the second part of this paper. The high-density LHCD experiment is one of the emphasized topics on HT-7, which is given in the third part of the paper. The ICRF start-up, heating and conditioning are introduced in the forth and fifth parts. Two different fueling experiments, pellet injection and supersonic beams filling are presented in the sixth and seventh parts. The summary and conclusion come at the end of the paper.

2. Outline of HT-7 experiments

The construction of HT-7 had finished in the end of 1994. After a few years of engineering tests and operation, all the design parameters were achieved. Toroidal magnetic field reached 2.5T. Plasma current reached 220kA, Electron temperature was above 1keV and ion temperature was around 0.3~0.6 keV. Plasma density reached $6.5 \times 10^{19}m^{-3}$. The plasma duration time was above 3 seconds in 1997. Since 1998, new feedback control systems are installed and HT-7 is normally running for

Ip=150KA, B_T = 2T, a = 28.5cm, with Mo. limiter configuration. The LHCD experiments were successfully carried out in the expected manner. The plasma confinement was improved by LHCD. The full wave current lasting for 3.5 seconds was obtained. Since the presence of permanent toroidal field, ICRF conditioning has been routinely used during experiments, which has proved to be a very effective and powerful way for the impurity cleaning, boronization and recycling control. Very strong wall isotope exchange capability of deuterium RF conditioning was demonstrated. High performance long pulse length discharges were carried out with the pulse length up to 3.9 seconds. The MHD instability suppressing by LHCD and Ip modulation, the operation region exploration, error field, lower loop voltage start-up, pellet injection, supersonic beam gas filling, as well as ICRF experiments were carried out. Some interesting results were obtained which will be described in the following sections.

3. High density LHCD experiments

Good plasma confinement under non-inductive steady-state high-density condition is a key issue for HT-7. The reversed magnetic shear could be obtained and sustained by lower hybrid current drive, which is predicted by theory and observed in experiment [1-2]. The quasi-steady state ($t_H > 10\ \tau_{Eoh}$) H-mode with a plasma density of 60% Greenwald density limit was obtained by the injection of LH Heating and LHCD in HT-6M tokamak [3]. The same method was used on the HT-7. Under high plasma density condition, the LH waves could not be absorbed in the plasma center, so a large fraction of non-inductive current is driven in the outer region of plasma. LHCD system consists of a multijunction 2 × 12 grill that has changeable $n_{||}$. The frequency is 2.45GHz. The magnetic field was 1.9T and plasma density is about $3 \sim 5.5 \times 10^{19} m^{-3}$, so that the weak absorption dormant condition was satisfied. By enhanced ICRF boronization and helium discharge, very good wall condition and high plasma performances were achieved. LH wave was injected to the plasma flat top and the density increased more than two times by the strong gas puffing. The H_a dropped which indicated increase in the particle confinement time. The stored energy increased by nearly a factor of three and the energy confinement time is about two times higher than the L-mode scaling shown as in Figure 1a. The H-phase at the 75% Greenwald density limit remains as long as 5 times the energy confinement time. To investigate the density limit that LHCD H-phase can sustain, plasma current was ramped down. The plasma confinement began to decline when the density accessed the Greenwald density limit. And plasma was disrupted at 1.25 Greenwald density limit shown in Figure 1b.

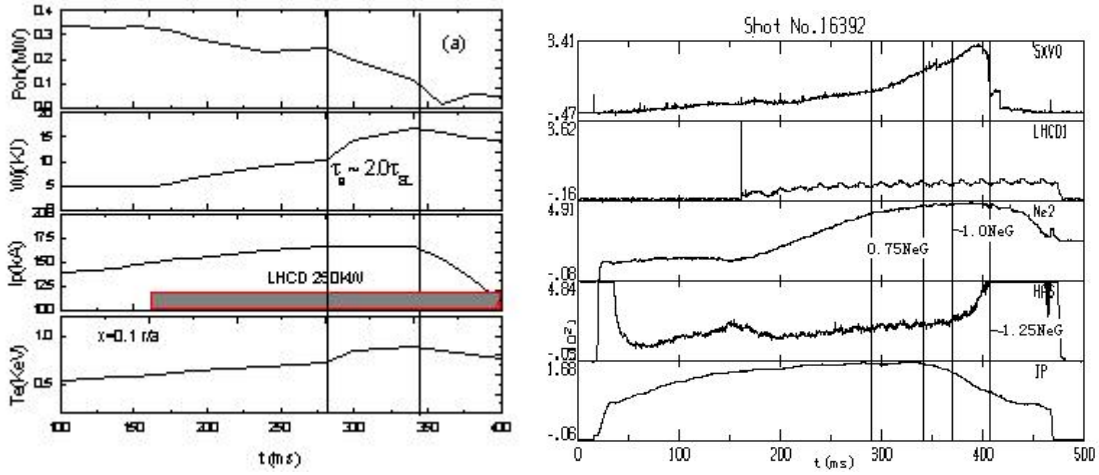

FIG. 1. High density H-mode by LHCD. B_T =1.9T, P_{LHCD} = 250 kW, $n_{//}$ = 2.8.

To fully understand the mechanism of the LH deposition profiles in the weak absorption regimes, the wave diffusion/Fokker-Planck (WD/FP) mode was used, which was derived from the phase averaging of wave kinetic equation. In this multipass absorption regime, the initial $n_{||}$-spectrum is broadened and

upshifted to very high $n_{||}$ values. The power is absorbed. The electromagnetic energy density U(r, k, t) tended to be uniform. The diffusion equation for <U>(m,t) could be obtained by averaging the wave kinetic equation over wave orbit as follows:

$$(\tau \frac{\partial}{\partial t} - \frac{\partial}{\partial m} D_{wave} \frac{\partial}{\partial m} + 2\tau < \gamma >) < U >= \tau < S >$$

Where the brackets < > denote the orbit averaging. $D_{wave} = \Delta m^2/2$ and m is the RMS step in m per transit time. τ, γ are the damping rate and S is the RF source term which is assumed to have δ-like form.

By simplifying and integrating Fokker-Planck equation, the LH waves power deposition, the current density and safety factor profiles could be obtained. The clear off-axis LH wave power deposition is shown in Figure 2.

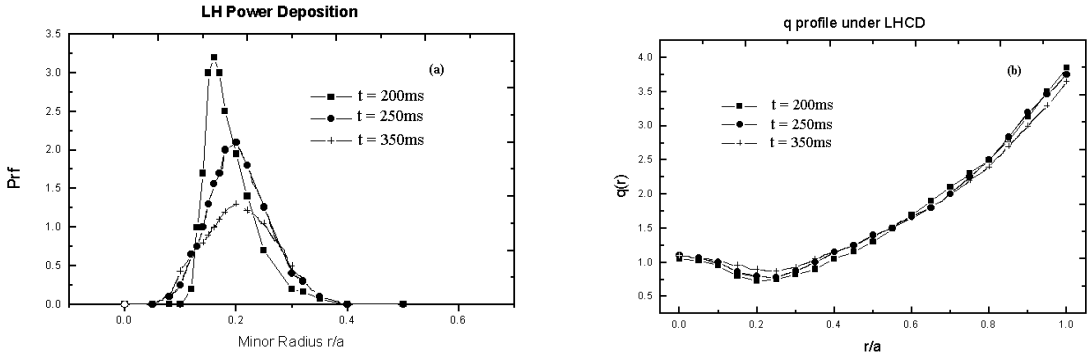

FIG. 2. WD/FP mode calculation for shot 16392. (a) LH wave power deposition. (b) q profiles.

The q profile is weakly reversed. When a certain of fraction of the plasma current (50% to 10% for the line average density $1.0 \times 10^{13}cm^{-3}$ to $4.5 \times 10^{13}cm^{-3}$) is non-inductively sustained by the lower hybrid waves, the hollow current density profile was formed and the magnetic shear was reversed at the normalized plasma radius of 0.2. This off-axis hollow current profile and enhanced confinement improvement lead to a strong reduction of electron thermal diffusivity in the reversed shear region. The off-axis non-inductive current profile by LHCD improved the confinements and sustained the reversed magnetic shear for more than 180ms which was about 10 times longer than the energy confinement time.

4. ICRF heating and start-up

The minority heating mechanism was chosen on HT-7 tokamak. The ratio of H/(H+D) was kept under 12%. The RF frequency was 30MHz that correspond to the first hydrogen harmonic layer with 2 Tesla in the plasma center. The two step tuner system was used for the marching the generator and the antenna. The injected power was above 100kw and ion temperature increased about 200 eV. Plasma density increased and its profile peaked. The RF power was also injected in the start-up phase of plasma. The delay time of break down was shortened by the injection of 120kW RF power. Proper adjustment of the poloidal field and the pre-filling gas pressure gradually reduced the loop voltage of the breakdown. About 15~25% flux saving was achieved during the start-up phase by ICRF. It seems possible that ICRF assisted low loop voltage start-up could be obtained.

5. ICRF conditioning

The important role of first wall conditioning to reduce plasma impurities has been recognized for decades and many efforts have been done in most pulsed tokamaks. The future superconducting reactor, like ITER, will need new techniques for wall conditioning and the particle recycling control

since the standard glow discharge would not work in the presence of toroidal field. A new technique for wall conditioning with a permanent magnetic field has been tested and developed on a few machines and HT-7 tokamak by ICRF wave injection in the past few years[4-7]. RF plasma has been produced by injection of ICRF power ranging from 5kw to 50kw in both helium and deuterium working gas. In order to get best conditioning efficiency, wide range parameters have been tested, such as toroidal field (0.1 ~ 2.0T), gas pressure (8×10^{-4} Pa ~ 1×10^{-1} Pa), radio frequency (RF) (18MHz~30MHz) and antenna configuration (with and without Faraday shielding). With the help of diagnostic measurement and theoretical calculations, the different optimized ICRF conditioning operational modes were achieved according to the different wall conditions. It was demonstrated that ICRF conditioning was very effective and powerful way for the impurity cleaning and recycling control on HT-7 tokamak. It has been routinely used during experiments.

Since two factors governing the conditioning efficiency were outgass rate of impurities from the wall and the ionization rate of desorbed molecules which induced a redeposition, the optimized pulsed RF mode with 0.5s RF power on and 1.5s time interval was used. Helium ICRF discharge was used mainly for the replacement of deuterium (and its isotopes). This made plasma start up and particle recycling well controlled. Electron temperature estimated from visible spectrum is about 4eV ~ 10eV and density is in the $1 \times 10^{17} m^{-3}$ range which depended on RF input power and gas pressure. The pulsed mode with pressure of 1×10^{-2} Pa increased the conditioning efficiency by controlling electron density and temperature separately to minimize the hydrogen redeposition portability. Results showed that ICRF wall conditioning efficiency was independent of injected RF frequency and weakly related to toroidal magnetic field. High hydrogen removal rates have been obtained. The RF injection power level played a very important role in helium ICRF wall conditioning experiment. In the lower power level (i.e. the power is lower than 20kw), the hydrogen removal rate went up quickly and reached a saturation status when P_{RF} was great than 30KW. As RF injection power went up, the ion and electron temperature increased, the interaction section of charge exchange became smaller. By 15 minutes helium ICRF discharge of 20 kW between normal plasma shots, very reproducible shots were obtained.

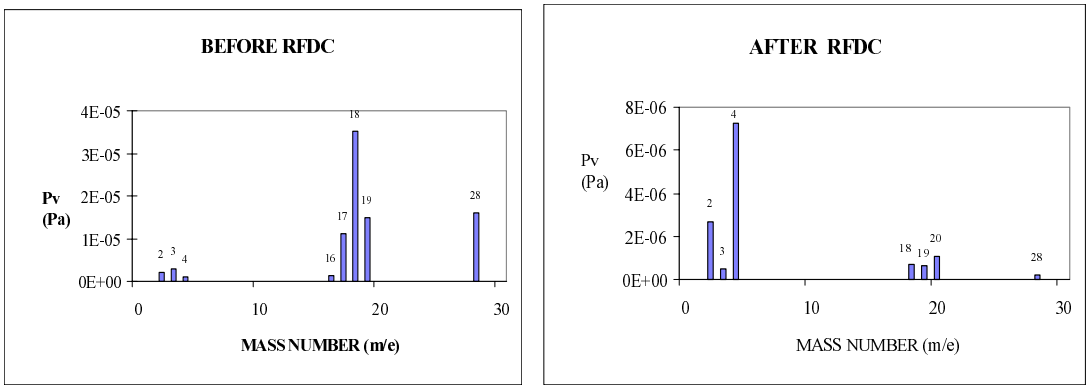

Fig. 3. Comparison of QMS data before and after ICRF wall conditioning.

Deuterium ICRF discharge was used for surface cleaning and wall isotope control. The pulsed mode with optimized pressure of $1x10^{-2}$ Pa was used. The electron temperature was lower (2~3 eV) compared with helium discharge. And T_e was almost constant with different levels of injected RF power. The low temperature minimized the strong plasma reionization and wall redeposition of neutral species. High temperature deuterium ion and its energetic tail were observed. Both energetic and reactive particles bombarded the first wall that induced the desorption of molecular impurities. These were the main reasons for the good conditioning efficiency of D_2 ICRF discharge. This point could be seen from the quadruple mass spectrometer (QMS) data. Fig. 3 shows QMS data before and after 35 minutes of pulsed 25KW RF discharge. After ICRF wall conditioning, the impurity part was decreased, and the working gas part was greater than 80%. The very strong wall isotope exchange

capability of deuterium RF conditioning was observed. The H/(H+D) ratio was normally around 20% and could be down to 12% after a few times of D_2 - ICRF discharge.

6. ICRF boronization

ICRF boronization has been successfully tested on HT-7, which is the first time on tokamak. This new technique has proved itself a highly efficient, fast and easy controllable method for the future large device, like ITER, especially for the superconducting tokamaks. The antenna was used for ICRH heating without Faraday shielding. The nontoxic and nonexplosive solid carborane ($C_2B_{10}H_{12}$) powder was used for the boronization material. 40 minutes RF cleaning was carried out with helium working gas to remove the impurity on the first wall before ICRF boronization. The liner temperature was 150^o C and wall temperature was about 80~ 120^{o}C. After that, the carborane container was heated to 60^{o}C to keep stable gas pressure and RF discharge. All the pump valves were nearly closed, only leaving little pumping. The base pressure was 3×10^{-1} Pa with the mixture of helium to carborane 1:1. To improve toroidal uniformity, the pulse RF power of 10 kW was coupled to the plasma with 2.4 seconds power on and 2 seconds power off. The plasma color changed from pure green to pink when the carborane vapor was injected to the chamber. The ion cyclotron resonant layers were clearly seen, shown as in Figure 4.

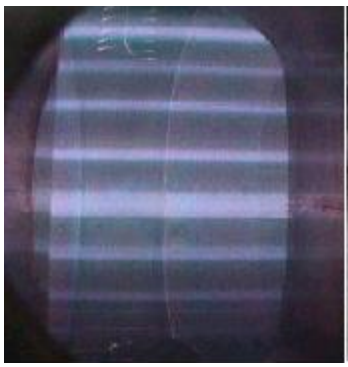

Fig. 4. The ICRF resonant layers could clearly be seen

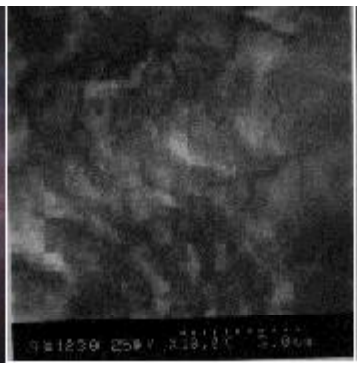

FIG. 5a. Fresh film on C Sample material.

FIG. 5b. Boron film after 250 shots which still looks good

RF plasma parameters were measured by different diagnostics. The electron temperature was about a few eV. Plasma density was about $1x10^{17}m^{-3}$, and the ion temperature is 2KeV with high-energy tail up to a few tens of keV. The ion temperature was a very important parameter since it governed the boron ion energy that compacts the wall. The residual gas analysis (RGA) was done during boronization. The results shown a totally different pattern with boronization using glow discharge clearing (GDC) on HT-7 and other device. The mass 144($C_2B_{10}H_{10}$) was the only peak mass that was detected during GDC boronization in HT-7. The partial pressure for the mass 11 and the group of 22 were 50 times higher than that of mass 144. This means that the carborane molecule was cracked into smaller pieces by the bombardment of high-energy ions of RF plasma. The 4g carborane was used and the boronization process lasted for 65 minutes. The carborane container was heated up to 120^{o}C at the end to evaporate all the carborane. After that, all the pump ducts were fully opened. Helium RF plasma continued for 20 minutes but the RF power was reduced to 3 kW to prevent the heavy bombardment on the fresh boron film. The another purpose for the RF conditioning is to remove the huge hydrogen content that was absorbed in the film during boronization. The RGA results after boronization showed that the partial pressures of oxygen containing gases (H_2O, CO, CO_2) were all reduced by more than one order.

X ray photoelectron spectroscopy was done on the films. The B/C ratio varied from 2.8 ~ 3 for a depth of 250nm for all the sample materials. Analysis of B/C coating showed that it consisted of a

fine amorphous C/B: H film with very strong adhesion to the first wall. Even after 250 shots with ICRF and LHCD (about 400 kW RF power), most parts of the film looked good except some hot spots which were bombarded by energetic electrons and ions. Figure 5 shows the film structure on the graphite base material. The depth distribution for all the elements (B, C, O, and Fe) was uniform. Figure 6 (a) shows one important unique feature. There was no clear boundary of the B/C film on the graphite base (also true to other materials). The boron contents could be detected at a depth of 500nm that was well beyond the coating depth. This meant that the high-energy boron ions (also other kinds of ions) hit the wall and penetrated into the base materials and deposited into the first wall. The film thickness of the coating was about 240 ~320nm. The distribution along the toroidal direction was nearly uniform. The thickness analysis and calculation showed that the ICRF boronization efficiency was close to 86%, which is a very promising number. Figure 6b shows that oxygen content increased from 15% to 26% and boron content decreased from 60% to 50% after 250 shots. This demonstrated that boron film has very strong oxygen capture capacity. The thickness of the film was reduced about 80nm after 250 shots. In general, the lifetime of the coating was 1500~2000 shots. The film property was much better than the film obtained by GDC method. The disadvantage of the film was that it contained some metal contents in it. Reducing the RF power, the metal contents in the film were also reduced to a neglected level during the second and third RF boronization.

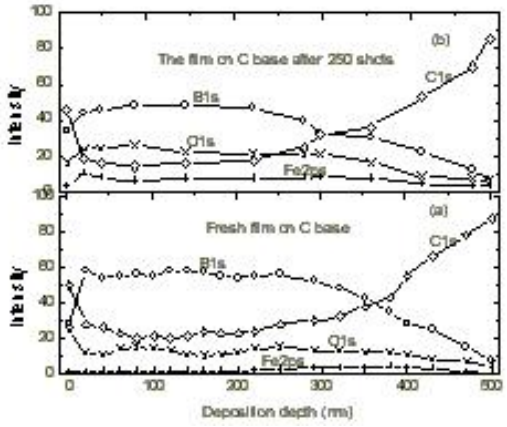

FIG. 6. The boron film property for the fresh film and the film after 250 shot.

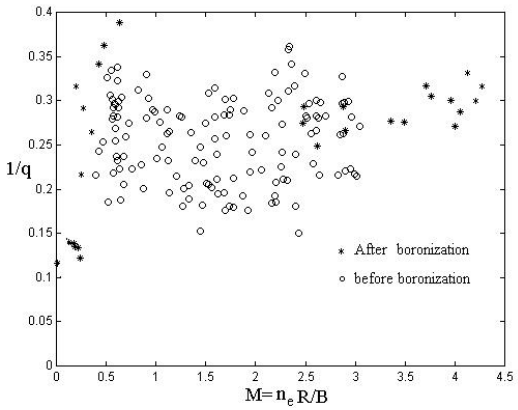

Fig. 7. The Hugill diagram was extended after ICRH boronization.

Standard ohmic discharges were fired after boronization. Impurity contamination was almost same with other successfully boronized device. The remarkable feature of the ICRF boronization was the fast vessel transition from the unconditioned state (such as air leak, major disruption, inter structure damage) to the very low impurity level. All the procedures took only a few hours. Loop voltage dropped dramatically and the Z_{eff} changed from 4 to a value close to 1. The light impurity line radiation (C, O) was reduced by a factor of three and the metal lines almost disappeared. The total radiation power dropped sharply to the level of 10% ~ 18% of ohmic power. The increase of density limit was also an important fact, which showed boronization merit. The density limit in standard ohmic discharge for the boronized wall with GDC was $5.3\times10^{19}m^{-3}$ (Ip = 150 kA, B_T = 2.0T), which was close to the Greenwald density limit. After ICRF boronization, the density limit reached $6.5 \times 10^{19}m^{-3}$. The Greenwald density limit was exceeded. On the other hand, a very low density ($2\times10^{18}m^{-3}$) plasma without run-away was obtained. Boronization resulted in an extension of Hugill stable operation diagram that is shown in Figure 7.

X ray photoelectron spectroscopy was done on the films. The B/C ratio varied from 2.8 ~ 3 for a depth of 250nm for all the sample materials. Analysis of B/C coating showed that it consisted of a fine amorphous C/B: H film with very strong adhesion to the first wall. Even after 250 shots with ICRF and LHCD (about 400 kW RF power), most parts of the film looked good except some hot spots which were bombarded by energetic electrons and ions. Figure 5 shows the film structure on the graphite base material. The depth distribution for all the elements (B, C, O, and Fe) was uniform. Figure 6 (a) shows one important unique feature. There was no clear boundary of the B/C film on the

graphite base (also true to other materials). The boron contents could be detected at a depth of 500nm that was well beyond the coating depth. This meant that the high-energy boron ions (also other kinds of ions) hit the wall and penetrated into the base materials and deposited into the first wall. The film thickness of the coating was about 240 ~ 320nm. The distribution along the toroidal direction was nearly uniform. The thickness analysis and calculation showed that the ICRF boronization efficiency was close to 86%, which is a very promising number. Figure 6b shows that oxygen content increased from 15% to 26% and boron content decreased from 60% to 50% after 250 shots. This demonstrated that boron film has very strong oxygen capture capacity. The thickness of the film was reduced about 80nm after 250 shots. In general, the lifetime of the coating was 1500~2000 shots. The film property was much better than the film obtained by GDC method. The disadvantage of the film was that it contained some metal contents in it. Reducing the RF power, the metal contents in the film were also reduced to a neglected level during the second

The improving effects of ICRF boronization were also shown in ICRF heating and LHCD experiments, especially hose on the LHCD. During LHW operation, Z_{eff} increased before boronization typically from 3.5 to 6. After boronization, Z_{eff} dropped by a factor of two and changed from 1.5 to 2.5. Sometimes it remained unchanged. Higher current driven efficiency η_{CD} was achieved because of the important role of Z_{eff} to the current driven efficiency. The full wave current driven with 3.5 seconds plasma duration was achieved.

7. Pellet injection

Both hydrogen and deuterium pellets were fired to the plasma with the speed of 0.5 ~ 1.2 km/s. Different size pellets were chosen according to different plasma conditions. Very peaked density profile was obtained after the injection of the pellet under normal ohmic discharge. Up to three pellets were injected to the same shot. Each pellet increased the density by about 50%. Figure 8 shows an

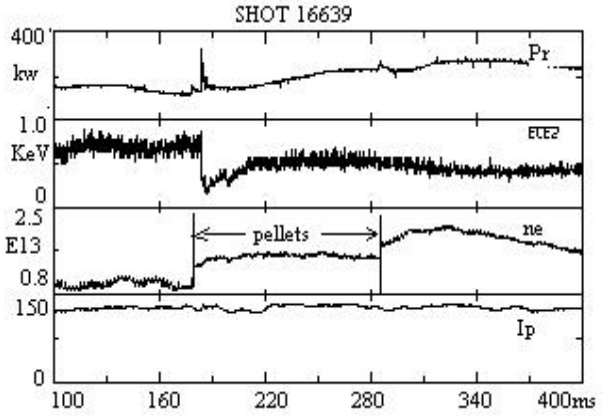

FIG. 8. OH shot with Two pellets case.

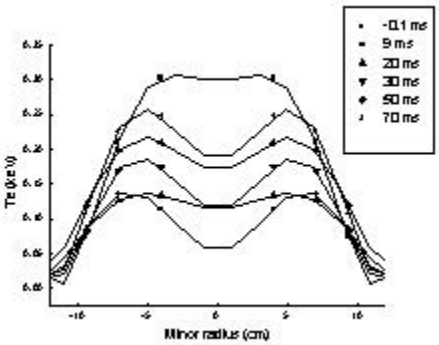

Fig. 9. Te profiles for the pellet injection by ECE measurement.

ohmic shot with two pellets case. The pellets could penetrate to the plasma center and a PEP like improved confinement was obtained, which indicated suppression of MHD activities, peaked density profile, reduction of Z_{eff} , increased stored energy, improvement in energy and particle confinement and hollow temperature profile (shown as Figure 9).

Pellets were also fired into LHCD plasma. The fueling efficiency was higher than the Ohmic shots. The run-away electrons were greatly reduced when the pellet injected to the LHCD plasma. The density increased by a factor of three during LHCD with pellets. The temperature recovering time was shorter. The current driven efficiency seemed unchanged with the density increase by the pellet. But larger size pellets easily terminated plasma discharge. The deuterium pellets were injected to the ICRF heated plasma that increased the RF wave coupling to the plasma. The high plasma density, which exceeded the Greenwald density limit, was obtained. It seemed that higher RF power and higher density could be reached. The detail scaling of the density limit by pellet under ICRH condition needed to be carried out in more detail.

8. Supersonic beam injection

Fueling tokamak plasma in more efficient way is very important for fusion research. According to aerodynamic principle, Laval nozzle is the key device to produce supersonic molecular beam, which is more effective fueling method than the normal gas puffing. The design of a Laval nozzle depends mainly on the diameter of its throat section, the diameter of its exit section, the curve from its inlet section to its throat section, and the curve from its throat section to its exit section. A complex computer simulation and 1-D aerodynamic theory were used to design optimum Laval nozzle for HT-7 tokamak. By eliminating expansion wave and compression wave from the nozzle wall, the flow parameters in the flow field of the nozzle were calculated in detail and the shape of the nozzle were determined. Two kinds of calculations gave little difference to a few sets of parameters. According to that theory and the conditions in the tokamak plasma, we could calculate the size and shape of a Laval nozzle and determine the velocity of the gas beam. Taking the diameter on the throat section of the Laval nozzle as 1 mm, and the diameter on exit section as 10 mm, the temperature in gas reservoir as 300^0K, the velocity of gas beam at the exit section of the Laval nozzle is 2800m/s for hydrogen and 1750m/s for helium.
The Laval nozzle has been installed in the HT-7 superconducting tokamak and experiments have been carried out. The density of plasma could easily be controlled by pulsed high-speed molecular beam that came from the Laval nozzle. The speed of the hydrogen beam was about 1.5~ 2.8 km/s that was mainly dependent on the temperature of the injected gas and the plasma condition. With penetration depth up to 15cm, the density peaking factor was almost same with the one achieved by pellet injection. Improvements for both energy and particle confinements were made by molecular beam injection. The fueling efficiency of about 60% demonstrated that it was an useful tool for the steady-state tokamak operation. The penetration and transport of neutral hydrogen have been measured and analyzed.

9. Summary and conclusion

The high performance steady-state plasma was obtained after finishing the engineering tests on the HT-7 superconducting tokamak. The confinement was improved by pellet injection, supersonic beam gas filling and LHCD. The off-axis LH waves deposition played a key role to improve the confinements. The weak absorption and multipass mechanisms were responded for the very high-density improved mode by LHCD, which was about Greenwald density limit. The efforts remained to be made for getting full wave current drive under Greenwald density limit by LHCD. The Ion Bernstein Wave (IBW) heating and IBW current drive will be carried out soon on the HT-7 to get on-axis heating and current drive. Even the ICRF wall conditioning techniques were very effective and very useful to the superconducting tokamak, the particle and heat flux control in the view of very long wall time constants were still under investigation. For the long time scale in-time control of particle and heat flux, the radiative layer and pump limiter would be tried in near future. Multi-pellet and high-speed supersonic beam were used for fueling of the plasma, which proved very effective to get high

plasma density. The combination of these with the high power ICRH and LHCD would be carried out soon to get higher plasma parameters.

REFERENCES

[1] C.KESSEL, et al., Phys. Rev. Lett. 72(1994)1212.
[2] M.HUGON, et al., Nucl. Fusion. 32(1992)33.
[3] J.LI et. Al., 17th IAEA Fusion Energy Conference, IAEA-CN-CD-69/CDP15, , Japan, 1998.
[4] E.J.STRAIT, et al., Phys. Rev. Lett. 75(1995)4421.
[5] Y.P.ZHAO, Chin. Phy. Lett. 14 (1997)916.
[6] A. LYSOJVAN et al., proc. 22nd EPS conf. Vol. 19c (1995) Part III, p341.
[7] E.GAUTHIER et al., J.Nucl.Mater. 241-243(1997)553.

OVERVIEW OF LHCD AND LONG-PULSE OHMIC OPERATION ON HL-1M

LHCD GROUP, HL-1M TEAM
(Presented by Liu Yong)

Southwestern Institute of Physics,
Chengdu, Sichuan, China

Abstract

HL-1M tokamak is a circular cross-section device with conventional toroidal magnetic field coils (R/a = 102 cm/26 cm). The goal of the LH-1M programme is to develop high power auxiliary heating (NBI, ICRH, ECRH) and non-inductive current drive (LHCD) technology and physics which are required for our next tokamak, HL-2A. This paper describes experiments using LHCD and ohmic discharges lasting up to 4 seconds.

1. Introduction

Up to now, on HL-1M, the maximum plasma current up to 320 kA (0.3s) and the longest discharge duration up to 4 second have been achieved with a very stable and reproducible plasma performance. An H-mode induced by biased electrode has been achieved with the information of an internal transport barrier [1]; Beside a pellet injection system with up to eight pellets, a new method of gas fueling was developed to inject supersonic molecular beam to the plasma [12]. Ohmic shear reversed configurations have been obtained by proper control of the plasma current rise and the supersonic beam injection. The ICRH and NBI experiments are being conducted on HL-1M. In this paper, we concentrate only on the subject related with long-pulse operations on HL-1M, i.e. non-inductive current drive and long-pulse ohmic operation with the wall conditioning.

2. LHCD experiments on HL-1M

In past few years LHCD experiments were conducted extensively, with a RF system composed of a 2 x 12 multijunction launcher and two klystron of 500 kW, in various aspects of the subjects, such as current drive efficiency dependence on plasma parameters and sawtooth suppression, on HL-1M tokamak [3].

It was found that the characteristic features of LHCD plasma at low density are quite different than those at high density. The current drive efficiency increase with the plasma current. The MHD activities were completely suppressed by LHCD. The improvement of particle confinement during LHCD was observed. The impurity confinement during LHCD was studied with laser blow-off. It was observed that the improvement of confinement was always accompanied with the increase of the poloidal rotation and the suppression of the fluctuation of the boundary plasma. The confinement improvement seems to be related with the production of radial electric field during LHCD. The suppression of the fluctuation during LHCD in the case of boronized wall showed different behavior with that in the case of siliconized wall.

Recently, some progress as follows have been made [4]. The ELM mode induced by LHW was observed under the condition of low density of about 1.0×10^{13} cm^{-3} accompanying with the improvement of confinement. At the condition of density around 0.5×10^{13} cm^{-3}, complete LHW driven plasma current was realized with zero loop voltage for 300 ms. The effective ion heating by LHW was observed when the plasma density exceeded 3.5×10^{13} cm^{-3}.

3. Long-pulse ohmic operation on HL-1

Even for non-superconducting tokamak, the ability to have long-pulse operation is an important sign of a n excellent device and an important issue of tokamak engineering. It involves not only plasma control technique, but also wall conditioning technology.
Up to 4 second ohmic discharge has been achieved due to the advanced wall conditioning technique and excellent feed-back control system for plasma parameters.

For the achievement of long-pulse operation on HL-1M, a well-conditioned wall is indispensable for two reasons, i.e. recycling and impurity. First, the hydrogen recycling has to be reduced by an efficient wall conditioning technique so that the plasma density could be well controlled. Second, a relatively clean plasma has to be sustained under a good wall condition to keep a low loop-voltage for saving ohmic transformer flux (only 1.7 VS for HL-1M) which is a critical factor for long pulse ohmic discharge.

Several different wall conditioning technique have been tried on LH-1M, such as baking of the vessel, glow discharge cleaning, boronization, siliconization, and lithium coating. The boronization is carried out in a helium glow discharge with $C_2B_{10}H_{12}$ addition, while siliconization is done in similar way with SiH_4-He gas mixture. The lithium coating is performed by evaporation during He glow discharge. As a regular way, the helium glow discharge cleaning was used everyday during experimental session to reduce hydrogen recycling after wall conditioning such as boronization and siliconization.

On HL-1M, the total plasma radiation power is reduced by 3 to 6 times after boronization. Siliconization is even more effective than the boronization to reduce plasma radiation. Furthermore, silicon has good oxygen gettering properties which is very important for obtaining high performance discharge. It is the siliconization after which a long pulse ohmic discharge up to 4 second was achieved with plasma current of 100kA.

For a discharge up to 4s, precise and stable control for plasma position and plasma-current is also indispensable. A computer-oriented fast feedback control system for ohmic current and vertical field was adopted on HL-1M.

REFERENCES

[1] WANG Enyao, HL-1M Team, in Fusion Energy 1996, (Proc. 16th Int. Conf. on Fusion Energy, Montreal) Vol. 1, IAEA, Vienna (1997) 693.
[2] YAO Lianghua, TANG Nianyi, CUI Zhengying et al, Nucl. Fusion, 1998, 38(4) 631.
[3] LIU Yong, LI Xiaodong et al., Proc. of IAEA TCM on Research Using Small Tokamak, Prague, Czech, 1996.
[4] LIU Yong, LI Xiaodong, et al., Confinement studies during LHCD and LHW ion heating on HL-1M, submitted to 17th IAEA Fusion Energy Conf. and numbered as IAEA-F1-CN-69/EXP2/17.

LHCD SYSTEM AND EXPERIMENTS ON HT-7 SUPERCONDUCTING TOKAMAK

G. KUANG, Y. LIU, D. LIU, W. XU, Q. ZHANG, J. SHAN, F. LIU,
G. ZHENG, J. WU, J. LIN, B. DING, H. XU, L. SHANG, W. SHEN, Y. FANG
Institute of Plasma Physics, Chinese Academy of Sciences,
Hefei, China

Abstract

A Lower Hybrid Current Drive (LHCD) system was built on HT-7 superconducting tokamak to deliver 1.2 MW microwave power at a frequency of 2.45 GHz for a pulse length up to 5 seconds. Partial non-inductive current drive and full non-inductive current drive for several seconds by means of LHCD have been demonstrated on HT-7. It has been observed that plasma confinement can be considerably improved by means of LHCD.

1. Introduction

HT-7 superconducting tokamak [1] was reconstructed from original Russian T-7 tokamak. A lower hybrid wave (LHW) launcher system [2] was constructed on HT-7 in 1996. To sustain long pulse discharges and to improve plasma confinement are the main objectives to develop LHCD technology on HT-7.

To operate HT-7 with LHCD in a mode of long pulse length or even steady state in the future, CW klystron amplifiers were chosen as the wave generators. Since the highest toroidal magnetic field of the machine can only be as high as 2.5 T, HT-7 was planned to be operated with plasma densities below 4×10^{19} m^{-3} and plasma currents around 200kA in the mode of long pulse performance, thus, the lower hybrid wave (LHW) frequency was chosen as 2.45GHz which corresponds to a density limit about 4.5×10^{19} m^{-3} for electron Landau damping. According to a theoretical estimation and LHCD experimental results from variety of machines, a current drive efficiency $I_{CD} = I_{CD}\overline{n}_e R_p/P_{LHW} 0.6 \times 10^{19}$ Am^{-2}/W for LHCD on HT-7 was quite possible provided that the wave spectrum width was less than 1 and HT-7 plasma parameters were taken as $\overline{n}_e = (0.5\text{-}3)\times 10^{19}$ m^{-3}, $T_e(0)$1 keV, and Z_{eff} 2-3. It implied that 1.2 MW of wave might sustain more than 200kA in HT-7 plasmas with line averaged densities about 2×10^{19} m^{-3}, provided that 25% of the wave was lost during the launching process. Therefore it was decided to use 12 pieces of klystron amplifiers (2.45GHz, output power 100kW × 12, CW) as the wave generators. A wave launcher with its distinguished structure was designed to ensure flexible adjustment of launched wave spectra and low wave reflection.

LHCD research on HT-7 has been performed since the establishment of the LHCD system, preliminary experimental results have been reported elsewhere [2, 3]. During the Spring experimental campaign in 1998, a feedback control system to simultaneously control plasma current and position was developed and put into daily operation. With the new control system, the experiments to extend the pulse duration of discharge and to improve plasma confinement by means of LHCD have been performed.

The LHCD system is described and the experiments are discussed in this paper. The experimental setup is described in section 2; LHCD experiments to extend discharges are depicted in section 3; Section 4 is devoted to describe and discuss the LHCD experiments on the improvement of plasma confinement; At the last a summary is given.

2. The LHCD system on HT-7

The LHCD system is composed of the following main subsystems:
- low power wave exciter;
- High Power klystron Amplifiers (HPA);
- High power isolators and connected waveguide transmission lines;
- Grill coupler (an arrays of 2 × 12 waveguides);
- High Voltage Power Supplies (HVPS);
- Wave monitoring & phase feedback control system;
- Protection system;
- Water cooling system.

The 12 klystron amplifiers in the LHCD system are fed by 2 high voltage power supplies and driven by one wave exciter. Their waves are launched to HT-7 plasmas by one grill coupler. The $N_{//}$-spectrum can be feed-back controlled in a preset value from $N_{//}$ = 1 to 4. At present the system can be operated in the following parameters:

Frequency	2.45 GHz
Power output	1.2 MW
Pulse length	5 seconds, max.
Pulse repetition period	8 minutes
Designed power density in the coupler	<3.5 kW / cm^2 on averaged
$N_{//}^{peak}$	from 1 to 4
$N_{//}$	0.8

2. 1. Wave exciter

The wave exciter mainly consists of one master oscillator, one PIN modulator, one 1:12 power divider, twelve identical wave drive chains. Each of the chains consists of a digital phase shifter, a semiconductor wave balance amplifier, a voltage control attenuator, a power detector, etc. The master oscillator has three outputs, one among the three delivers 100 mw for phase reference, either of other two delivers 1 w. The PIN modulator can switch off wave power in 10 μs with a cut-off level of 20 dB. The phase adjustment range of the digital phase shifter is 360° with an adjustment step of 2.8°. The semiconductor amplifier has a constant output about 3 w when its input changes in a range of 5 dB. The attenuator has a dynamic range of 20 dB. Each of the twelve wave drive chains connects to the input of one klystron amplifier.

2. 2. High Power klystron amplifiers

The klystron amplifiers (Type KU-2.45) were designed and constructed by a Russian company. The main parameters of the devices are listed in the following table:

Frequency	2.45 GHz
Power output	100 kW, CW, 130 kW at its max.
Beam voltage	~33 kV
Beam current	5 ~ 7 A
Efficiency	>50%
Gain	>50 dB

At present the klystrons are operated in pulse mode with a pulse length determined by the high voltage power supplies.

2.3. High power isolators and connected transmission lines

The klystrons are protected from the reflected wave power by high power isolators. The isolator is composed of a 4-port differential phase shift circulators and two water dummy loads. The high power isolator can be used to transmit 130kW of microwave (2.45GHz, CW) with a reflected power of 35kW and can withstand 100 kW of reflected power for 10 ms max. The wave power from each klystron is transmitted to the grill coupler through a standard rectangular waveguide (WR430) transmission line over a length of about 10 meters, including a section of flexible rectangular waveguide (0.6 m). There are waveguide components such as twists, bends, one DC-break, and two bi-directional wave couplers on each line. The transmission losses on the line are totally 0.5 dB max. Dry air is occasionally pumped into the waveguides to remove moisture, but no pressurization and cooling are used for the transmission lines during the operation of the LHCD system.

2. 4. Grill coupler

One grill type coupler is used to couple the waves from the 12 klystrons to the HT-7 tokamak plasmas. The coupler is composed of 2 × 12 waveguides (2 rows × 12 columns). The wave from each klystron is transported to the coupler by a rectangular waveguide transmission line which is changed in sizes by step transformer and then divided into two waveguides by a 3dB divider. The two waveguides compose one column of the grill and have a phase difference of 45º. By such arrangement, adjacent waveguides in either row of the grill emit waves from different klystrons, therefore, the wave phase difference can be flexibly controlled. On each of the 12 transmission lines there is one BeO ceramic RF window which is located in the standard rectangular waveguide section and is 1.8 m away from the mouth of the coupler. No ceramic RF window is located in the position close to the mouth of the coupler. The waveguide of the grill coupler is 13.1 mm wide and 109.2 mm high. The septum between the waveguides is 2 mm. The grill coupler is made of stainless steel and has guard limiters (made of 2 mm thick molybdenum) around its mouth. The mouth of the grill coupler has a toroidal and poloidal shape to match to the plasma surface. The grill coupler is evacuated by a turbo-pump. For long pulse (even up to steady state) operations the waveguide array of the coupler is cooled by two water cooling plates which are put on the top and the bottom of the array respectively and are cooled by circulating pure water with a total flow rate of 150l/min. There is no coating on the inner surfaces of the stainless steel waveguides in the vacuum section of the wave coupler. Before starting LHCD experiments, usually about 10 hours are spent for launching short pulse of microwave (150kW/50ms, a shot / 5 minutes) to HT-7 vacuum chamber through the wave coupler (the wave phase difference between adjacent waveguides is set in 0^0) while the waveguide array is kept to be about 100^0 C by heating. It has been demonstrated to be very effective for outgassing of the coupler and also for increasing the wave launching ability of the coupler.

2. 5. High voltage power supplies

Two identical high voltage power supplies are used in the LHCD system, each feeding 6 klystrons in parallel. The high voltage power supplies normally acquire about two third of electrical power from a flying wheel AC generator and the rest from the electricity network. The main purpose for using two systems of input power is to reduce the load to the electricity network and to adjust the output DC voltage conveniently. Ignitrons are used for fast switching-off the high DC voltage on klystrons. The main parameters of the HVPS are listed in the following table:

Input	10 kV (3 phases, 50 Hz) +2 kV (6 phases, 70 Hz)
Output	2 × (-35 kV)/40 A, max.
Ripple	<1%
Pulse length	5 sec. max.
Fast switch-off time	150 μs
Normal switch-off time	50 ms

The klystron beam voltage can be controlled by a star point voltage regulator.

2. 6. Wave monitoring & phase feedback control system

The measurements of wave phase and power are essential for the control of desired $N_{//}$-spectra. To monitor the wave phase and power in each of the 12 waveguides at the coupler, a 12-channel wave phase and power detecting system was developed. The response time of the phase detector is about several microseconds. The 11 phase signals (the 12th is taken as a reference) are compared with their pre-set values by a computer which generates the control digital signals for the 11 phase shifters in the wave exciter. The time to complete one control cycle of the 11-channel wave phases is less than 180 μ s. The phase control of the system has an accuracy of 5^o over a range of 360^o. The phase signals are stored by the computer and can be displayed after each shot. The wave power control is realized by pre-setting proper control voltage to the attenuators which are connected to the outputs of the semiconductor wave balance amplifiers in the wave exciter. The input and output wave powers of each klystron as well as the reflected wave power from the wave coupler in each waveguide transmission line are detected and stored by another computer.

2. 7. Protection system

A wave protection system is developed to switch off the wave signals to the 12 semiconductor amplifiers in less than 20 μ s and to switch off the high voltage on the klystron cathodes in less than 50 ms if any of the following faults occur:

(1) VSWR > 1.3 at the klystron output;
(2) VSWR > 3 at the circulator output;
(3) wave breakdown at the klystron output window;
(4) wave breakdown in the transmission line;
(5) wave breakdown in the grill coupler.

A high voltage protection system was developed to ensure a reliable operation of the klystron. The ignitrons of the HVPS are triggered to fast switch off the klystron cathode voltage in less than 150 μ s in either of the following cases:
(1) The current in any klystron cathode circuit rises up to 7.5 A;
(2) The current of any klystron resonator rises up to 250 mA.

Normal switch-off of the HVPS functions within a time less than 50 ms in any of the following cases:
(1) When the wave protection system is triggered;
(2) When the ignitrons are triggered;
(3) When the solenoid current falls to below the nominal value by 10%;
(4) When the flow rate of water in any channel of the cooling system falls to the allowed minimum.

3. LHCD experiments on HT-7

On HT-7 superconducting tokamak a feedback control technology to simultaneously keep plasma current and plasma position in their preset values was developed during the Spring 1998. After the improvement of the control technology LHCD experiments on extending HT-7 discharges and improving plasma confinements have been performed. Partial non-inductive current drive, full non-inductive current drive, and recharge of transformer by means of LHCD have been respectively demonstrated.

3.1. Partial non-inductive current drive

Shot 18067 is a typical discharge in which the current is partially sustained by LHCD. Shown in Fig.1 is the waveforms in the shot. An LHW (200kW, $N_{//}{}^{p} = 2.45$, $N_{//} = 0.8$) is launched into the

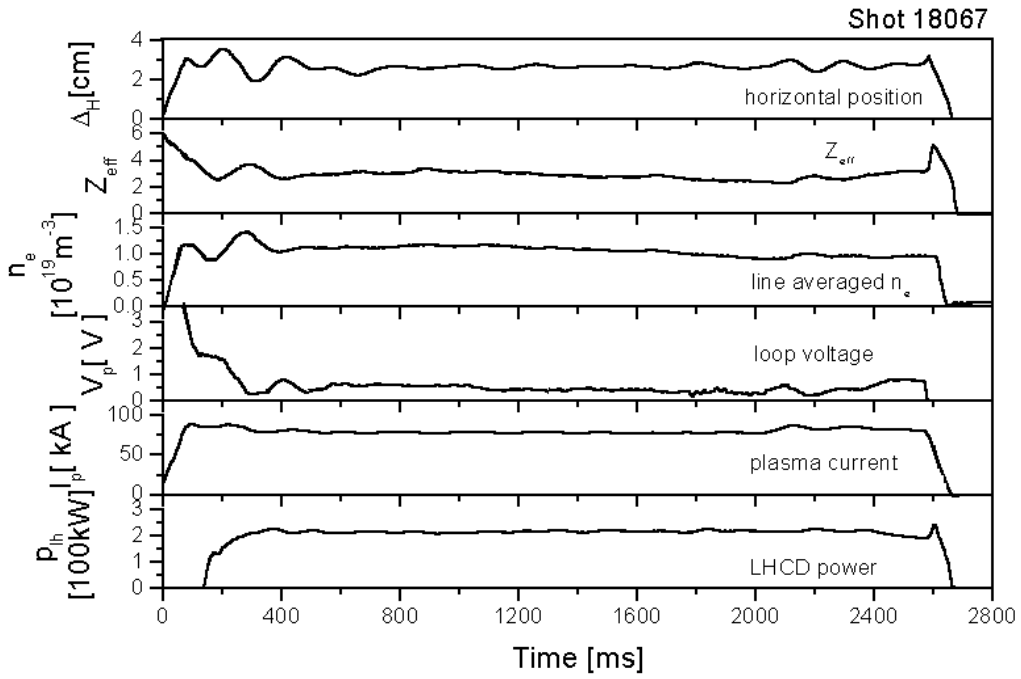

FIG. 1. The waveforms of a typical partial non-inductive current drive discharge on HT-7. After the onset of LHCD (200kW, $N_{//}^{p}$ = 2.9, $N_{//}$ = 0.8) the loop voltage drops from 1.8V to about 0.4V, meanwhile, plasma current, density, horizontal position, and Z_{eff} almost remain unchanged.

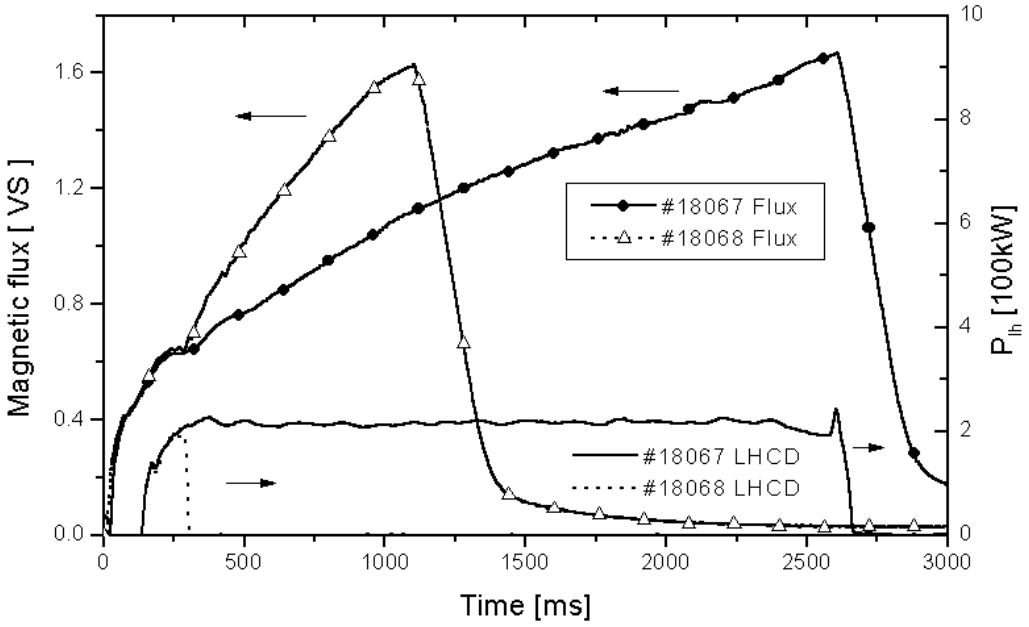

FIG. 2. Temporal evolution of the magnetic fluxes of the tokamak transformer in two sister shots (#18067 & #18068). The two discharges have almost same plasma parameters and same operational conditions except different times of LHCD.

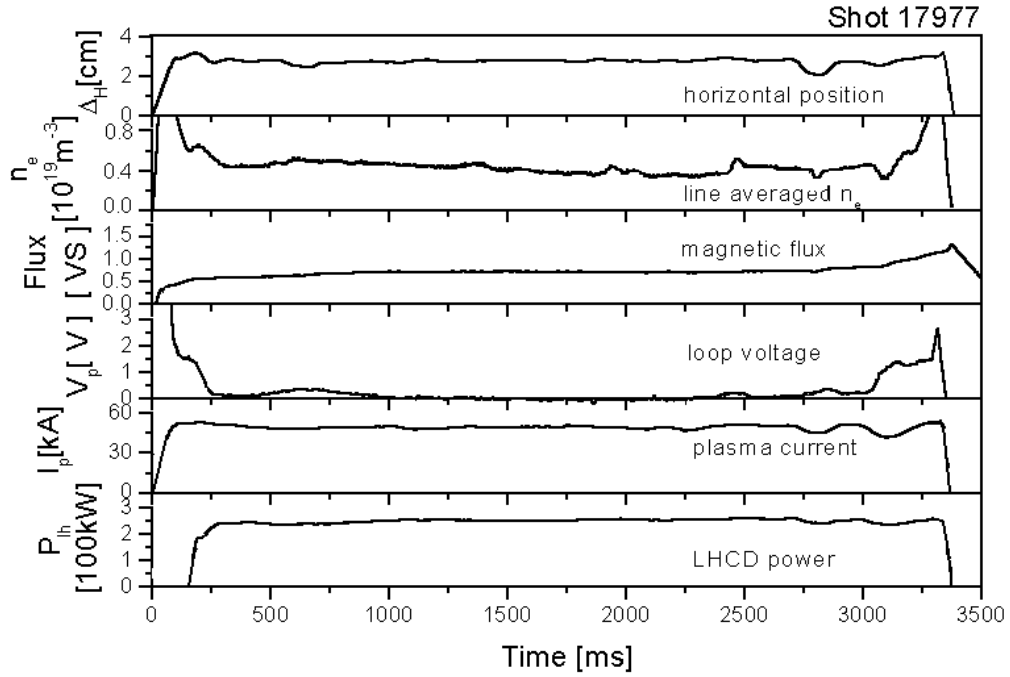

FIG. 3. The waveforms of a full non-inductive current drive discharge on HT-7. During the LHCD (250kW, $N_{//}^{p}$ =2.45, $N_{//}$ =0.8) phase the loop voltage remains zero for more than 2 sec, meanwhile, the magnetic flux of the tokamak transformer remains constant and no considerable changes occur in plasma current, density and horizontal displacement.

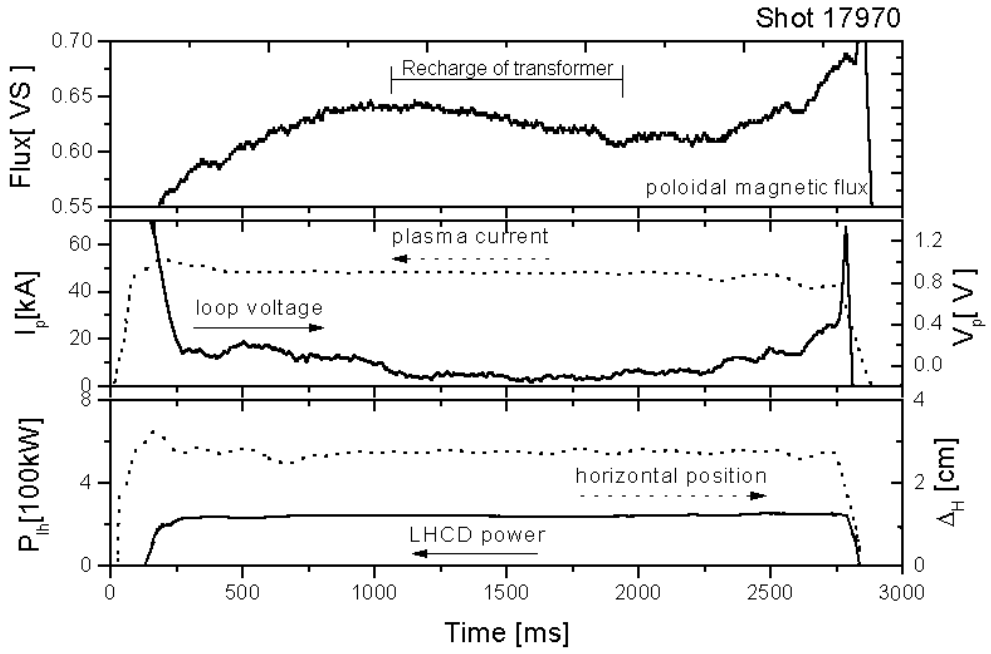

FIG. 4. The tokamak transformer is recharged in the indicated time interval when magnetic flux of the transformer gradually decreases and the loop voltage remains negative (-0.1V). The plasma current and horizontal displacement are kept constant in the phase.

plasma after 160ms when plasma current is already in its flat phase. The loop voltage drops from about 1.8V to about 0.4V due to LHCD. The merit of the current drive ($\eta_{CD} = \boldsymbol{I}_{CD} \bar{\boldsymbol{n}}_e \boldsymbol{R}_p / \boldsymbol{P}_{LH}$) is calculated to be about $0.54 \times 10^{19} \mathrm{Am}^{-2}/\mathrm{W}$.

LHCD effects on extension of discharge can be clearly seen from the temporal evolution of MFT in shot18067 and shot18068, as shown in Fig.2. Both shots have same performance conditions and nearly same plasma parameters, but LHW only lasts for 150ms in shot18068. The two discharges have different pulse lengths (1.1 sec, 2.6 sec respectively), but exhaust almost same MFT.

3.2. Full non-inductive current drive

Full non-inductive current drive is achieved on HT-7 by launching LHW into plasma during current flat phase. The waveforms of a typical shot are shown in Fig.3. The loop voltage drops to around zero after the onset of LHW and remains zero for more than 2 sec. The MFT is kept constant when the loop voltage is zero. The discharge terminates at last due to large vertical displacement of the plasma. The merit of the current drive in the zero loop voltage phase is calculated to be about $0.17 \times 10^{19} \mathrm{Am}^{-2}/\mathrm{W}$. The low drive efficiency is suspected to be due to too low a plasma density that may lead to poor particle confinement.

3.3. Recharge of transformer

In low density LHCD discharges, recharge of transformer is achieved during LHCD phase, as shown in Fig.4. It is indicated by the gradual decrease of MFT that the plasma ring delivers magnetic energy to the primary coils of the transformer, i.e., recharging the transformer. During the recharge phase, plasma current is fully sustained by LHCD and the LHW power is larger than what is demanded for sustaining the plasma current. Because the plasma current is feedback controlled to a preset value by adjusting input OH power, part of the surplus LHW power is thus coupled to the primary circuit of the transformer. The recharged energy is deposited in the transformer and may be delivered afterwards when the LHW is unable further to alone sustain the plasma current.

3.4. Improvement of plasma confinements by means of LHCD

It has been tested to improve plasma confinement by means of LHCD on HT-7. By adjusting plasma parameters and LHW parameters, improved confinement has been observed in the discharges in which the plasma currents are partially sustained by LHCD. An example is shown in Fig.5. In this shot LHW (300kW, $N_{//}{}^{p} = 2.45$, $N_{//} = 0.8$) is launched into the plasma in the current flat phase (I_p= 150kA), loop voltage drops from 2.5V to 1.1V after the onset of the wave. The discharge can be divided into four phases (OH, I, II, III), as indicated in the Figure. During the LHCD phases the ion temperature in plasma central region remains about 500eV (measured by a neutral particle analyzer), but the electron temperature gradually increases from 550eV to 900eV (measured by a soft X ray energy spectrum analyzer). HCN laser interferometer signals (three channels: r = -18.5cm, 0, 18.5cm) show that electron density slightly increases in phase III, but the shape of the density profile almost remains unchanged in the LHCD phases. The electron thermal energy increases from phase II to phase III by a factor of 1.5, as roughly estimated according to measured electron density and electron temperature. Multi-channel soft X ray signals show a gradually peaked soft X ray emissivity profile in phase III which suggests a very peaked electron temperature profile since Z_{eff} does not change from phase II to phase III. It was observed that sawtooth activity is visible in soft X ray signals in the LHCD phases but no m=1 mode oscillation is observed from soft X ray signals and Mirnov coil signals until the final termination of the discharge. The final disruption is attributed to increasing m=2 mode instability.

The improvement in phase III can not be attributed to the suppression of sawteeth and m=1 mode, as on ASDEX , because sawtooth activity exists but there is no m=1 mode activity in phase II and phase III. The improvement may be due to the change of magnetic shear, as suggested by the evolution of $\beta_p + \boldsymbol{l}_i / \mathbf{2}$ (shown in Fig.5) that is deduced from equilibrium measurements. The gradual decrease of

$\beta_p + \boldsymbol{l}_i / \mathbf{2}$ should be due to gradual decrease of $\boldsymbol{l}_i$ /2 because β_p is expected to gradually increase from phase II to phase III, therefore, it should be attributed to the redistribution of plasma current density in the outer region of the plasma since the current profile in the central region should not change much as suggested by the fact that sawtooth activity exists in the two phases. MHD modes seems not stable with such current profile, usually m=2 mode activity is stimulated and leads to plasma disruption.

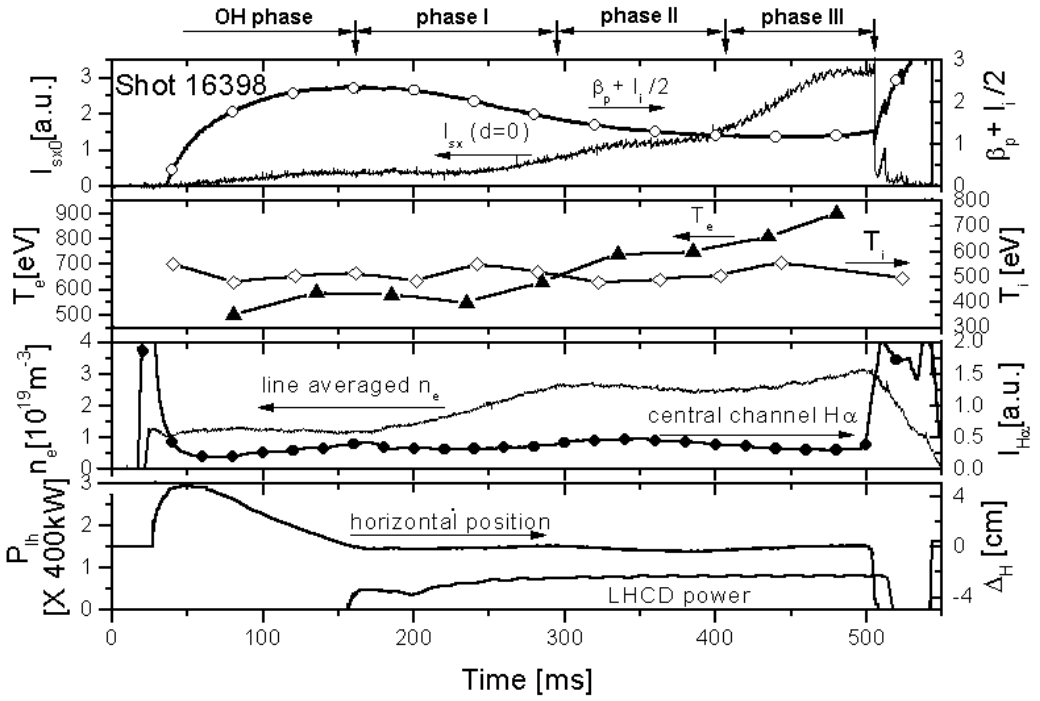

FIG. 5. The waveforms in an LHCD improved discharge. After the onset of LHW plasma density increases with even reduced Hradiation. As $\beta_p + \boldsymbol{l}_i / \mathbf{2}$ *decreases, electron temperature greatly increases, especially in phase III. A drastic increase of the electron thermal energy in phase III is indicated by the temporal evolution of the central channel soft X ray radiation.*

4. Summary

A LHCD system with a maximum output of 1.2 MW (2.45GHz) has been built on the superconducting tokamak HT-7. Its wave source consists of 12 klystrons. The grill coupler consists of 24 narrow rectangular waveguides (2 rows 12 columns). The wave launcher ensures a low wave reflection and a flexibly adjusted wave spectrum. HT-7 LHCD system has been used for experiments, partial non-inductive current drive, full non-inductive current drive, and recharge of transformer by means of LHCD have been respectively demonstrated. It has also been tried to improve plasma confinements by means of LHCD. Experimental evidences demonstrate that plasma electron thermal energy confinement can be greatly improved during LHCD phase. It is suggested by the evidences that the improvement might be attributed to the current redistribution in the outer region of the plasma.

REFERENCES

[1] Xie, J.K., HT-7 Group, "HT-7 superconducting tokamak and its operation", IAEA-CN-64/AP1-13, 1996.

[2] Kuang, G., LHCD group of ASIPP, in Proc.24th European Conf. on Contr. Fusion and Plasma Physics, Berchtesgaden (1997), Vol. 21A, part I, 457-460.

[3] Kuang, G., Xu, W., et al., Chinese Physics Letters, Vol.15, No.6 (1998) 435.

LIST OF PARTICIPANTS

Becoulet, A.
Association Euratom-CEA sur la Fusion,
CEA-Cadarache, 13108 Saint-Paul-lez-Durances, France
Tel.: +33-4-4225-6488
Fax: +33-4-422S-6233
e-mail: becoulet@cea.fr

Bi, Y.F.
Institute of Plasma Physics, Chinese Academy of Sciences,
P.O. Box 1126, Hefei, Anhui 230031, China
Tel.: +86-551-5591374
Fax: +86-551-5591310
e-mail: yfbi@ipncl.hfcas.ac.cn

Bora, D.
Institute for Plasma Research,
Nr. Indira Bridge, Bhat, Gandhinagar 382 428, India
Tel.: +91-79-2864690
Fax: +91-79-2864310
e-mail: dbora@plasma.ernet.in

Chen, Y.P.
Institute of Plasma Physics, Chinese Academy of Sciences,
P.O. Box 1126, Hefei, Anhui 230031, China
Tel.: +86-551-5591397
Fax: +86-551-5591310
e-mail: ypchen@ipncl.hfcas.ac.cn

Dolan, T.
Physics Section, International Atomic Energy Agency,
Wagramer Strasse 5, P.O. Box 100, A-1400 Vienna, Austria
Tel.: +43-1-2060-21756
Fax: +43-1-20607
e-mail: t.dolan@iaea.org

Dong, S.H.
Institute of Plasma Physics, Chinese Academy of Sciences,
P.O. Box 1126, Hefei, Anhui 230031, China
Tel.: +86-551-5591601
Fax: +86-551-5591310
e-mail: shdong@ipncl.hfcas.ac.cn

Gao, B.J.
Institute of Plasma Physics, Chinese Academy of Sciences,
P.O. Box 1126, Hefei, Anhui 230031, China
Tel.: +86-551-5591326
Fax: +86-551-5591310
e-mail: bjgao@ipncl.hfcas.ac.cn

Gao, D.M.
Institute of Plasma Physics, Chinese Academy of Sciences,
P.O. Box 1126, Hefei, Anhui 230031, China
Tel.: +86-551-5592302-4
Fax: +86-551-5591310
e-mail: dmgao@ipncl.hfcas.ac.cn

Gao, X.
Institute of Plasma Physics, Chinese Academy of Sciences,
P.O. Box 1126, Hefei, Anhui 230031, China
Tel.: +86-551-5591604
Fax: +86-551-5591310
e-mail: xgaoi@ipncl.hfcas.ac.cn

Ge, M.Y.
Headquarters,
Chinese Academy of Sciences,
52, Sanlihe road, Beijing 100864, China
Tel.: +86-10-68597240
Fax: +86-10-68111095

Hanada. K.
Advanced Fusion Research Center, RLM,
Kyushu University,
Kasuga-koen 6-1, Kasuga, Fukuoka 816, Japan
Tel.: +81-92-583-7482
Fax: +81-92-573-6899
e-mail: fusion@triam.kyushu-u.ac.jp

He, Y.Y.
Institute of Plasma Physics, Chinese Academy of Sciences,
P.O. Box 1126, Hefei, Anhui 230031, China
Tel.: +86-551-5591601
Fax: +86-551-5591310
e-mail: yyh@ipncl.hfcas.ac.cn

Hu, X.W.
University of Science & Technology of China,
Hefei, Anhui 230026, China
Tel.: +86-551-3603744
Fax: +86-551-3631760

Ivanov, D.P.
Institute of Nuclear Fusion, Russian Research Centre (Kurchatov Institute),
Ploshchad' akademika Kurchatova 46,
123182 Moscow, Russian Federation
Tel.: +7-095-196-1700
Fax: +7-095-943-0073
e-mail: aj@nfi.kiae.su(and/or "kev@isssph.kiae.ru")

Jacob, S.
Institute for Plasma Research,
Nr. Indira Bridge, Bhat, Gandhinagar 382 428, India
Tel.: +91-79-2864690
Fax: +91-79-2864310
e-mail: saji@plasma.ernet.in

Kaw, P.K.
Institute for Plasma Research,
Nr. Indira Bridge, Bhat, Gandhinagar 382 428, India
Tel.: +91-79-2864690
Fax: +91-79-2864310
e-mail: kaw@plasma.ernet.in

Kuang, G.L.
Institute of Plasma Physics, Chinese Academy of Sciences,
P.O. Box 1126, Hefei, Anhui 230031, China
Tel.: +86-551-5591381
Fax: +86-551-5591310
e-mail: kuang_gl@ipncl.hfcas.ac.cn

Li, D.
University of Science & Technology of China,
Hefei, Anhui 230026, China
Tel.: +86-551-3603107
Fax: +86-551-3631760
e-mail: dli@lx04.mphy.ustc.edu.cn

Li, J.G.
Institute of Plasma Physics, Chinese Academy of Sciences,
P.O. Box 1126, Hefei, Anhui 230031, China
Tel.: +86-551-5591332
Fax: +86-551-5591310
e-mail: j_li@ipnc1.hfcas.ac.cn

Li, Q.R.
Southwestern Institute of Physics,
P.O. Box 15, Chengdu, Sichuan 610041, China
Tel.: +86-28-5581122
Fax: +86-28-5581053
e-mail: liqr@swip.edu.cn

Liu, P.
Southwestern Institute of Physics,
P.O. Box 15, Chengdu, Sichuan 610041, China
Tel.: +86-28-5581122-6609
Fax: +86-28-5581053
e-mail: liuping@swip.edu.cn

Liu, W.D.
Modern Physics Department,
University of Science & Technology of China,
Hefei, Anhui 230026, China
Tel.: +86-551-3603744
Fax: +86-551-3631760
e-mail: wdliu@ustc.edu.cn

Liu, Y.
Southwestern Institute of Physics,
P.O. Box 15, Chengdu, Sichuan 610041, China
Tel.: +86-28-5581122-6555
Fax: +86-28-5581053
e-mail: liuyong@swip.edu.cn

Luo, J.R.
Institute of Plasma Physics, Chinese Academy of Sciences,
P.O. Box 1126, Hefei, Anhui 230031, China
Tel.: +86-551-5591332
Fax: +86-551-5591310
e-mail: luojr@ipncl.hfcas.ac.cn

Matto, S.K.
Institute for Plasma Research,
Nr. Indira Bridge, Bhat, Gandhinagar 382 428, India
Tel.: +91-79-2864623
Fax: +91-79-2864310
e-mail: shiban@plasma.ernet.in

Nin, Q.
Institute of Plasma Physics, Chinese Academy of Sciences,
P.O. Box 1126, Hefei, Anhui 230031, China
Tel.: +86-551-5591300
Fax: +86-551-5591310
e-mail: qnin@ipncl.hfcas.ac.cn

Qian, S.J.
Southwestern Institute of Physics,
P.O. Box 15, Chengdu, Sichuan 610041, China
Tel.: +86-28-5581122-6321
Fax: +86-28-5581053
e-mail: qiansj@swip.edu.cn

Qiu, L.J.
Institute of Plasma Physics, Chinese Academy of Sciences,
P.O. Box 1126, Hefei, Anhui 230031, China
Tel.: +86-551-5591300
Fax: +86-551-5591310
e-mail: qiulj@ipncl.hfcas.ac.cn

Saoutic, B.
Service de Physique des Plasmas de Fusion,
Association Euratom-CEA sur la Fusion,
CEA-Cadarache, 13108 Saint-Paul-lez-Durances, France
Tel.: +33-4-4225-4815
Fax: +33-4-4225-6233
e-mail: saoutic@drfc.cad.cea.fr

Saxena, Y.C.
Institute for Plasma Research,
Nr. Indira Bridge, Bhat, Gandhinagar 382 428, India
Tel.: +91-79-2864758
Fax: +91-79-2864310
e-mail: saxena@plasma.ernet.in

Wan, B.N.
Institute of Plasma Physics, Chinese Academy of Sciences,
P.O. Box 1126, Hefei, Anhui 230031, China
Tel.: +86-551-5591332
Fax: +86-551-5591310
e-mail: bnwan@ipncl.hfcas.ac.cn

Wan, Y.X.
Institute of Plasma Physics, Chinese Academy of Sciences,
P.O. Box 1126, Hefei, Anhui 230031, China
Tel.: +86-551-5591340
Fax: +86-551-5591310
e-mail: wanyx@ipncl.hfcas.ac.cn

Wang, K.J.
Institute of Plasma Physics, Chinese Academy of Sciences,
P.O. Box 1126, Hefei, Anhui 230031, China
Tel.: +86-551-5591301
Fax: +86-551-5591310
e-mail: kjwang@ipncl.hfcas.ac.cn

Wang, N.L.
Chinese Academy of Sciences,
52, Sanlihe Road, Beijing 100864, China
Tel.: +86-10-68597242
Fax: +86-10-68111095

Wang, S.J.
Institute of Plasma Physics, Chinese Academy of Sciences,
P.O. Box 1126, Hefei, Anhui 230031, China
Tel.: +86-551-5591300
Fax: +86-551-5591310
e-mail: sjwan@ipncl.hfcas.ac.cn

Wang, W.H.
Modern Physics Department,
University of Science & Technology of China,
Hefei, Anhui 230026, China
Tel.: +86-551-3603744
Fax: +86-551-3631760

Wen, Y.Z.
Modern Physics Department
University of Science & Technology of China,
Hefei, Anhui 230026, China
Tel.: +86-551-3601190
Fax: +86-551-3631760
e-mail: yzwen@staff.ustc.edu.cn

Weng, P.D.
Institute of Plasma Physics, Chinese Academy of Sciences,
P.O. Box 1126, Hefei, Anhui 230031, China
Tel.: +86-551-5591609
Fax: +86-551-5591310
e-mail: pdweng@ipncl.hfcas.ac.cn

Wu, S.T.
Institute of Plasma Physics, Chinese Academy of Sciences,
P.O. Box 1126, Hefei, Anhui 230031, China
Tel.: +86-551-5592302-4
Fax: +86-551-5591310
e-mail: stwu@ipncl.hfcas.ac.cn

Wu, Y.C.
Institute of Plasma Physics, Chinese Academy of Sciences,
P.O. Box 1126, Hefei, Anhui 230031, China
Tel.: +86-551-5591601
Fax: +86-551-5591310
e-mail: ycwu@ipncl.hfcas.ac.cn

Wu, D.
Institute of Plasma Physics, Chinese Academy of Sciences,
P.O. Box 1126, Hefei, Anhui 230031, China
Tel.: +86-551-5591601
Fax: +86-551-5591310
e-mail: dwu@ipncl.hfcas.ac.cn

Xiao, W.W.
Institute of Plasma Physics, Chinese Academy of Sciences,
P.O. Box 1126, Hefei, Anhui 230031, China
Fax: +86-551-5591310
e-mail: xiaoww@ipncl.hfcas.ac.cn

Yin, F.X.
Institute of Plasma Physics, Chinese Academy of Sciences,
P.O. Box 1126, Hefei, Anhui 230031, China
Tel.: +86-551-5591332
Fax: +86-551-5591310
e-mail: yinfx@ipncl.hfcas.ac.cn

Yu, C.X.
Modern Physics Dept.,
University of Science & Technology of China,
Hefei, Anhui 230026, China
Tel.: +86-551-3601186
Fax: +86-551-3631760
e-mail: chxyu@staf£ustc.edu.cn

Yu, Q.Q.
Institute of Plasma Physics, Chinese Academy of Sciences,
P.O. Box 1126, Hefei, Anhui 230031, China
Tel.: +86-551-5591302
Fax: +86-551-5591310
e-mail: szhu@ipncl.hfcas.ac.cn

Zhang, S.Y.
Institute of Plasma Physics, Chinese Academy of Sciences,
P.O. Box 1126, Hefei, Anhui 230031, China
Tel.: +86-551-5591604
Fax: +86-551-5591310
e-mail: svzhang@ipncl.hfcas.ac.cn

Zhao, Y.P.
Institute of Plasma Physics, Chinese Academy of Sciences,
P.O. Box 1126, Hefei, Anhui 230031, China
Tel.: +86-551-5591601
Fax: +86-551-5591310
mail: ypzhao@ipncl.hfcas.ac.cn

Zheng, S.B.
Institute of Physics, Chinese Academy of Sciences,
P.O. Box 603, Beijing 100080, China
Tel.: +86-10-62559131
Fax: +86-10-62562605